Taxonomic characterization of a novel marine *Streptomyces* and its application in nybomycin production enhancement through systems metabolic engineering

Dissertation

zur Erlangung des Grades

des Doktors der Naturwissenschaften

der Naturwissenschaftlich-Technischen Fakultät

der Universität des Saarlandes

von

Wei Shu

Saarbrücken

2025

Tag des Kolloquiums:	17.10.2025
Dekan:	Prof. Dr.-Ing. Dirk Bähre
Berichterstatter:	Prof. Dr. Christoph Wittmann
	Prof. Dr. Andriy Luzhetskyy
Akad. Mitglied:	Dr. Mark Lommel
Vorsitz:	Prof. Dr. Uli Kazmaier

Publications

Partial results of this work have been published in advance authorized by the Institute of Systems Biotechnology represented by Prof. Dr. Christoph Wittmann.

Peer-reviewed articles

Seo K, **Shu W**, Rückert-Reed C, Gerlinger P, Erb T, Kalinowski J, Wittmann C. (2023) From waste to health-supporting molecules: biosynthesis of natural products from lignin-, plastic- and seaweed-based monomers using metabolically engineered *Streptomyces lividans*. *Microb. Cell Fact.* 22:262.

Stegmüller J, Rodríguez Estévez M, **Shu W**, Gläser L, Myronovskyi M, Rückert-Reed C, Kalinowski J, Luzhetskyy A, Wittmann C. (2023) Systems Metabolic Engineering of *Streptomyces albidoflavus* at the level of primary and secondary metabolism enhances production of the reverse anitbiotic nybomycin against multi-resistant *Staphylococcus aureus*. *Metab. Eng*. 81:123-143.

Beganovic S, Rückert-Reed C, Sucipto H, **Shu W**, Gläser L, Patschkowski T, Struck B, Kalinowski J, Luzhetskyy A, Wittmann C. (2023) Systems biology of industrial oxytetracycline production in *Streptomyces rimosus*: the secrets of a mutagenized hyperproducer. *Microb. Cell Fact*. 22:222.

Shu W, Rückert-Reed C, Gromyko O, Tistechok S, Kalinowski J, Luzhetskyy A, Wittmann C. (2025) Description of *Streptomyces explomaris* sp. nov., isolated from the coastal soil rhizosphere of *Juniperus excelsa* and reclassification of *Streptomyces libani* as later heterotypic synonym of *Streptomyces nigrescens*. *Int. J. Syst. Evol. Microbiol*. 75(5).

Shu W, Stegmüller J, Rodríguez Estévez M, Rückert-Reed C, Kalinowski J, Gromyko O, Rebets Y, Luzhetskyy A, Wittmann C. (2025) Metabolic engineering of *Streptomyces explomaris* for increased production of the reverse antibiotic nybomycin. *Microb. Cell Fact*. 24, 227.

Conference contributions

Shu W, Stegmüller J, Rückert-Reed C, Luzhetskyy A, Wittmann C. Systems metabolic engineering of *Streptomyces* LV1-4 for production of the reverse antibiotic nybomycin. Next-Generation Synthetic Biology (5th edition), 2024, Ghent, Belgium.

Acknowledgment

I would first like to express my deepest gratitude to my supervisor, Prof. Dr. Christoph Wittmann, whose guidance, support, and encouragement have been invaluable throughout my PhD journey. Your insightful advice, patience, dedication, and wisdom have shaped my research, inspired my scientific curiosity, and greatly enriched my academic and personal growth. Your mentorship has profoundly influenced my professional trajectory, and I am immensely grateful for the countless hours spent discussing and refining my ideas.

I would like to also express my sincere gratitude to my second supervisor Prof. Dr. Andriy Luzhetskyy, for coordinating the research project EXPLOMARE, for excellent collaboration over the past few years, and for reviewing my thesis.

I sincerely appreciate my scientific colleague Dr. Christian Rückert-Reed for his assistance in transcriptomic analysis, genome analysis of *Streptomyces explomaris*, providing constructive feedback, insightful suggestions, and valuable discussions about taxonomic research. Thank you Julian, for sharing me the knowledge of genetic engineering about *Streptomyces*. Many thanks Dr. Marta Rodríguez Estévez for screening nybomycin hosts. I would like to express my gratitude to Michael Marx for his valuable support in the collection of SEM data.

Many thanks to all members of iSBio, who have brought me numerous memorable moments. Special thanks to Michel for developing analytical methods and keeping the machines running smoothly. Thank you, Susanne, for your generous assistance with administrative tasks. Fabian, thank you for your encouragement and for joining me on hikes. My sincere appreciation goes to Kyoyoung, Anna and Iza for sharing many laughs, patiently listening to my complaints, and truly understanding me. Many thanks to Jens and Sarah for inviting me to various activities, which truly enriched my life in Saarbrücken.

Special thanks also to my Chinese friends Muzi and Peng, for helping me quickly adapt to life in Germany and for all the memorable moments we had, especially our unforgettable “online talking”. Hang and Yingying, thank you for going to Mensa daily with me and the enjoyable

lunch time we spent.

My heartfelt thanks go to my family, especially my wife, whose unwavering support, constant encouragement, and love have been my greatest source of strength. Your belief in me has guided and propelled me forward through challenging times.

Table of Contents

Summary

Members of the genus *Streptomyces* are renowned for their ability to produce variety of natural products. Given the rising concern over the antibiotics resistance in the past decades, nybomycin has emerged as promising candidate to re-establish clinical effectiveness of fluoroquinolone antibiotics against *Staphylococcus aureus*. Consequently, isolating novel *Streptomyces* strains capable of efficiently producing known antibiotics remains crucial. Here we identified a new isolate from the coastal rhizosphere soil of *Juniperus excelsa* M. Bieb. on the Crimean Peninsula by a multiphase identification method. This isolate has been designated as *Streptomyces explomaris*. *S. explomaris* revealed promising performance as heterologous nybomycin producer when compared to other hosts. Global transcriptomic analysis indicated unfavorably downregulated genes, related to precursor supply including the pentose phosphate and the shikimate pathways. In contrast, the regulatory genes *nybW* and *nybX* were found up-regulated. Guided by these insights, stepwise metabolic engineering globally addressed the observed bottlenecks. After several rounds of optimization, *S. explomaris* NYB-3B achieved a significantly improved nybomycin titer of 57 mg L^{-1}, about five-fold more than parental strain. Finally, *S. explomaris* NYB-3B was successfully applied to valorize commercially available seaweed hydrolysates, demonstrating the potential of sustainable marine-derived feedstocks for enhanced antibiotic production.

Zusammenfassung

Die Vertreter der Gattung *Streptomyces* sind bekannt für ihre Fähigkeit, eine Vielzahl natürlicher Produkte zu synthetisieren. Angesichts der zunehmenden Besorgnis über Antibiotikaresistenzen in den letzten Jahrzehnten ist Nybomycin als vielversprechender Kandidat hervorgetreten, um die klinische Wirksamkeit der Fluorchinolon-Antibiotika gegenüber *Staphylococcus aureus* wiederherzustellen. Daher ist die Isolierung neuer *Streptomyces*-Stämme, die bekannte Antibiotika effizient produzieren können, von großer Bedeutung. In der vorliegenden Studie wurde mittels eines mehrstufigen Identifikationsverfahrens ein neuer Stamm aus der küstennahen Rhizosphären-Erde von *Juniperus excelsa* M. Bieb. auf der Halbinsel Krim isoliert. Dieser Stamm wurde als *Streptomyces explomaris* benannt. Im Vergleich zu anderen heterologen Produktionswirten zeigte *S. explomaris* eine vielversprechende Leistung als Produzent von Nybomycin. Eine globale transkriptomische Analyse offenbarte eine unerwünschte Herunterregulierung von Genen, die mit der Vorstufenversorgung in Verbindung stehen, insbesondere in den Stoffwechselwegen des Pentosephosphats und des Shikimats. Im Gegensatz dazu wurden die regulatorischen Gene *nybW* und *nybX* hochreguliert vorgefunden. Auf Basis dieser Erkenntnisse wurden schrittweise metabolische Optimierungen durchgeführt, um die beobachteten Engpässe systematisch zu beseitigen. Nach mehreren Optimierungsrunden erreichte der Stamm *S. explomaris* NYB-3B eine signifikant verbesserte Nybomycinausbeute von 57 mg L^{-1}, etwa das Fünffache des Ausgangsstamms. Schließlich wurde der Stamm *S. explomaris* NYB-3B erfolgreich eingesetzt, um kommerziell verfügbare Algenhydrolysate aufzuwerten, was das Potenzial mariner nachwachsender Rohstoffe für eine nachhaltige und verbesserte Antibiotikaproduktion demonstriert.

1 Introduction

1.1 General introduction

Actinomycetes, particularly *Streptomyces*, are prolific producers of secondary metabolites, contributing nearly half of all known microbial natural products (Bilyk and Luzhetskyy, 2016). Many of these bioactive compounds exhibit diverse pharmaceutical activities, including antibacterial, anticancer, and antiviral properties (Beganovic et al., 2023; Campbell, 1985; Gläser et al., 2021; Seo et al., 2023; Stegmüller et al., 2024). As a result, the isolation, taxonomic classification, and further study of novel *Streptomyces* species remain a focus of extensive research (Goodfellow et al., 2017). While terrestrial environments have traditionally been the focus of *Streptomyces* research, marine ecosystems are increasingly recognized as valuable sources of novel strains (Yang et al., 2019). The extreme conditions of marine habitats, such as high salinity, nutrient limitations, high hydrostatic pressure, low pH, and low temperature (Genilloud, 2017), drive the evolution of unique metabolic adaptations. As a result, marine-derived *Streptomyces* may have special physiological and biochemical characteristics, as well as different metabolic pathways (Barakat and Beltagy, 2015; Lee et al., 2014; Li et al., 2011). These findings emphasize the biotechnological potential of *Streptomyces* isolated from marine environments as a valuable source of novel metabolites with pharmaceutical applications.

The industrial fermentation of natural products has historically relied on agriculture-based carbon sources, including glucose and starch (Ögmundarson et al., 2019; Seo et al., 2023). However, the growing demand for food has intensified competition for these resources, emphasizing the need to explore renewable feedstocks. As a third-generation biomass, macroalgae (seaweed) presents a promising alternative (Poblete-Castro et al., 2020). Rich in carbohydrates, with concentrations reaching up to 75% (Milledge et al., 2014), seaweed presents an attractive carbon source. Unlike traditional feedstocks, it requires neither arable land nor freshwater (Torres et al., 2019), and has minimal lignin content (Offei et al., 2018), reducing the need for extensive pretreatment prior to enzymatic hydrolysis.

Although seaweed-derived sugars have been extensively studied for bulk chemical and biofuel production, including butanol (Hou et al., 2017), ethanol (Enquist-Newman et al., 2013; Kim et al., 2011), 2,3-butanediol (Mazumdar et al., 2013), and L-lysine (Hoffmann et al., 2021), their potential for synthesizing high-value bioproducts remains largely uninvestigated. However, recent research has shown that the viability of seaweed hydrolysates serve as a carbon source for bioactive compound biosynthesis, the antibiotic peptide bottromycin and the anti-insecticidal polyketide pamamycin in *Streptomyces lividans* using brown algae hydrolysate(Seo et al., 2023). These findings highlight the vast potential of seaweed biomass as a renewable feedstock for the sustainable production of bioactive molecules.

Nybomycin which referred as a “reverse antibiotic”, exhibits potent activity against fluoroquinolone-resistant *Staphylococcus aureus*, effectively restoring the therapeutic potential of fluoroquinolones (Bardell-Cox et al., 2019). However, its low natural production yield (Rodríguez Estévez et al., 2018; Wang et al., 2019) remains a major challenge for clinical application, necessitating the development of efficient production strategies. One promising approach to increasing natural product titers involves the heterologous expression of biosynthetic gene clusters (BGCs) in genetically optimized *Streptomyces* hosts (Liu et al., 2018; Myronovskyi and Luzhetskyy, 2019). Therefore, utilizing seaweed hydrolysate for nybomycin biosynthesis in metabolically engineered marine-derived *Streptomyces* presents a sustainable and promising biotechnological application.

1.2 Objectives

This study aims to enhance nybomycin production in *Streptomyces* hosts through systems metabolic engineering while exploring the feasibility of seaweed-derived feedstocks as a sustainable resource for nybomycin biosynthesis.

The initial goal involved determining the taxonomic identity of a novel marine-derived isolate, designated as *Streptomyces explomaris*, which was obtained from the coastal rhizosphere sediment associated with *Juniperus excelsa* M. Bieb. on the Crimean Peninsula. Following taxonomic characterization, its potential as a nybomycin producer should be assessed and compared to other known *Streptomyces* hosts. To further improve nybomycin biosynthesis, transcriptional analysis should be performed to identify key regulatory and metabolic targets. Subsequently, a rational metabolic engineering strategy would be applied to optimize both nybomycin biosynthetic pathways and supporting metabolic networks to increase production.

Finally, the further objective was to evaluate the most promising engineered mutant strain for nybomycin biosynthesis using seaweed hydrolysate, assessing its potential as a renewable feedstock for antibiotic production.

2 Theoretical Background

2.1 The genus of *Streptomyces*

The genus *Streptomyces* is one of the most well-characterized genera within Actinobacteria, recognized for its ecological adaptability and widespread presence in terrestrial, aquatic, and host-associated environments (van der Meij et al., 2017). These bacteria are widely recognized for their capability to synthesize a broad spectrum of bioactive metabolites, such as antibiotics, which contribute to their survival for competition and adaptation in diverse ecosystems (Barka et al., 2016). Furthermore, *Streptomyces* produces extracellular enzymes such as cellulase, xylanase, chitinase, amylase, protease, and lipase (Prakash et al., 2013), enabling the breakdown of complex biopolymers, which serve as nutrient sources for *Streptomyces*.

Streptomyces are aerobic, Gram-positive bacteria that develop spores and form an extensive branched mycelial network, including both substrate and aerial mycelium during growth (Flardh and Buttner, 2009). The special features among bacteria are that they possess high GC-content (>70%) and relatively large, linear genomes (5–12 Mb) (Harrison and Studholme, 2014; Hopwood, 2019), which include a “core” region essential for fundamental cellular functions and flanking “arms” enriched with dispensable genes under laboratory conditions, which are probably obtained by horizontal transfer to adapt the environment changes (Hopwood, 2006).

The life cycle of *Streptomyces* is distinguished by its multicellular and filamentous growth, bearing resemblance to fungal development (**Figure 1**). It begins with spore germination, giving rise to vegetative hyphae, which extend and branch to form a complex vegetative mycelial structure (Chater, 1972). Unlike most bacteria, *Streptomyces* does not divide by binary fission; instead, it develops cross-walls that separate its hyphae into multinucleated compartments (Claessen et al., 2014; Wildermuth and Hopwood, 1970). This unique trait making *Streptomycetes* as unusual example of a multicellular bacterium.

Under unfavorable conditions, particularly nutrient depleted, vegetative mycelium will differentiate into aerial hyphae, a process fueled by lipids and amino acids derived from

autolyzed substrate mycelium through a programmed cell death-like mechanism (Méndez et al., 1985; Miguélez et al., 1999; Wildermuth, 1970). These aerial hyphae ultimately mature into spore chains, formed via simultaneous cell division and maturation.

The shift from substrate-associated growth to aerial mycelium formation is closely linked to the activation of secondary metabolism, leading to the synthesis of antibiotics and other bioactive molecules. The synchronization of morphological differentiation and metabolite biosynthesis indicates that both processes are regulated by shared genetic mechanisms (Worrall and Vijgenboom, 2010). Antibiotic bioproduction during the stage from substrate to aerial mycelium transition provides a competitive edge against coexisting microorganisms (Bibb, 2005; van Wezel and McDowall, 2011) and plays an important role in cell signaling and microbial interactions, influencing both gene expression and interspecies dynamics (Yim et al., 2007).

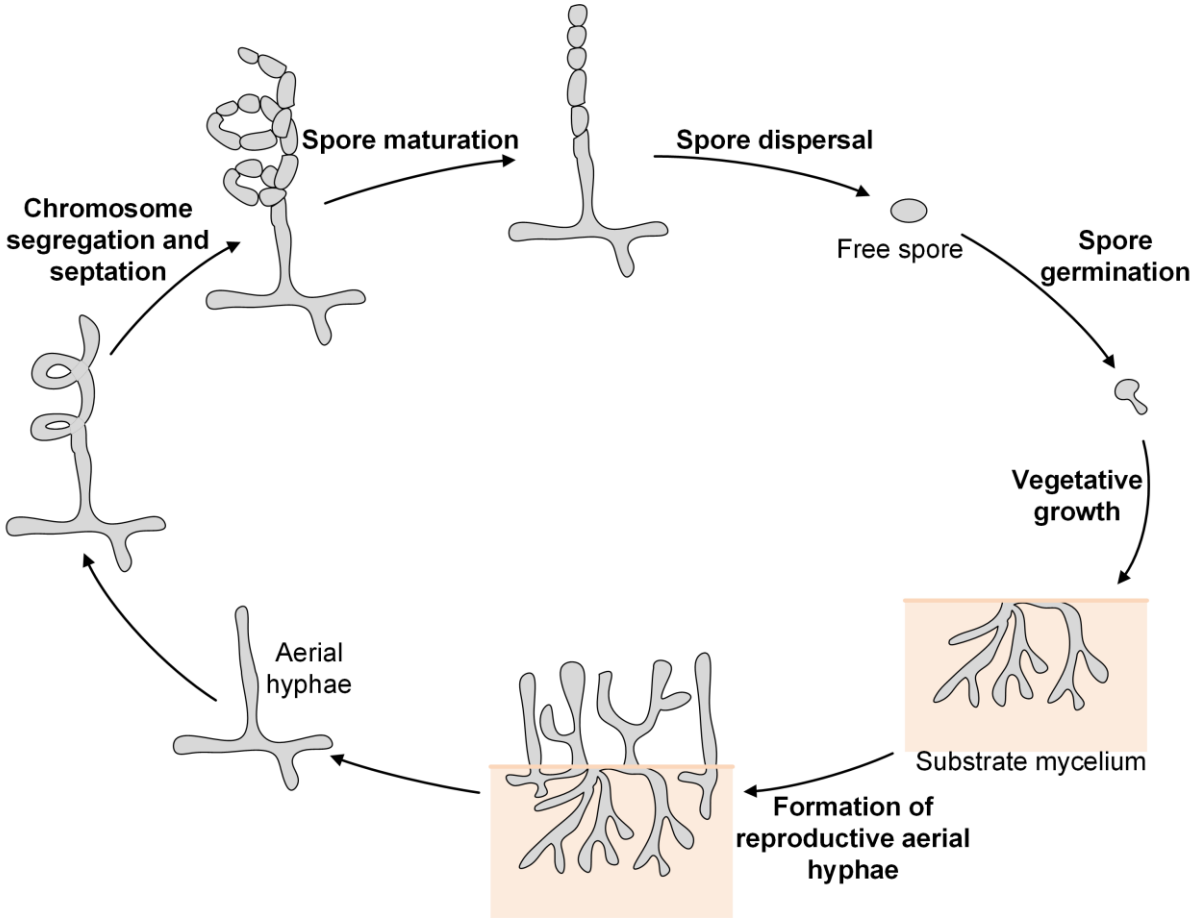

Figure 1: Developmental life cycle of *Streptomyces*. Adapted from (van der Meij et al., 2017). In a nutrient rich environment, free spores start to germinate to develop into substrate mycelium, followed by progressing into aerial hyphae growth. Eventually, these aerial hyphae

undergo division to produce uninucleate cells, which further mature into spores, completing the developmental cycle.

2.1.1 Polyphasic taxonomy of *Streptomyces*

Microbial taxonomy involves the classification, identification, and nomenclature of microorganisms based on similar characteristics (Garrity, 2016; Gupta, 2021; Hugenholtz et al., 2021; Moore et al., 2010). Establishing an accurate taxonomic framework is fundamental to comprehending microbial diversity and function, making the development of reliable and standardized classification methods a priority. Currently, polyphasic taxonomy (Anderson and Wellington, 2001) is the predominant approach for microbial classification and identification, including both phenotypic and genotypic analyses. Phenotypic characterization relies on morphological, physiological, and chemotaxonomic traits (Vandamme et al., 1996), whereas genotypic analysis is primarily based on 16S rRNA gene sequencing and whole-genome sequencing (Coenye et al., 2005; Komaki, 2023; Meier-Kolthoff et al., 2014).

As a representative genus of actinomycetes, *Streptomyces* constitutes the largest taxonomic group of prokaryotes (Komaki, 2023). The extensive diversity within this genus presents challenges for accurate species classification and identification. The polyphasic taxonomic approach has significantly contributed to the accurate delineation and classification of many species within the genus *Streptomyces*. For instance, a strain isolated from Atacama Desert soil was identified as *Streptomyces bullii* sp. nov. (Santhanam et al., 2013), while *Streptomyces rimosus* subsp. *paromomycinus* was reclassified as *Streptomyces paromomycinus* sp. nov. (Komaki and Tamura, 2019).

2.1.2 Phenotypic analysis

The classification of *Streptomyces* at both the genus and species levels is primarily depends on morphological, physiological, and chemotaxonomic traits. Morphological analysis is relied on the observation of cultures on a series of agar media from International *Streptomyces* Project (ISP) (Shirling and Gottlieb, 1966) after full maturation. Morphological characteristics assessed include pigmentation of vegetative mycelium, coloration of aerial spore masses, and

production of diffusible pigments. Moreover, the spore chain morphology by microscope also serves as a critical criterion for species identification.

Physiological and biochemical profiling plays a crucial role in defining *Streptomyces* species. Those studies include evaluation of the assimilation of different carbon sources, growth under varying temperatures and pH conditions, tolerance to varies NaCl concentrations, susceptibility to antibiotics, and analysis on ability to produce various enzymes (Landwehr et al., 2018; Risdian et al., 2021; Tian et al., 2012).

Chemotaxonomy, which categorizes organisms based on their cellular chemical composition, is another key approach in microbial classification (Goodfellow and Minnikin, 1985; Goodfellow et al., 1988). The predominant chemical components utilized in this classification scheme include amino acids in the cell wall, mycolic acids, lipids, proteins, menaquinones, and carbohydrate components (Embley et al., 1988; Stackebrandt et al., 1997). A distinguishing chemotaxonomic trait of *Streptomyces* is the consistent presence of LL-diaminopimelic acid and dominant menaquinones in the cell walls (Alderson et al., 1985; Mary P. Lechevalier, 1970). However, no specific whole-cell sugar profile has been identified as a defining taxonomic feature for this genus (Alderson et al., 1985; McKerrow et al., 2000).

2.1.3 Genomic and phylogenetic analysis

Recent progress in genomic analysis has markedly improved the classification and identification of actinomycetes by employing 16S rRNA gene sequence, DNA-DNA hybridization (DDH), multilocus sequence typing (MLST), and whole genome sequence (WGS) (Anderson and Wellington, 2001; Daquioag and Penuliar, 2021). Among these, phylogenetic evaluation based on the 16S rRNA gene sequence is typically served as an initial step in identification. However, the low resolution limits its effectiveness in accurately delimitating *Streptomyces* (Alam et al., 2010; Han et al., 2012; Komaki, 2023; Labeda et al., 2012). Notably, some *Streptomyces* strains that exhibit nearly identical 16S rRNA gene sequences have been classified into distinct taxonomic groups (Antony-Babu et al., 2017), underscoring the inherent complexity of *Streptomyces* taxonomy and the need for higher-resolution methodologies for

species differentiation.

DDH has traditionally been employed to evaluate genetic similarity among closely related microbial species by comparing their genomic content. The cut-off value 70% of DDH serves as a species boundary, meaning that strains exceeding this threshold are considered to belong to the same species (Tindall et al., 2010; Wayne et al., 1987). The progress in bioinformatics technology has facilitated the adoption of digital DDH, eliminating the need for tedious laboratory experiments by enabling in silico genome comparisons.

MLST has emerged as a robust alternative for prokaryotic species identification, utilizing a set of five housekeeping genes. Due to its high reproducibility and resolution, MLST provides taxonomic insights comparable to DDH (Rong et al., 2009). Studies have shown a strong correlation between DDH and MLSA, with an MLSA evolutionary distance of 0.007 corresponding to the 70% DDH threshold used for species delineation in the *Streptomyces* (Glaeser and Kampfer, 2015; Rong and Huang, 2010; Rong and Huang, 2012). The application of housekeeping genes enhances both classification accuracy and resolution, making it a valuable tool for taxonomic studies. Many phylogenetic investigations in *Streptomyces* have utilized protein-coding genes due to their superior discriminatory power. For instance, MLSA has been employed in taxonomic identifications of *Streptomyces griseus* (Rong and Huang, 2010) and *Streptomyces hygroscopicus* (Rong and Huang, 2012), as well as in studies examining diversity within the *Streptomycetaceae* family(Han et al., 2012; Labeda et al., 2012).

The increasing availability of WGS data from type strains has further revolutionized microbial taxonomy, driven by the declining cost of high-throughput sequencing technologies and large-scale genome sequencing projects (Wu and Ma, 2019). Whole-genome data now become a critical resource for taxonomy in Actinobacteria, allowing for the assessment of genome-relatedness indices such as OGRI (Overall Genome Relatedness Index) (Chun and Rainey, 2014), and phylogenomic analyses. The Type (Strain) Genome Server (TYGS) is a notable online platform providing genome-based taxonomic insights (Meier-Kolthoff and Goker, 2019). By submitting WGS data, researchers can obtain accurate species identification, perform

phylogenetic analyses utilizing both 16S rRNA and complete genome sequences, and conduct pairwise genome comparisons with closely related species.

2.2 Natural products formation in *Streptomyces*

Streptomyces exhibits a highly versatile secondary metabolism, allowing it to thrive in extreme and dynamic environments while producing a broad spectrum of bioactive natural products (Genilloud, 2017; Sardari, 2017; Xia et al., 2020). As a result, *Streptomyces* is regarded as a valuable source of secondary metabolites, many of which exhibit complex chemical structures, including macrolides (Wu et al., 2007), polyketides (Deng et al., 2017), peptides (Xu et al., 2020), saccharids (McCulloch et al., 2015), alkaloids (Fang et al., 2020), and terpenes (Martin-Sanchez et al., 2019). Given their extensive structural diversity, these compounds exhibit varied biological activities, including antimicrobial, antiviral, anticancer, immunosuppressive, antihypertensive, insecticidal, antioxidative, herbicidal, and plant growth-promoting effects (Ikeda et al., 2014). These properties have made them indispensable in pharmaceutical, biotechnology, and agricultural industries.

In *Streptomyces*, the synthesis of secondary metabolites is regulated by biosynthetic gene clusters (BGCs), containing clusters of genes with related functions dedicated to producing specific natural products (Medema et al., 2015). The genome sequencing of *Streptomyces coelicolor* A3(2), completed in 2002 (Bentley et al., 2002), marked the beginning of large-scale genomic analysis of this genus (Medema et al., 2010; Ohnishi et al., 2008; Pullan et al., 2011). Subsequent genomic studies have identified more than 20 secondary metabolite BGCs within various *Streptomyces* genomes. The size of these BGCs can vary significantly depending on the compound they encode, with the daptomycin BGC spanning 65 kb (Seunghee et al., 2019), and the vancoresmycin pathway requiring a 141 kb BGC (Kepplinger et al., 2018).

Despite the presence of numerous BGCs, many remain silent or exhibit low expression under standard laboratory cultivation conditions (Moussa et al., 2019), complicating the isolation and subsequent structural characterization of the encoded metabolites. Heterologous expression systems have emerged as robust approaches for activating silent gene clusters and enhancing

the biosynthesis of secondary metabolite. Several cloning methodologies have been developed to facilitate the transfer and expression of BGCs, including Gibson assembly (Gibson et al., 2009), site-specific recombination-based tandem assembly (SSRTA) (Zhang et al., 2011), the bacterial artificial chromosome (BAC) system (Deng et al., 2017), and transformation-associated recombination (TAR) (Kim et al., 2010). The selection of expression hosts and vector systems depends on the specific requirements of the target metabolite.

During the stationary phase, *Streptomyces* synthesize secondary metabolites, including antibiotics, which provide a competitive advantage in natural ecosystems. Actinomycetes contribute to over two-thirds of all known antibiotics (Hopwood, 2006), with *Streptomyces* alone responsible for approximately 80% of these bioactive compounds (**Table 1**) (Alam et al., 2022). Several clinically important antibiotics, including chloramphenicol (Vining and Stuttard, 1995), tetracycline (Nelson and Levy, 2011), daptomycin (Miao et al., 2005) and streptomycin (Schatz et al., 1944) originate from *Streptomyces* strains.

Table 1: Bioactive compounds originating from *Streptomyces*

Compound	Species	Reference
Cephamycin	*Streptomyces clavuligerus*	(Nagarajan et al., 1971)
Chloramphenicol	*Streptomyces venezuelae*	(John Ehrlich et al., 1947)
Tetracycline	*Streptomyces aureofaciens*	(Marjorie A Darken et al., 1960)
Kanamycin	*Streptomyces kanamyceticus*	(Umezawa et al., 1957)
Spectinomycin	*Streptomyces spectabilis*	(Bergy et al., 1961)
Monencin	*Streptomyces cinnamonensis*	(Agtarap et al., 1967)
Mitomycin	*Streptomyces caespitosus*	(Hata et al., 1956)
Lincomycin	*Streptomyces lincolnensis* ssp. *lincolnensis*	(MacLeod et al., 1964)

Rapamycin	*S. hygroscopicus*	(Vézina et al., 1975)
Streptomycin	*S. griseus*	(Schatz et al., 1944)
Daptomycin	*Streptomyces roseosporus*	(Debono et al., 1988)
Actinomycin D	*Streptomyces antibioticus*	(Waksman and Woodruff, 1940)
Avermectins	*Streptomyces avermitilis*	(Burg et al., 1979)
Tacrolimus	*Streptomyces tsukubaensis*	(Goto et al., 1987)
Doxorubicin	*Streptomyces peucetius*	(Bonadonna et al., 1969)
Bleomycin	*Streptomyces verticillus*	(Umezawa et al., 1966)
Kasugamycin	*Streptomyces kasugaensis*	(Umezawa et al., 1965)
Neomycin	*Streptomyces fradiae*	(Waksman and Lechevalier, 1949)
Streptochlorin	*Streptomyces* sp. *SF2583*	(Watabe, 1988)
Hygromycin B	*S. hygroscopicus*	(Mann and Bromer, 1958)
Oligomycin	*Streptomyces diastatochromogenes*	(Smith et al., 1954)
Candicidin	*S. griseus* IMRU3570	(Waksman et al., 1965)
Amphotericin B	*Streptomyces nodosus*	(Stiller et al., 1955)

Streptomyces is a well-established producer of bioactive compounds, such as the most of valuable clinically antibiotics (Dhakal et al., 2019; Takahashi and Nakashima, 2018). However, its industrial application in antibiotic production faces several limitations. Due to its filamentous growth and intricate developmental cycle, *Streptomyces* fermentation processes tend to be prolonged, negatively affecting production efficiency (Sigle et al., 2015); Additionally, under conventional laboratory conditions, approximately 90% of its BGCs remain inactive or cryptic,

preventing the expression of many potential antibiotics (Mao et al., 2018).

As genome sequencing technology advances quickly, with the combination of omics and systems biology approaches, have facilitated the mining of important *Streptomyces* enzymes and the study of synthesis processes. Systems metabolic engineering has emerged as a potent strategy to boost secondary metabolite production by expanding substrate availability, minimizing byproduct formation, optimizing cell physiology, and heterologous expressing BGCs for novel compound biosynthesis (Kern et al., 2007).

2.2.1 Expand degradable sugar spectrum

Carbon sources significantly influence biomass accumulation and metabolite biosynthesis, thus critically affecting the production of secondary metabolites, including antibiotics (Sánchez et al., 2010). Selecting an appropriate substrate is essential for optimizing *Streptomyces* metabolism and triggering bioactive compound synthesis (Ruiz et al., 2010). The carbon catabolite repression (CCR) mechanism can regulate the activation or suppression of genes related to morphological development and secondary metabolite production, though its effects vary depending on the strain (Ruiz et al., 2010; Sánchez et al., 2010).

When utilizing mixed sugar substrates, especially combination of hexoses and pentoses, CCR may negatively impact co-fermentation. For example, mixing other sugars alongside D-glucose inhibited validamycin A biosynthesis (Zhou and Zhong, 2015). While various strategies have been explored to counteract CCR effects in co-fermentation processes (Wu et al., 2016; Yao and Shimizu, 2013), specific methodologies for *Streptomyces* remain limited, further research is needed to find solutions for CCR deactivation in *Streptomyces*. The use of alternative sugars instead of glucose may help mitigate CCR (Wu et al., 2016; Yao and Shimizu, 2013). Studies investigating xylose and arabinose mixtures for *Streptomyces* fermentation highlight the potential benefits of diverse sugar utilization (Park et al., 2015; Zhou and Zhong, 2015). In industrial settings, polysaccharides, oligosaccharides, and oils are often employed as alternative carbon sources to bypass CCR (Zhu et al., 2014).

Several metabolic engineering strategies have been implemented to enhance antibiotic

production through carbon source optimization. Overexpression of the maltose ABC transporter gene (*malEFG-a*) in *S. avermitilis* improved avermectin titer approximately threefold (Li et al., 2010). Similarly, amplifying the glycerol consumption gene cluster (*glpK1D1*) significantly enhanced clavulanic acid production in both wild-type and engineered strains of *S. clavuligerus* (Banos et al., 2009). Furthermore, knocking out *nagA* encoding N-acetylglucosamine-6-phosphate deacetylase, led to an increased yield of actinorhodin, a pigmented antibiotic in *S. coelicolor* (Swiatek et al., 2012).

These studies highlight the critical role of metabolic engineering for broadening the substrate spectrum to enhance antibiotic productivity in *Streptomyces*, enabling the degradation and assimilation of diverse carbohydrates. In this context, seaweed-derived carbohydrates present a promising source, aligning sustainable feedstock utilization with enhanced metabolic versatility in *Streptomyces*.

Seaweed represents a promising third-generation biomass source owing to its abundant carbohydrate content (up to 75%) (Milledge et al., 2014), and low lignin content (Offei et al., 2018), which facilitate enzymatic hydrolysis with minimal pretreatment. Unlike terrestrial feedstocks, seaweed can be cultivated without the need for arable land, freshwater, or chemical fertilizers, making it a viable alternative to first- and second-generation biomass sources (Goh and Lee, 2010; Torres et al., 2019). Additionally, seaweeds can be harvested multiple times a year, achieving a 2- to 8-fold higher yield per hectare compared to conventional crops such as corn and soybeans (Forster and Radulovich, 2015). Beyond its industrial applications, seaweed contributes to marine ecosystems by providing habitats for diverse organisms, reducing greenhouse gas emissions, and mitigating ocean acidification and deoxygenation (Kraan, 2010). Due to these advantages, the global seaweed industry has experienced rapid growth, with aquaculture producing 32 million metric tons valued at $12 billion USD in 2017, and market projections exceeding $40 billion USD by 2030 (Poblete-Castro et al., 2020).

Seaweeds are classified as brown, red, and green algae based on their pigment composition,

each characterized by distinct polysaccharide profiles. Brown seaweed predominantly contain laminarin, mannitol, alginate, and fucoidan; red seaweed mainly consist of agarose, starch, carrageenan, and cellulose; and green seaweed contain cellulose, ulvan, starch, and mannan xyloglucan (Offei et al., 2018). The high carbohydrate fraction of seaweed biomass offers great potential for microbial fermentation, primarily for biofuel production, including 2,3 butanediol (Mazumdar et al., 2013) and ethanol (Enquist-Newman et al., 2013; Kim et al., 2011), and lactic acid (Mazumdar et al., 2014) and L-lysine (Hoffmann et al., 2021). However, its application in bioactive natural product biosynthesis in *Streptomyces* remains underexplored. To date, successful heterologous production of bottromycin and pamamycin in *S. lividans* using brown algae hydrolysates has been reported (Seo et al., 2023). Effective utilization of seaweed biomass in *Streptomyces* fermentation requires hydrolysis of complex polysaccharides into fermentable carbohydrates including glucose, arabinose, mannitol, galactose, xylose, and mannose. Three industrially relevant seaweed species (**Figure 2**): *Himanthalia* elongata (brown seaweed), *Ulva lactuca* (green seaweed), and *Palmaria palmata* (red seaweed) were chosen for the following study.

Himanthalia elongata *Ulva lactuca* *Palmaria palmata*

Figure 2: Photos of different fresh seaweeds. Credit for the photo of *H. elongata*: Willem van Kruijsbergen, Saxifraga Foundation, http://www.freenatureimages.eu/; *U. lactuca*: Sytske Dijksen, Saxifraga Foundation, http://www.freenatureimages.eu/; *P. palmata*: Voctir, Wikimedia Commons, CC BY-SA 4.0, https://creativecommons.org/licenses/by-sa/4.0.

Efficient seaweed hydrolysis is essential for obtaining high-yield fermentable sugars, with the primary methods being chemical treatment and enzymatic hydrolysis. Chemical hydrolysis, particularly with sulfuric acid, achieves effective breakdown at high temperatures (El-Tayeb et

al., 2012). However, enzymatic hydrolysis is more efficient and environmentally friendly, offering higher conversion rates and fewer toxic by-products. Cellulase is commonly used for polysaccharide degradation (Carere et al., 2008), while enzyme cocktails with complementary activities enhance saccharification efficiency. Optimizing combined chemical and enzymatic approaches is key to developing sustainable and high-yield hydrolysis strategies.

Despite its potential, several challenges remain in using seaweed hydrolysates as fermentation feedstocks. First of all, not all sugars in seaweed hydrolysates are efficiently metabolized by microbes, requiring strategies to enhance sugar utilization. Additionally, how to efficiently hydrolyze seaweed to obtain fermentable sugars is another major challenge. For example, acid hydrolysis generates inhibitory by-products, which negatively impact microbial growth and productivity. Although activated charcoal is commonly used to remove these inhibitors, it also reduces fermentable sugar content (Hargreaves et al., 2013), leading to decline of fermentable sugars content in the hydrolysates. Furthermore, seasonal and species-dependent variations in carbohydrate composition (Poblete-Castro et al., 2020; Reboleira et al., 2021), necessitate the identification of stable seaweed sources for industrial fermentation.

2.2.2 Improvement of supporting pathways

Secondary metabolites are primarily derived from simple primary metabolites, emphasizing the critical role of precursor and intermediate availability in maximizing natural product biosynthesis. Modulating carbon flux through the central metabolic network by eliminating competing pathways or overexpressing key enzymes can increase precursor availability and enhance metabolite production (Bilyk and Luzhetskyy, 2016; Reeves et al., 2006; Ryu et al., 2006).

Genetic modifications in glycolysis and the pentose phosphate pathway (PPP) have been effectively utilized to optimize antibiotic production, including clavulanic acid, actinorhodin, and undecylprodigiosin. (Olano et al., 2008). In *S. clavuligerus*, inactivation of the glyceraldehyde-3-phosphate dehydrogenases gene expression led to increased glyceraldehyde-3-phosphate (G3P) accumulation, a key precursor for clavulanic acid biosynthesis. Supplementation with L-

arginine, another essential precursor, further boosted production by 3.1-fold (Li and Townsend, 2006).

In *S. lividans*, the PPP was altered by deleting *zwf1* and *zwf2* (glucose-6-phosphate dehydrogenase encoding genes) and *devB* (6-phosphogluconolactonase). These modifications shifted carbon flux from the PPP to glycolysis, increasing acetyl-CoA levels and subsequently enhancing undecylprodigiosin and actinorhodin production (Butler et al., 2002). Similarly, deletion of *meaA*, a gene involved in (2S)-ethylmalonyl-CoA (EMCoA) metabolism, resulted in a four-fold increase in intracellular EMCoA levels in *S. venezuelae*. When tylosin biosynthesis was coexpressed with an extra copy of PikD, a pathway-specific regulator, tylactone production increased 10-fold upon ethylmalonate supplementation (Jung et al., 2014). In a word, enhancing precursor supply through metabolic engineering remains a key strategy for improving secondary metabolite production in *Streptomyces*.

2.2.3 Heterologous expression of BGCs in *Streptomyces*

Heterologous expression is a crucial strategy for secondary metabolite production in *Streptomyces*, particularly when native hosts exhibit slow growth rates, poor genetic tractability, or challenging fermentation control. Given the limited genetic manipulation tools available for *Streptomyces*, heterologous expression provides an effective solution to these challenges. Selecting a suitable heterologous host strain is essential for successful expression of BGCs. Ideal heterologous hosts should: (i) be genetically accessible and easy to manipulate, (ii) efficiently express exogenous BGCs without requiring extensive genetic refactoring, and (iii) provide adequate precursor supply while minimizing competition from native metabolic pathways (Kang and Kim, 2021; Xu et al., 2022).

Given that approximately 70% of natural products discovered originate from the genus *Streptomyces*, several species have been extensively utilized as heterologous hosts for BGC expression, including *S. coelicolor*, *S. lividans*, and *Streptomyces. albus* (Anne et al., 2012; Baltz, 2010; Gomez-Escribano et al., 2014; Ikeda et al., 2014; Myronovskyi and Luzhetskyy, 2019). Among these, *S. coelicolor* has emerged as a versatile expression host attributing to its

well-established synthetic biology tools (Leipoldt et al., 2017; Tong et al., 2015). For example, an engineered mutant *S. coelicolor* M1152 successfully expressed the marine-drived *als* cluster, leading to the produce of the novel aromatic polyketide prealnumycin B (Xu et al., 2023). *S. lividans* has been widely employed due to its genetic tractability, particularly its ability to accept methylated DNA, which facilitates the expression of complex non-ribosomal peptide synthetase (NRPS) and ribosomally synthesized and post-translationally modified peptide (RiPP) BGCs (Myronovskyi and Luzhetskyy, 2019). Numerous peptide-based natural products have been successfully expressed in *S. lividans*, including capreomycin (Felnagle et al., 2007), daptomycin (Penn et al., 2006), pamamycin (Seo et al., 2023), bottromycin (Horbal et al., 2018), viomycin (Barkei et al., 2009).

S. albus, particularly strain J1074, has also become prominent as a heterologous expression host for secondary metabolites. Several biosynthetic pathways have been successfully expressed in this strain, producing compounds such as fredericamycin (Chen et al., 2008), isomigrastatin (Feng et al., 2009), pamamycin (Kuhl et al., 2020), napyradiomycin (Winter et al., 2007), grecocyline (Bilyk et al., 2016), and nybomycin (Rodríguez Estévez et al., 2018).

2.2.4 Regulatory mechanisms of *Streptomyces*

The production of secondary metabolites in *Streptomyces* is regulated by intricate transcriptional networks, which are broadly categorized into pathway-specific and global regulators (Hwang et al., 2014). Pathway-specific regulators typically reside within corresponding BGCs and directly controlling genes responsible for metabolite synthesis. In certain contexts, TetR-family regulators exert inhibitory effects on secondary metabolite production. For instance, in *S. avermitilis*, the TetR regulator AccR represses the biosynthesis of malonyl-CoA and methylmalonyl-CoA, both crucial precursors for avermectin B1a production. The deletion of *accR* increased avermectin production by 14.5% compared to the wild-type, indicating its indirect role in modulating secondary metabolism by controlling acyl-CoA availability (Lyu et al., 2020).

Global regulators, in contrast, are located outside BGCs and influence secondary metabolism

by controlling primary metabolic pathways and morphological differentiation processes. WblA can repress the production of daptomycin in *S. roseosporus* by downregulating regulator genes *atrA*, *dptR2*, *dptR3* and the structural gene *dptE*. Deletion of *wblA* resulted in a 51% higher daptomycin titer while also inhibiting sporulation and long-chain spore formation (Huang et al., 2017). An in-depth understanding of such regulatory networks is critical to strategically refine metabolic engineering methods, ultimately enhancing secondary metabolite production efficiency in *Streptomyces*.

2.3 Nybomycin: a promising reverse antibiotic bioproduction in *Streptomyces*

Antibiotics are indispensable not only for human therapeutic purposes but also have extensive applications in agriculture and livestock production. While advances in industrial antibiotic production have made these compounds more accessible, their excessive and improper use—particularly in livestock farming—has contributed to the rise of antibiotic-resistant bacteria, reducing the clinical efficacy. The emergence and spread of antimicrobial resistance (AMR) are largely driven by overuse, improper dosing, and misuse of antibiotics in both human and agricultural settings (Aslam et al., 2018). This has led to severe global health concerns, with antibiotic-resistant infections causing roughly 25,000 deaths per year in the European Union (EU) alone and approximately 700,000 deaths worldwide (Bennani et al., 2020). Without intervention, projections estimate by 2050, drug-resistant pathogens could result in up to 10 million annual deaths (Bennani et al., 2020).

Historically, the discovery of antibiotics occurred at a rate sufficient to match bacterial resistance development. However, this trend has reversed in recent decades, with resistant pathogens emerging faster than new antibiotics can be developed. This reinforce the urgent need to identify novel antimicrobial compounds while promoting the responsible use of existing antibiotics to mitigate further resistance. Employing “reverse antibiotics” is one of the strategies to against AMR.

2.3.1 Nybomycin natural producers

Nybomycin, a pyridoquinolinedione-based metabolite, was first identified in 1955 from the terrestrial *Streptomyces* sp. A717 (Strelitz et al., 1955). Its chemical structure (**Figure 3**) was fully elucidated, and the total synthesis was achieved 15 years later (Kenneth et al., 1970). Another producer, *Streptomyces hyalinus* NBRC 13850 (Naganawa et al., 1970), was discovered in the rhizosphere in 1970 and found to synthesize both nybomycin and its structural analogue deoxynybomycin. Nybomycin-producing *Streptomyces* strains have since been discovered in diverse ecological niches, including marine sediments (Arai et al., 2015; Rodríguez Estévez et al., 2018) and insect hosts (Zakalyukina et al., 2019), highlighting their environmental adaptability.

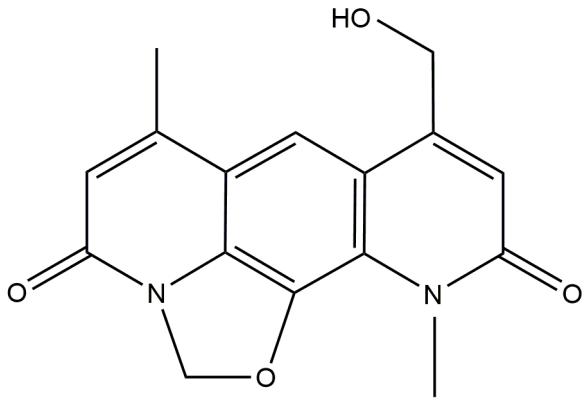

Figure 3: Chemical structure of nybomycin

Nybomycin possesses a distinctive pyridoquinolone scaffold with an angularly fused oxazoline ring, making it a structurally unique secondary metabolite. The oxazoline moiety, an important N-heterocyclic pharmacophore, contributes significantly bioactivity due to its oxygen and nitrogen atoms, which facilitate strong interactions with molecular targets (Liu et al., 2023; Zhang et al., 2018). This pharmacophore is present in various synthetic drugs, including the antitumor agent A-289099 (Li et al., 2002), the antibacterial compound L-161,240 (Onishi et al., 1996), and the commercial pesticide etoxazole (Nauen and Smagghe, 2006). Given its structural uniqueness, nybomycin exhibits different biological activities.

Extensive studies has demonstrated nybomycin's efficacy against Gram-positive bacteria (Hiramatsu et al., 2012; Strelitz et al., 1955). It is also active against *Mycobacterium*

tuberculosis in both proliferative and dormant states in aerobic and hypoxic environments (Arai et al., 2015). Certain nybomycin analogues exhibit cytotoxicity against cancer cells, likely through NAD(P)H quinone oxidoreductase 1 (NQO1)-mediated bioreductive activation, leading to intracellular reactive oxygen species (ROS) generation (Lee et al., 2017; Parkinson et al., 2013; Parkinson and Hergenrother, 2015). Moreover, some derivatives can inhibit cell division cycle 25 (CDC25) phosphatases, which are key enzymes that regulate cell-cycle progression and are commonly overexpressed in many cancer type (Sur and Agrawal, 2016). Nybomycin D shows bioactive to against cancer cell line and gram-positive bacteria (Wang et al., 2019). However, nybomycin and its derivates lack activity against Gram-negative bacteria including *Pseudomonas aeruginosa* and *Acinetobacter baumannii*, and show only modest efficacy on *Escherichia coli* with permeable mutation (Parkinson et al., 2015).

Nybomycin is particularly notable for its role as a “reverse antibiotic”. Fluoroquinolones, including ciprofloxacin and levofloxacin, are extensively employed to treat infections caused by both Gram-positive and Gram-negative bacteria (Andersson and MacGowan, 2003). These antibiotics act by inhibiting DNA gyrase (*gyrA*/*gyrB*) and topoisomerase IV (*parC*/*parE*) (Cozzarelli, 1980; Gellert et al., 1977; Wolfson and Hooper, 1989), which are crucial for DNA supercoiling and chromosome segregation. By interfering with these enzymes, fluoroquinolones induce DNA fragmentation and bacterial cell death (Fukuda et al., 1998; Hooper, 1999; Pommier, 2013). However, the clinical efficacy of fluoroquinolones has been significantly compromised by the emergence of resistant bacterial strains, notably methicillin-resistant *S. aureus* (MRSA). Resistance often arises from mutations within the quinolone-resistance determining region (QRDR) (Redgrave et al., 2014; Yoshida et al., 1990), which disrupts the magnesium bridge essential for quinolone enzyme interaction (Aldred et al., 2013; Redgrave et al., 2014; Sissi et al., 2013). In contrast, nybomycin and deoxynybomycin selectively target fluoroquinolone-resistant bacteria by binding to mutant type II topoisomerases, the mutant *gyrA* by replacing serine-84 with leucine, but have no any effects on intact *gyrA* (Hiramatsu et al., 2012). Additionally, deoxynybomycin has demonstrated efficacy against vancomycin-resistant *Enterococcus* species by inhibiting DNA gyrase *in vitro*

(Parkinson et al., 2015).

Although nybomycin itself can induce resistance, the rate at which resistance develops is considerably lower than for fluoroquinolones (Hiramatsu et al., 2012). Sequencing of nybomycin-resistant bacteria revealed a point mutation at codon 84 (T → C), resulting in a leucine-to-serine reversion, which restores fluoroquinolone susceptibility (Hiramatsu et al., 2012; Hiramatsu et al., 2015). This critical observation led to the innovative concept of "reverse antibiotics", where combining use of nybomycin and fluoroquinolones forces bacteria into an evolutionary loop—continuously cycling between fluoroquinolone-sensitive and nybomycin-sensitive states (**Figure 4**). This strategy presents a novel approach to combating AMR by leveraging bacterial evolutionary constraints, potentially reducing the need for new antibiotics.

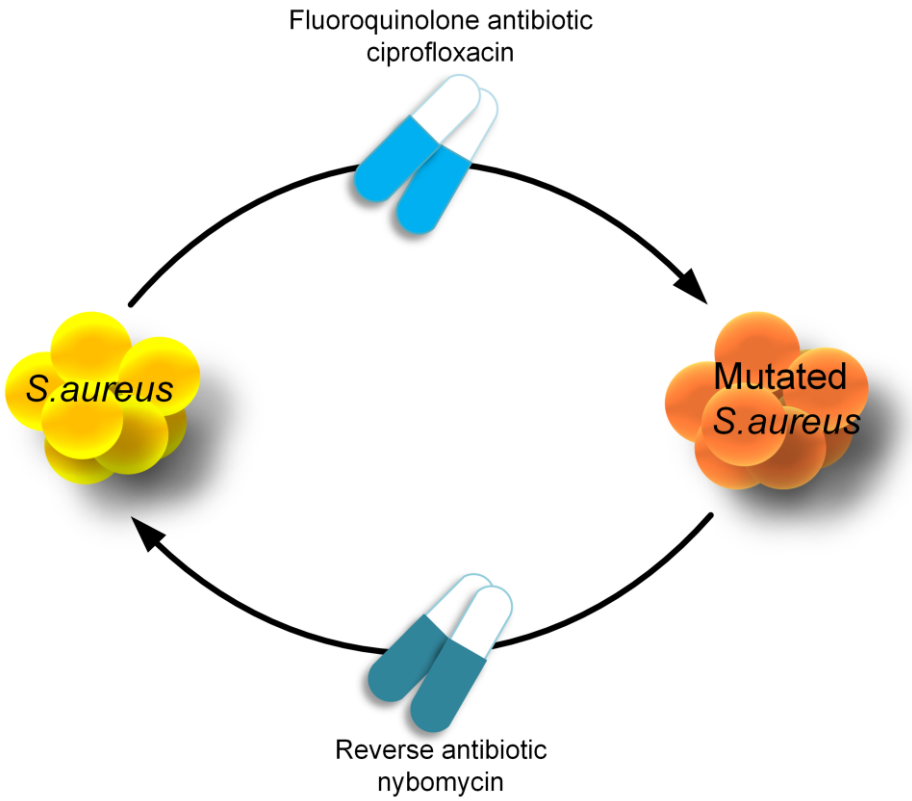

Figure 4: Reverse antibiotics mechanism of nybomycin. Adapted from (Bardell-Cox et al., 2019). The fluoroquinolone antibiotic ciprofloxacin is effective against wild-type *S. aureus* (depicted in yellow). However, mutations by replacing serine-84 with leucine in *gryA* result in a resistant mutant strain (shown in orange), rendering ciprofloxacin ineffective. The reverse antibiotic nybomycin can inhibit mutant *S. aureus* strains, resistance to nybomycin by reversing leucine-to-serine. Therefore, the resistance mechanism against nybomycin restores the wild-

type target conformation, making the bacteria once again susceptible to fluoroquinolones.

2.3.2 Biosynthesis of nybomycin

In bacterial genomes, genes encoding secondary metabolites are commonly organized in BGCs. A BAC 4N24, harboring the nybomycin BGC was firstly isolated from *S. albus* subsp. *chlorinus* NRRL B-24108 (Rodríguez Estévez et al., 2018). This genomic segment spans approximately 36 kb and contains 33 open reading frames (ORFs) (**Figure 5a**). Sequence analysis revealed that nine of these ORFs share significant homology with genes involved in streptonigrin biosynthesis, a structurally related compound.

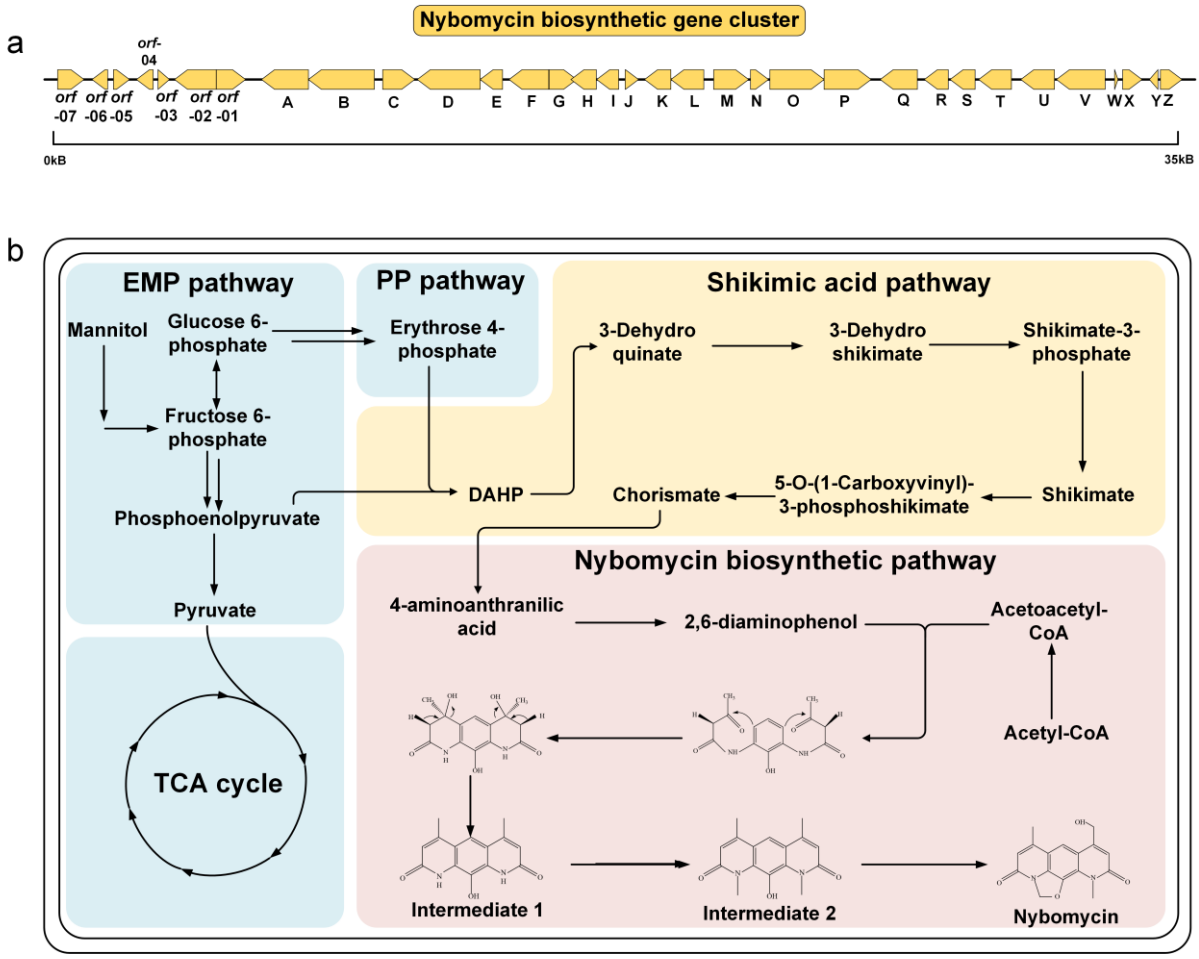

Figure 5: Nybomycin biosynthetic pathway in *Streptomyces*. The overview illustrates the nybomycin gene cluster (a) and biosynthesis pathway (b). The biosynthesis of nybomycin begins with erythrose 4-phosphate (E4P) and phosphoenolpyruvate (PEP), derived from the pentose phosphate (PP) and Embden-Meyerhof-Parnas (EMP) pathways, which are converted

into shikimic acid and chorismic acid. The transformation of chorismic acid into 4-aminoanthranilic acid is catalyzed by NybC, NybD, NybE, and NybL, followed by its conversion into 2,6-diaminophenol, a reaction mediated by NybP. The aromatic core structure is then extended through the incorporation of two acetoacetyl-CoA molecules, sourced from the ethylmalonyl-CoA pathway. This step is followed by the cyclization of the pyridine rings, leading to the formation of intermediate 1, which undergoes methylation of its nitrogen atoms, yielding intermediate 2. The subsequent formation of an oxazoline ring results in deoxynybomycin, which is finally hydroxylated to produce nybomycin. The completed nybomycin molecule is then exported via NybV for secretion (Rodríguez Estévez et al., 2018).

To identify essential genes for nybomycin biosynthesis, 4N24 was compared with truncated variants 4M14 and 6M11, lacking genes downstream of *nybR* and *nybL*, respectively (Rodríguez Estévez et al., 2018). Predicted gene functions are summarized in **Table 2**. LC-MS analysis confirmed that *nybS* to *nybZ* are essential, while further homology analysis with genes in streptonigrin BGC suggested that *nybA* to *nybZ* might form the complete *nyb* BGC. This was refined by single gene deletion in 4N2 (Stegmüller et al., 2024), showing that *orf02* disruption abolished nybomycin production, while *nybA* and *nybC* deletions also blocked synthesis. *nybB* deletion reduced production but did not eliminate it. Inactivating *nybV*, *nybW*, *nybX*, *nybY*, and *nybZ* significantly lowered yields, except *ΔnybW*, which slightly increased production. *ΔnybT* and *ΔnybU* mutants showed weak production, intriguingly, with *ΔnybT* generating a new derivative, possibly nybomycin D.

Table 2: Proposed function of genes in nybomycin biosynthetic gene cluster (Rodríguez Estévez et al., 2018).

Gene	Proposed function
orf-07	Streptomycin 3'-adenylyltransferase
orf-06	Hypothetical protein
orf-05	ATP-binding protein
orf-04	Hypothetical protein

orf-03	Hypothetical protein
orf-02	Hypothetical protein
orf-01	Hypothetical protein
nybA	3-carboxy-cis,cis-muconate cycloisomerase
nybB	FAD-binding protein
nybC	NADPH:quinone reductase
nybD	Anthranilate synthase
nybE	Isochorismatase
nybF	DAHP synthase
nybG	Hypothetical protein
nybH	Vicinal oxygen chelate protein
nybI	NAD(P)H:dehydrogenase
nybJ	Hypothetical protein
nybK	N-acetyltransferase
nybL	Amidohydrolase
nybM	Acetoacetyl-CoA synthase
nybN	Aromatase/cyclase
nybO	Long-chain acyl-CoA synthetase
nybP	Salicylate hydroxylase
nybQ	Hypothetical protein
nybR	NAD-dependent epimerase

nybS	SAM-dependent methyltransferase
nybT	Isopenicillin N synthase family oxygenase
nybU	Isopenicillin N synthase family oxygenase
nybV	MFS transporter
nybW	Transcriptional regulator
nybX	Transcriptional regulator
nybY	Hypothetical protein
nybZ	Transcriptional regulator

Integrating sequence homology insights with BAC-based heterologous expression data, a biosynthetic pathway closely resembling streptonigrin biosynthesis was proposed for nybomycin (**Figure 5b**) (Rodríguez Estévez et al., 2018). It begins with the shikimate pathway, where 3-deoxy-D-arabino-heptulosonate 7-phosphate (DAHP) is synthesized from PEP and E4P, catalyzed by NybF (DAHP synthase). Feeding experiments confirmed that nybomycin's central ring carbons originate from a shikimate-type intermediate (Nadzan and Rinehart, 1976). Since genes responsible for DAHP to chorismate conversion are absent, the host bacterium likely provides these enzymes (Vitayakritsirikul et al., 2015). Chorismate is then converted into 4-aminoanthranilic acid by NybC, NybD, NybE, and NybL, a key precursor in nybomycin biosynthesis.

Subsequently, 4-aminoanthranilic acid undergoes hydroxylation and decarboxylation, yielding 2,6-diaminophenol. Two units of acetoacetate are subsequently attached to this intermediate by NybK (N-acetyltransferase). NybM (acetoacetyl-CoA synthase) generates acetoacetyl-CoA from acetyl-CoA and malonyl-CoA, ensuring sufficient precursor supply. Feeding studies suggest acetate contributes to the pyridone ring carbons (Knoell et al., 1973).

Cyclization of the pyridone rings is catalyzed by NybN (putative cyclase), forming an intermediate. Methylation of the pyridone nitrogen atoms follows, likely mediated by NybS (SAM-dependent methyltransferase). The oxazoline ring, a defining feature of nybomycin, is proposed to be formed by NybT or NybU, both encoding isopenicillin N synthases (IPNS-like enzymes). The final step, hydroxylation, is facilitated by NybB (oxidoreductase), completing the nybomycin structure. After synthesis, nybomycin is exported via NybV (membrane transporter). Additionally, regulatory genes *nybW*, *nybX*, and *nybZ*, encoding putative transcriptional repressors, are supposed to modulate the expression levels of nybomycin biosynthetic genes.

3 Material and Methods

3.1 Strains and plasmids

The strain *S. explomaris*, a recently classified isolate from the coastal rhizosphere soil of *Juniperus excelsa* M. Bieb. (Crimean Peninsula) (LIT). Strains *Streptomyces libani* subsp. *libani* NBRC 13452T (JCM 4322) and *Streptomyces nigrescens* NBRC 12894T (DSM 40276) were obtained from German Collection of Microorganisms and Cell Cultures (DSMZ, Braunschweig, Germany). And the sponge-associated marine strains *Streptomyces* sp. PVA 94-07 and *Streptomyces* sp. GBA 94-10 (Ian et al., 2014), as well as *S. albus* 4N24, which was obtained from previous research (Stegmüller et al., 2024). Additionally, three uncharacterized *Streptomyces* isolates (EXG1, EXG2, EXG3) were taken from our laboratory stocks.

For molecular biology applications, *E. coli* DH10B (Thermo Fisher Scientific, Karlsruhe, Germany) was used for cloning, while *E. coli* ET12567/pUZ8002 served as the donor strain for intergeneric conjugation (Kieser et al., 2000). The BAC 4N24 containing *nyb* BGC was isolated from *S. albus* subsp. *chlorinus* (Rodríguez Estévez et al., 2018). A detailed list of all strains and plasmids used in this study is provided in following section (**Table 3**).

Table 3: Strains and plasmids

Strains/plasmids	Description	Reference
Escherichia coli		
DH10B	F– mcrA Δ(mrr-hsdRMS-mcrBC) φ80lacZΔM15 ΔlacX74 recA1 endA1 araD139 Δ (ara-leu)7697 galU galK λ– rpsL (Str^R) nupG	Thermo Fisher Scientific
ET12567/pUZ8002	Methylation deficient ET12567 containing nontransmissible RP4 derivative plasmid pUZ8002, Cm^R, Kan^R	(Kieser et al., 2000)

Streptomyces		
Streptomyces libani subsp. *libani* NBRC 13452^T	Wild type strain	JCM 4322
Streptomyces nigrescens NBRC 12894^T	Wild type strain	DSM 40276
Streptomyces sp. PVA 94-07	Natural isolate	(Ian et al., 2014)
PVA 94-07 4N24	Heterologous expression of BAC 4N24	This work
Streptomyces sp. GBA 94-10	Natural isolate	(Ian et al., 2014)
GBA 94-10 4N24	Heterologous expression of BAC 4N24	This work
Streptomyces sp. EXG1	Natural isolate	Laboratory stock
EXG1 4N24	Heterologous expression of BAC 4N24	This work
EXG2	Natural isolate	Laboratory stock
EXG2 4N24	Heterologous expression of BAC 4N24	This work
EXG3	Natural isolate	Laboratory stock
EXG3 4N24	Heterologous expression of BAC 4N24	This work
Streptomyces albus 4N24	Heterologous expression of BAC 4N24	(Rodríguez Estévez et al., 2018)
S. explomaris DSM 117375^T	Natural isolate	This work
4N24	Heterologous expression of BAC 4N24	This work
P_{ermEp*}-*araBDAE*	Genome-based integration of *araBDAE* from *Corynebacterium glutamicum*	This work

	31831 under control of *ermEp** promoter into *attB* site of *S. explomaris*	
NYB-1	4N24 with in-frame deletion of *nybWX* in *S. explomaris*	This work
NYB-2	4N24 with in-frame deletion of *nybWXYZ* in *S.explomaris*	This work
NYB-3A	NYB-1 expressing *nybF* (FM076 RS29120) from *S. albus* subsp. *chlorinus* NRRL B- 24108 and *tkt* (B591 RS24355) from *Streptomyces* sp. GBA 94–10 under control of P_{kasOP*}	This work
NYB-3B	NYB-1 expressing *nybF* (FM076 RS29120) and *zwf2* (B591 RS24345) from *Streptomyces* sp. GBA 94–10 under control of P_{kasOP*}	This work
NYB-3C	NYB-1 expressing *tkt* (B591 RS24355) and *zwf2* (B591 RS24345) under control of P_{kasOP*}	This work
NYB-4	NYB-1 expressing *nybF* (FM076_RS29120), *tkt* (B591_RS24355) and *zwf2* (B591_RS24345) under control of P_{kasOP*}	This work
NYB-5A	NYB-2 expressing *nybF* (FM076 RS29120) and *tkt* (B591 RS24355) under control of P_{kasOP*}	This work

NYB-5B	NYB-2 expressing *nybF* (FM076 RS29120) and *zwf2* (B591 RS24345) under control of P_{kasOP*}	This work
NYB-5C	NYB-2 expressing *tkt* (B591 RS24355) and *zwf2* (B591 RS24345) under control of P_{kasOP*}	This work
NYB-6	NYB-2 expressing *nybF* (FM076_RS29120), and *tkt* (B591_RS24355) and *zwf2* (B591_RS24345) under control of P_{kasOP*}	This work
NYB-7A	Integrative expression of *araBDAE*(*Corynebacterium glutamicum 31831*), *xylA*(*Xanthomonas campestris pv. campestris* ATCC 33913), *xylB* (*C. glutamicum* ATCC 13032) and *xylE* (*E. coli* MJ1655) under the control of P_{ermEp*} in *S. albus* 4N24	This work
NYB-7B	NYB-7A expressing *araBDAE* and *xylABE* under the control of P_{kasOP*}	This work
Plasmids/BAC		
4N24	BAC including the nybomycin biosynthetic gene cluster	(Rodríguez Estévez et al., 2018)
pBT1HP	Integrative plasmid containing *oriT*, *attP*, *int phiBT1*, *hph*, P_{ermEp*}, *tfd*	(Stegmüller et al., 2024)
pBT1H	Integrative plasmid containing *oriT*, *attP*, *int phiBT1*, *hph*	(Stegmüller et al., 2024)

pBT1HP- P_{ermEp*}- araBDAE	integrative plasmid containing *araB*, *araD*, *araA*, *araE,* Hyg^R	This work
4N24 *ΔnybWX*	4N24 with in-frame replacement of *nybW* (FM076 RS29200), *nybX* (FM076_RS29205) by Kan^R	This work
4N24 *ΔnybWXYZ*	4N24 with in-frame replacement of *nybW* (FM076 RS29200), *nybX* (FM076_RS29205), *nybY* (FM076_RS29210), and *nybZ* (FM076_RS29215) by Kan^R	This work
pBT1H- P_{kasOP*}- nybF tkt	integrative plasmid containing P_{kasOP*} *nybF*, *tkt*, Hyg^R	This work
pBT1H- P_{kasOP*}- nybF zwf2	integrative plasmid containing P_{kasOP*} *nybF*, *zwf2*, Hyg^R	This work
pBT1H- P_{kasOP*}- tkt zwf2	integrative plasmid containing P_{kasOP*} *tkt*, *zwf2*, Hyg^R	This work
pBT1H- P_{kasOP*}-nybF tkt zwf2	integrative plasmid containing P_{kasOP*} *nybF*, *tkt*, *zwf2*, Hyg^R	This work
pBT1H- P_{ermEp*}- araBDAE xylABE	integrative plasmid containing P_{ermEp*}, *araBDAE*, *xylABE*, Hyg^R	This work
pBT1H- P_{kasOP*}- araBDAE xylABE	integrative plasmid containing P_{kasOP*}, *araBDAE*, *xylABE*, Hyg^R	This work

3.2 Chemicals

API 50 CH and API ZYM stripes were purchased from bioMérieux (Nürnberg, Germany). ISP (Shirling and Gottlieb, 1966) solid media 3 and ISP 7 media were purchased from HiMedia Laboratories (Modautal, Germany). Agar, yeast extract, malt extract, soluble starch, peptone,

proteose peptone were obtained from Difco Laboratories (Detroit, MI, USA). All other chemicals were purchased from Sigma-Aldrich (Steinheim am Albuch, Germany), Fluka (Buchs, Switzerland), Merck (Darmstadt, Germany), or Carl Roth GmbH (Karlsruhe, Germany).

3.3 Genetic engineering

3.3.1 Construction of transformation vectors

Strain design, primer selection, and plasmid construction were performed using SnapGene software (GSL Biotech LLC, San Diego, USA). Gibson assembly was employed to assemble plasmids (Gibson et al., 2009). Specifically, DNA fragments intended for cloning were amplified via PCR using primers containing homologous regions of 20 bp. Amplified products were assessed for correct fragment size by gel electrophoresis and subsequently purified with a commercial DNA clean-up kit (WIZARD SV Gel and PCR Clean-up System, Promega Madison, WI, USA) according to the manufacturer's instruction. The concentrations of obtained purified DNA fragments were measured by a spectrophotometer (NanoDrop1000, Thermo Fisher Scientific, Waltham, MA, USA). Following quantification, DNA fragments were incorporated into a linearized empty vector via Gibson assembly, and the reactions was incubated at 50 °C for 1 h in a thermal cycler (peQSTAR, Peqlab Biotechnology GmbH, Erlangen, Germany). Plasmid DNA was subsequently isolated using the QIAprep Spin MiniPrep Kit (Qiagen, Hilden, Germany). The resulting constructs were verified through PCR screening, restriction digestion analysis, and DNA-sequencing to confirm the accuracy of plasmid assembly.

3.3.2 Transformation of *E. coli* by heat shock

Transforming corrected plasmid into *E. coli* DH 10B was carried out using the heat shock method. A 100 µL aliquot of competent cells was thawed on ice, followed by the addition of 100–500 ng of plasmid DNA. The mixture was incubated on ice for 30 minutes, after which the cells were subjected to heat shock in water bath for 45 seconds at 45 °C. Immediately after, the cells were placed back on ice for 2 minutes before 900 µL of Luria-Bertani (LB) medium was added. For cell recovery, the transformed cells were incubated at 37 °C for 1-2 h in a thermo block (ThermoMixer, Eppendorf, Hamburg, Germany) at 800 rpm. After the

regeneration, cells were collected by centrifugation (6000 x *g*, 3 min). The most supernatant was removed, and the remaining around 100 µL of residual medium was used to resuspend the cell pellet. Followed by spread cells onto the LB agar plate supplemented with 50 µg mL^{-1} hygromycin B for selection and incubated at 37 °C for 24 h. The resulting colonies were screened for successful transformation via PCR analysis, restriction digestion, and sequencing.

3.3.3 Preparation of electrocompetent *E. coli* cells

To prepare electrocompetent *E. coli* ET12567/pUZ8002 cells, a preculture was initiated by inoculating fresh cells into 50 mL of LB medium supplemented with kanamycin (50µg mL^{-1} final concentration) in a 500 mL shake flask without baffles and incubated overnight at 37 °C with shaking at 230 rpm. After overnight cultivation, 1.8 mL pre-culture broth was transferred into 100 mL of fresh LB medium containing kanamycin (50µg mL^{-1}) in in a 500 mL shake flask incubated under the same conditions until optical density (OD) at 600 nm reached 0.4-0.6. once the desired OD was achieved, the cells were harvested by centrifugation (8000 x *g*, 6 min, 4 °C) in precooled 50 mL falcon tubes, washed twice with 40 mL of iced cold deionized water to remove residual medium. Subsequently, two additional washes with 20 mL cold 10% (v/v) glycerol solution were performed to maintain osmotic stability. Finally, resuspend the cells in 1 mL cold 10% (v/v) glycerol solution and aliquot 100 µL per tube, immediately stored at -80 °C until further use.

3.3.4 Transformation of *E. coli* by electroporation

The selected plasmid was subsequently introduced into the methylation-deficient *E. coli* ET12567/pUZ8002 via electroporation. For this, 100 µL of obtained electrocompetent cells as describe above were thawed on the ice, followed by the addition of 0.5-1 µg plasmid DNA. The DNA-cell mixture was transferred into precooled 1 mm electroporation cuvette (Gene Pulser cuvette with 1 mm gap, Bio-Rad, Hercules, CA, USA) followed by incubation on ice for 5 min. Electroporation was performed using a Gene Pulser Xcell (Bio-Rad Laboratories Inc., Hercules, CA, USA) at 2.5 kV, 25 µF and 400 Ω. Immediately after pulsing, 900 µL of LB medium was added to the cuvette, and the suspension was transferred to a 2 mL tube. The transformed

cells were allowed to recover by incubation in a thermo block (ThermoMixer, Eppendorf) at 37 °C for 1-2 h at 800 rpm. After the regeneration, cells were collected by centrifugation (6000 x *g*, 3 min). The most supernatant was discarded and cell pellet was resuspended in residual about 100 µL of medium. Followed by spread cells onto the LB agar plate containing 50 µg mL^{-1} hygromycin B and 50 µg mL^{-1} kanamycin for selection and incubated at 37 °C for 24-48 h. The resulting colonies were screened for successful transformation using PCR verification. The confirmed transformants served as donor strains for intergeneric conjugation, enabling the transfer of the plasmid into *Streptomyces* strains (Kieser et al., 2000).

3.3.5 Conjugation of *S. albus* and *E. coli*

For conjugation in *S. albus*, *E. coli* ET12567/pUZ8002 was cultivated in 10 mL LB medium with appropriate antibiotics until an OD_{600} of 0.4–0.6 was reached. To remove residual antibiotics, the cells were harvested by centrifugation(6000 x *g*, 3 min), washed twice with fresh LB medium, and resuspended in 2 mL LB medium. The suspension was subsequently aliquoted into 0.5 mL fractions for use as donor cells. Meanwhile, *S. albus* spores were collected from MS agar plates after incubation at 30 °C for 4-5 days. The collected spores were resuspended in 5 mL deionized water, and aliquoted into 1 mL portions, and used as the recipient.

The donor and recipient strains were thoroughly mixed, and subsequently spread onto MS agar plates. The plates were incubated at 30 °C for 16 to 18 hours, allowing the conjugation process to occur. Following this initial incubation, 1 mL of sterile water containing 30 µL 200 µg mL^{-1} phosphomycin and 15 µL 50 µg mL^{-1} hygromycin B was evenly distributed over the surface of the agar to select for successful exconjugants and eliminate non-transformed cells. The plates were then incubated for an additional 2 to 3 days at 30 °C to promote the growth of exconjugants.

Emerging exconjugants were transferred to fresh mannitol-soy (MS) flour plates supplemented with the same antibiotics to maintain selective pressure and eliminate non-transformed cells. The accuracy of the exconjugant colonies was confirmed by PCR and subsequent Sanger sequencing. The successful integration of recombinant DNA into the chromosome was

achieved via site-specific recombination, facilitated by the *φBT1* integrase (Kieser et al., 2000).

3.3.6 Conjugation of *S. explomaris* and *E. coli*

The donor strain *E. coli* ET12567/pUZ8002 carrying the selected plasmid was obtained as described above. *S. explomaris* spores were collected from MS agar plates following incubation at 30 °C for 5-7 days, resuspended in 5 mL deionized water and aliquoted in 1 mL portions for use as the recipient. The donor and recipient cells were mixed and spread onto MS agar plates supplemented with 0, 20, 40, 60, and 80 mM $CaCl_2$ and $MgCl_2$. The plates were incubated at 30 °C for 16-18 h to facilitate conjugation. Following this incubation, 1 mL of sterile water containing 30 µL 200 µg mL^{-1} phosphomycin and 15 µL 50 µg mL^{-1} hygromycin B or 50 µg mL^{-1} apramycin was overlaid on the plate. The selection of antibiotics was according to specific vector used. The plates were further incubated at 30 °C for 3-5 days until exconjugant colonies appeared. Emerging exconjugants were subsequently transferred to fresh MS plates containing phosphomycin and hygromycin or apramycin to reinforce selection. The presence of the desired construct was confirmed by PCR and sequencing as described previously.

Deletion of target genes in BAC 4N24 was achieved using the *E. coli* Red/ET recombination system (Horbal et al., 2018). In brief, genes targeted for deletion were replaced by an antibiotic resistance cassette, which was flanked by appropriate homology arms (500 bp) for precise recombination. The obtained colonies were screened for successful gene deletion through PCR and sequencing. The validated BAC construct was subsequently introduced into *S. explomaris* via conjugation.

3.4 Extraction of sugars from seaweed

The extraction of sugars from brown seaweed (*Himanthalia elongata*) was performed as described previously (Hoffmann et al., 2021; Seo et al., 2023). The dried brown seaweed (50 g) (PureRaw, Klötze, Germany) was ground into a fine powder and mixed with 500 mL of deionized water. The mixture was subjected to thermal treatment at 121 °C for 15 minutes to facilitate sugar release. Following heat treatment, enzymatic hydrolysis was performed by

adding a blend of Celluclast 1.5 L and Viscozyme L (Sigma-Aldrich, Steinheim, Germany) at a concentration of 0.01 g per gram of the original dried biomass to maximize sugar yield. The hydrolysis reaction proceeded at 50 °C and pH 5.5 for 48 hours. The resulting hydrolysate was centrifuged at 4500 x *g* for 15 minutes at 4 °C to remove solid debris and clarify the solution. Prior to use in cultivation, the pH of the hydrolysate was adjusted to 7.0 using 6 M NaOH, followed by autoclaving at 121 °C for 15 minutes to ensure sterility. In addition, the same thermal and enzymatic hydrolysis procedure was applied to green seaweed (*Ulva lactuca*) and red seaweed (*Palmaria palmata*) (PureRaw), producing their respective hydrolysates.

3.5 Growth and production media

All media and solutions utilized in this study were prepared using ultrapure water. Sterilization for all media used in this work was conducted either by autoclaving at 121 °C for 20 minutes or by filtration, depending on the specific requirements of each preparation.

E. coli strains were cultivated in LB broth (**Table 4**) (Becton & Dickinson, Heidelberg, Germany). For solid media, LB broth was supplemented with 20 g L^{-1} Difco agar (Becton & Dickinson). For sporulation, *Streptomyces* strains were cultivated on MS agar (**Table 5**) with pH adjusted at 7.0. When required, antibiotics were added at the following concentrations: hygromycin B at 50 µg mL^{-1} for *Streptomyces* and 100 µg mL^{-1} for *E. coli*, kanamycin at 50 µg mL^{-1}, phosphomycin at 200 µg mL^{-1}, and apramycin at 50 µg mL^{-1}.

Table 4: Composition of LB medium

Components	Amount (g L^{-1})
Tryptone	10
Yeast extract	5
NaCl	10

Table 5: Composition of MS medium

Components	Amount (g L^{-1})
Mannitol	20
Soy flour	20
Agar	20

For liquid cultivation of *Streptomyces*, ISP 1 medium (Shirling and Gottlieb, 1966) was used for the initial preculture. The medium was composed of: 5 g L^{-1} tryptone (Becton & Dickinson) and 3 g L^{-1} yeast extract (Becton & Dickinson), with the pH adjusted to 7.0–7.2. The second preculture and main cultivation medium were chemically defined and prepared using two different approaches. In the first setup, the medium was formulated with fresh ultrapure water (**Table 6**), ensuring optimal sterility and consistency for microbial growth.

Table 6: Composition of defined minimal medium for growth of *Streptomyces*

Components	Amount (g L^{-1})
$MgCl_2$ • 6H2O	0.4
$CaCl_2$·• $2H_2O$	0.0265
$(NH_4)_2SO_4$	7
MOPS buffer (pH 7.0)	20
K_2HPO_4	0.5
Vitamin solution(mL)	40

Vitamin solution	Amount (mg L^{-1})

Biotin	10
Thiamine-HCl	4
Inositol	40
Pantothenic acid	8
Pyridoxine-HCl	4

In the second setup, fresh ultrapure water was substituted with artificial seawater, following the composition described by (Fang et al., 2015) (**Table 7**).

Table 7: Composition of artificial seawater

Components	Amount (g L^{-1})
NaCl	27.13
$CaCl_2$	1.17
$MgSO_4$	3.38
$MgCl_2$	2.5
KCl	0.74
$NaHCO_3$	0.21

In both freshwater and artificial seawater setups, the remaining medium composition was unchanged, while different carbohydrates were introduced as sole carbon source to each setup either individually or in combination. For single-sugar experiments, the medium was supplemented with 10 g L^{-1} of one of the following carbohydrates: glucose, xylose, arabinose, mannose, galactose, fucose, rhamnose, and mannitol. For mixed sugars conditions, the medium contained 2 g L^{-1} of each of glucose, xylose, galactose, mannose, mannitol, and

arabinose. These conditions were applied separately to both the fresh water and artificial seawater setups to evaluate the impact of seawater components on metabolism.

For cultivation in seaweed hydrolysates, *Streptomyces* strains were first grown in ISP 1 medium for preculture. The main cultivation medium was composed of 90% (v/v) macroalgae extract combined with 10% (v/v) 2 M MOPS buffer to maintain pH stability.

3.6 Growth and nybomycin production experiments

Liquid cultivations in defined media were conducted in 500 mL baffled shake flasks with a working volume of 10%. To enhance aeration, 30 g of soda-lime glass beads (5 mm, Sigma-Aldrich) were added. Cultures were incubated on an orbital shaker (Multitron, Infors AG, Bottmingen, Switzerland) at 230 rpm, 75% relative humidity, and 28 °C. For standard cultivation, spores from a single colony were inoculated into ISP 1 medium for the first preculture and incubated overnight. Cells were then harvested by centrifugation (5000 x *g*, 5 min, 25 °C) and resuspended in the second defined preculture medium. Following an additional overnight incubation, cells were collected again under the same centrifugation conditions and used to inoculate the main culture in defined medium. For cultivation in seaweed hydrolysate-based media, spores from a single colony were first inoculated into ISP 1 medium and incubated overnight. Cells were then harvested (5000 x *g*, 5 min, 25 °C) and directly transferred into the main cultivation medium containing seaweed hydrolysate. All growth experiments were performed in biological triplicates.

3.7 Taxonomic classification

3.7.1 Cultivation media

All media and solutions utilized in this study were prepared using ultrapure water. For all solid media except ISP 9 medium, 20 g L^{-1} of agar was added; in ISP 9 medium, 15 g L^{-1} of agarose was added for solidification, 10 g L^{-1} of glucose, arabinose, xylose, fructose, rhamnose, sucrose, mannitol, inositol, raffinose, and cellulose were added for carbon source assimilation test, respectively. Sterilization was conducted either by autoclaving at 121 °C for 20 minutes

or by filtration, depending on the specific requirements of each preparation. The compositions of each media are presented in the following list (**Table 8**).

Table 8: Media composition

Medium	Components	Amount (g L^{-1})	pH
ISP 1	Tryptone	5	7.0-7.2
	Yeast extract	3	
ISP 2 / GYM	Yeast extract	4	7.1-7.3
	Malt extract	10	
	Dextrose	4	
ISP 4	Soluble starch	10	7.0-7.4
	K_2HPO_4	1	
	$MgSO_4 \cdot 7H_2O$	1	
	NaCl	1	
	$(NH_4)_2SO_4$	2	
	$CaCO_3$	2	
	*Trace elements solution (mL)	1	
	*Trace elements solution contain:		
	$FeSO_4 \cdot 7H_2O$	0.01	
	$MnCl_2 \cdot 4H_2O$	0.01	
	$ZnSO_4 \cdot 7H_2O$	0.01	
ISP 5	L-Asparagine	1	7.0-7.4

	Glycerol	10	
	K_2HPO_4	1	
	*Trace elements solution (mL)	1	
ISP 6	Peptone	15	7.0-7.2
	Proteose peptone	5	
	Ferric ammonium citrate	0.5	
	K_2HPO_4	1	
	$Na_2S_2O_3$	0.08	
	Yeast extract	1	
ISP 9	$(NH_4)_2SO_4$	2,64	6.8-7.0
	KH_2PO_4	2,38	
	K_2HPO_4	4,31	
	$MgSO_4 \cdot 7H_2O$	1	
	#Trace element solution (mL)	1	
	#Trace element solution contains		
	$CuSO_4 \cdot 5H_2O$	0.064	
	$FeSO_4 \cdot 7H_2O$	0.011	
	$MnCl_2 \cdot 4H_2O$	0.079	
	$ZnSO_4 \cdot 7H_2O$	0.015	
	Carbon source	10	

3.7.2 Genome sequencing

Genomic DNA of isolate Je 1-4^T was extracted using the NucleoSpin Microbial DNA kit (Macherey & Nagel, Düren, Germany). Subsequently, DNA sequencing was subsequently performed using a combined Nanopore and Illumina approach. Libraries were constructed using the TruSeq DNA PCR-free high-throughput library preparation kit (Illumina, San Diego, CA, USA) for short-read sequencing and the SQK-LSK109 kit (Oxford Nanopore Technologies, Oxford, UK) for long-read sequencing, with no prior fragmentation of genomic DNA. Short reads were generated using a 2 × 300-nucleotide run (MiSeq reagent kit v3, 600 cycles, Illumina), while long-read sequencing was carried out on a GridION platform using an R9.4.1 flow cell (Nanopore). Raw sequencing data were processed through base-calling and demultiplexing using the software GUPPY v5.0.16 (Nanopore, 2023) applying the “super-accurate” base-calling algorithm.

Initial assemblies were generated using FLYE v.2.9 software for the Nanopore reads (Kolmogorov et al., 2019) and NEWBLER v2.8 for the Illumina data (Miller et al., 2010). The FLYE-based assembly was further refined through polishing steps employing MEDAKA v1.5.0 (Github) and PILON v1.22 (Bruce J. Walker, 2014), with BOWTIE2 (Langmead and Salzberg, 2012) employed for mapping. Following this, the FLYE and NEWBLER assemblies were integrated using CONSED v28.0 (Gordon et al., 1998). The resulting single contig, representing the linear genome, was checked with BUSCO (Manni et al., 2021) and CHECKM (Parks et al., 2015) for completeness and contamination, showing that the genome is indeed complete (BUSCO: 98.7% complete, 0.8% fragmented, 0.4% missing; CHECKM: 99.1% completeness) and free of contaminations (CHECKM: 0.71% contamination). The final genome was annotated with the PGAP pipeline (Li et al., 2021; Tatusova et al., 2016) and submitted to GenBank (CP106840).

3.7.3 16S rRNA classification

The sequences of the seven 16S rRNA genes (SLV14_001993, SLV14_002131, SLV14_003358, SLV14_004352, SLV14_004947, SLV14_006120, and SLV14_006859) were

extracted from the complete genome sequence and individually compared against the EzBioCloud 16S database (Yoon et al., 2017). From those seven sequences, the 16S rDNA consensus sequence was derived, resulting in two wobble bases at positions 179 ([CT] = Y) and 425 ([AG] = R). The consensus sequence was deposited in GenBank under the accession number OQ740289.

3.7.4 16S rRNA sequence verification

The 16S rDNA sequence was verified by performing a PCR reaction with 30 cycles using Q5 high fidelity DNA polymerase (New England Biolabs) with the 27F (AGRGTTYGATYMTGGCTCAG) and 1492R (RGYTACCTTGTTACGACTT) primers (Weisburg et al., 1991) using mycelial material as template and extending the initial denaturation step to 15 minutes . The obtained product was purified using Ampure XP beads, sequenced on an ABI 3730xl DNA Analyzer (Applied Biosystems) and compared to consensus sequence using SnapGene v5.0.8 (Dotmatics).

3.7.5 Genome-based phylogeny

ANI values were calculated using OrthoANIu (Yoon et al., 2017). The genome sequence data were uploaded to the TYGS (https://tygs.dsmz.de) for taxonomic classification based on genome comparisons, which includes recent methodological updates and additional analytical features (Meier-Kolthoff and Goker, 2019). TYGS provided detailed taxonomic data, including nomenclature, synonyms, and related literature through its partner resource, the List of Prokaryotic names with Standing in Nomenclature (LPSN, https://lpsn.dsmz.de) (Meier-Kolthoff and Goker, 2019). Results from the TYGS analysis were provided on 2024-07-22.

The TYGS analysis involved several steps. The closest type-strain genomes were determined through two complementary strategies. Firstly, submitted genomes underwent comparison against all type strain genomes present in the TYGS database via the MASH algorithm, determining the ten nearest type strains per user-submitted genome based on minimal MASH distances (Ondov et al., 2016). Secondly, ten additional closely related type strains were determined through 16S rDNA gene analysis. For this purpose, 16S rDNA sequences were

extracted from user genomes with RNAmmer (Lagesen et al., 2007), and subsequently compared via BLAST searches (Camacho et al., 2009) against a comprehensive database containing 16S rDNA gene sequences from 21,376 type strains. From these comparisons, the top 50 matches, ranked by BLAST bit scores, were further refined through precise genome distance calculations employing the Genome BLAST Distance Phylogeny (GBDP) method, using the “coverage” algorithm and d5 distance formula (Meier-Kolthoff et al., 2013). Ultimately, the ten most closely related type strain genomes for each user-submitted genome were identified from these precise distance calculations.

Phylogenomic inference involved pairwise genome comparisons using GBDP, where accurate genomic distances were computed employing the 'trimming' algorithm and distance formula d5, each performed with 100 replicates (Meier-Kolthoff et al., 2013). The dDDH values, including confidence intervals, were estimated using the Genome-to-Genome Distance Calculator (GGDC, version 4.0) with default parameters (Meier-Kolthoff et al., 2013). The resulting genomic distances were subsequently utilized to construct a balanced minimum evolution phylogenomic tree, implementing the FASTME software (version 2.1.6.1) with subtree pruning and regrafting (SPR) post-processing (Lefort et al., 2015). Support for tree branches was evaluated using 100 pseudo-bootstrap replicates. The resulting phylogenetic trees were midpoint-rooted (Farris, 1972) and visualized using the PhyD3 tool (Kreft et al., 2017).

Species-level clustering was performed based on a 70% dDDH threshold centered around each type strain, while subspecies-level clustering applied a more stringent 79% dDDH threshold (Meier-Kolthoff and Goker, 2019; Meier-Kolthoff et al., 2014). For MLST-based phylogenetic analyses, MEGA 11 was employed (Tamura et al., 2021). This software facilitated alignment using CLUSTAL, focusing on the *atpD, gyrB, recA, rpoB,* and *trpB* genes listed for *Streptomyces* spp. in PUBMLST (Jolley et al., 2018). Additionally, MEGA 11 was used to construct the corresponding phylogenetic trees. The methods employed for this analysis included Minimum-Evolution (ME), Maximum Likelihood (ML), Maximum Parsimony (MP), and

Neighbor-Joining (NJ). The MEGA ANALYSIS OPTION (MAO) parameters used for CLUSTAL alignment and tree generation are listed in the **Appendix Table A2-A6** .

3.7.6 In silico prediction of secondary metabolite clusters

Secondary metabolite biosynthesis clusters were predicted using the ANTISMASH web service (Blin et al., 2023), version 8.dev-0de8f3d7, with the annotated GenBank file as input.

3.7.7 Colony morphology analysis

Morphological observations of substrate and aerial mycelium were conducted after a 14-day incubation at 30°C on ISP solid media 1-7 (Shirling and Gottlieb, 1966). The colors of the mycelium and diffusible pigments were assessed using RAL-code color chips (Ivana Charousová, 2015).

3.7.8 Scanning electron microscopy analysis

Morphological characteristics of spore chains and surface ornamentation were visualized by scanning electron microscopy using cultures sporulated on ISP 3 agar medium after incubation for 28 days at 30°C. Sample preparation was adapted from previous work (Murtey and Ramasamy, 2021). For this purpose, a section (0.5 cm^2) of agar with bacterial lawn was cut off, fixed with 5% glutaraldehyde for 2 hours at 4 °C, twice resuspended in 0.1 M phosphate buffer (pH 7.2), thoroughly mixed for 10 min, and collected by centrifugation (5 min, 5000x *g*, RT). The sample was dehydrated using a series of ethanol solutions with increasing concentration (35%, 50%, 75%, 95%, 100%), washed three times with pure ethanol, freeze dried, sputtered with gold, and subsequently examined (Zeiss Sigma VP FEG-SEM).

3.7.9 Biochemical characterization

API 50 CH test

The capacity of *Streptomyces* to metabolize various carbon sources was evaluated using the API 50 CH system. All *Streptomyces* strains were cultured in 50 mL ISP 1 liquid medium and incubated in an orbital shaker (Multitron, Infors AG, Bottmingen, Switzerland) at 230 rpm, 75% relative humidity, and 28 °C for 1 day. Following incubation, the cell pellet were collected and

resuspended in API 50 CH medium until the turbidity matched 2 McFarland standard.

The prepared 100 µL of the spore suspension was then inoculated into the API 50 CH strips, followed by incubation for seven days at 30°C. After incubation, color changes in the medium were observed, with a positive reaction defined by a transition from red to yellow, indicating acid production due to metabolic utilization of the respective carbon sources.

API ZYM test

The assessment of enzyme activities of *Streptomyces* was conducted by API ZYM test kit. Following manufacturer's instruction, the results was recorded, a numerical scale from 0 to 5 was used to assess the reaction intensity, corresponding to the color changes observed.

Carbohydrate assimilation test

Carbohydrate assimilation was studied on ISP 9 agar supplemented with 1% of glucose, xylose, fructose, cellulose, mannitol, inositol, sucrose, arabinose, rhamnose, or raffinose (Shirling and Gottlieb, 1966). The cultivation was at 30°C for 7 days.

Antibiotic susceptibility test

Sensitivity to antimicrobial was investigated using disc-diffusion plate tests, with strains incubated for 7 days at 30°C on ISP 2 agar (Bauer et al., 1966). The following antibiotics were evaluated: ampicillin (10 µg/disc), erythromycin (15 µg/disc), gentamicin (30 µg/disc), tetracycline (30 µg/disc), vancomycin (30 µg/disc), cefotaxime (30 µg/disc), rifampicin (5 µg/disc), and penicillin G (6 µg/disc) (Risdian et al., 2021).

3.7.10 Physiological studies

Effect of temperatures

The *Streptomyces* strains were inoculated into shake flasks containing ISP 2 medium and incubated at 25, 28, 30, 37, and 45 °C for 7 days. After inoculation, the growth was recorded.

Effect of pH

The miniaturized incubator (Biolector, Beckmann Coulter, Baesweiler, Germany) with a 48-well microtiter plate was used for testing pH effects on growth. The pH of liquid ISP 2 medium was adjusted to different pH values (3.0, 4.0, 5.0, 6.0, 7.0, 8.0, 9.0, 10.0) and cultivations were carried out at 28 °C for 7 days, with growth monitored online (Pauli et al., 2023).

Effect of NaCl

The miniaturized incubator with a 48-well microtiter plate was used for testing tolerance to NaCl. The ISP 2 medium was adjusted to various NaCl concentrations (0, 2.5, 5.0, 7.5, 10.0%) and cultivations were carried out at 28 °C for 7 days, with growth monitored online (Pauli et al., 2023).

3.7.11 Chemotaxonomical analysis

For chemotaxonomic analyses, cell biomass was prepared from liquid ISP 2 medium cultures incubated at 28°C and agitated at 230 rpm for 48 hours. Cellular fatty acids, respiratory quinones, polar lipids, mycolic acids, whole-cell sugar profiles, and the stereochemistry of diaminopimelic acid were analyzed by the commercial analytical service provided by DSMZ, Leibniz-Institut DSMZ – Deutsche Sammlung von Mikroorganismen und Zellkulturen GmbH, Braunschweig, Germany.

3.8 Bioanalytical methods

3.8.1 Quantification of cell concentration

For OD measurements, 1 mL of culture broth was withdrawn and transferred to pre-weighed 1.5 mL centrifugation tube. The precise mass of sample was determined by an analytical balance (Quintix 224-1S, Sartorius, Göttingen, Germany). Cell densities were then measured by spectrophotometry at a wavelength of 600 nm using a UV-1600PC spectrophotometer (Radnor, PA, USA), with deionized water serving as the blank control.

Additionally, the dry cell weight (CDW) of *S. explomaris* was determined gravimetrically. For this, 10 mL of culture broth was transferred to sample tube, the precise amount of sample was

determined by measuring sample tube with and without sample on analytical balance. The cells were harvested by centrifugation (10,000 x *g*, 4 °C, 10 min), washed with 15 mL of 0.9 % (w/v) NaCl solution twice. Following washing, the pellet was freeze-dried using a lyophilizer (Alpha 3-4 LSCbasic, Christ, Osterode am Harz, Germany), and the final dry weight was determined by reweighing the sample tube (Kuhl et al., 2020). Therefore, this systematic measurements established a linear correlation (**Figure 6**) between OD_{600} and CDW for *S. explomaris*, which is described by the equation: CDW (g L^{-1}) = 0.56 × OD_{600}.

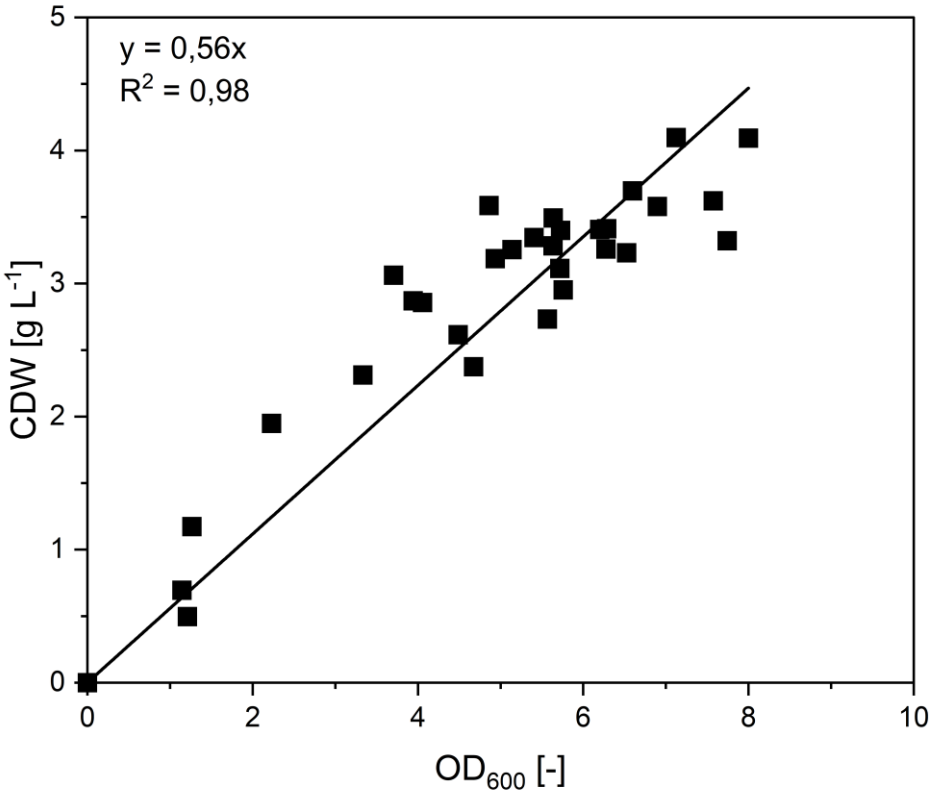

Figure 6: Correlation of optical density (OD_{600}) and cell dry weight (CDW) from batch cultures of *S. explomaris* 4N24 on minimal mannitol medium. Samples were taken from the entire culture process. n=3.

3.8.2 Quantification of sugar and sugar alcohol

Sugars and mannitol were quantified using high-performance liquid chromatography (HPLC) (1260 Infinity Series, Agilent, Darmstadt, Germany) equipped with a Nucleogel Sugar Pb

column (10 µm, 300 x 7.8 mm, Macherey-Nagel, Düren, Germany) and a Nucleodur C18 Isis guard column (3 µm, 100 x 3 mm, Macherey-Nagel). For separation, demineralized water was used as the mobile phase at a flow rate of 0.4 mL min^{-1} with the column temperature at 80 °C. Detection was performed using a refractive index detector. The injection volume of sample was based on type of water contained in the sample, injection volume was 5 µL under fresh water condition and 0.5 µL for the cultivation with artificial sea water. And quantification was achieved using external calibration standards.

3.8.3 Qualitative and quantification of sugars from seaweed

The identification of carbohydrates present in brown, green, and red seaweed extracts was performed using gas chromatography-mass spectrometry (GC-MS) (GC 7890A, 5975C quadrupole detector, Agilent Technologies). For analysis, 100 µL hydrolysates of each macroalgae were transferred into GC-MS vial and dried the sample under the N_2 stream. The dried sample was then subjected to methoximation by adding 50 µL pyridine (2% Methoxylamine), followed by incubated at 80°C for 25 min. Subsequently, derivatizatio was conducted by adding 50 µL *N*-methyl-*N*-trimethylsilyl-trifluoroacetamide (MSTFA; Macherey-Nagel, Düren, Germany) and incubating the mixture at 80°C for 30 min. The sample was then centrifuged (17,000 x g, 5 min), and the resulting supernatant was transferred to a fresh GC-MS vial for analysis. Carbohydrate identification was performed in scan mode, using pure standards as references (Kiefer et al., 2004; Wittmann et al., 2002).

Once the carbohydrate composition was determined for each type of seaweed, the quantification of sugars and sugar alcohols was conducted using HPLC. The seaweed extracts were analyzed directly using the method described in Section 3.8.2, with the injection volume adjusted to 2 µL. Quantification was carried out using external calibration standards to ensure accuracy.

3.8.4 Extraction and quantification of nybomycin

Nybomycin was extracted from the culture broth using 1-butanol. A 200 µL aliquot of culture broth was mixed with 600 µL of 1-butanol and incubated at 22 °C with shaking at 1500 rpm for

15 minutes using a Thermomixer F1.5 (Eppendorf, Wesseling, Germany). The organic phase was then separated by centrifugation (17,000 x *g*, 5 min, 4 °C) and collected. A second extraction step was performed by adding 450 µL of 1-butanol to the remaining aqueous phase, followed by centrifugation under the same conditions. The combined organic fractions were collected, and the solvent was removed by freeze-drying. The resulting solid was dissolved in a methanol-DMSO mixture (1:1, v/v) and clarified by centrifugation (17,000 x *g*, 5 min, 4 °C) to remove any residual debris.

Quantification of nybomycin was carried out using liquid chromatography-electrospray ionization tandem mass spectrometry (LC–ESI–MS/MS), employing a HPLC system (Agilent Infinity 1290 System, Santa Clara, CA, USA) coupled to a triple quadrupole mass spectrometer (QTRAP 6500+, AB Sciex, Darmstadt, Germany) as described in (Stegmüller et al., 2024). Briefly, Chromatographic separation was performed on a C18 reversed-phase column (Vision HT C18 HighLoad, 100 mm × 2 mm, 1.5 µm, Dr. Maisch, Ammerbuch-Entringen, Germany) maintained at 45 °C. A linear gradient elution was applied, with eluent B (0.1% formic acid in acetonitrile), increasing from 10% to 90% over 7 minutes, against eluent A (0.1% formic acid in water). The flow rate was maintained at 0.5 mL min^{-1}. Detection was performed in positive ion mode, employing selected ion monitoring (SIM) of the $[M + H]^+$ adduct at m/z 299.1 (Rodríguez Estévez et al., 2018). Quantification was carried out using external calibration standards obtained from Cayman Chemical (Ann Arbor, USA).

3.9 System biology analysis

RNA extraction and sequencing were followed previously established protocols (Stegmüller et al., 2024). Briefly, cells (1 mL culture broth) were harvested by centrifugation (16,000 x *g*, 4 °C, 1 min) and immediately flash-frozen in liquid nitrogen. RNA was isolated using the Qiagen RNA Mini Kit (Qiagen, Hilden, Germany), following the manufacturer's instructions. Residual DNA was removed with 10 U RNase-free DNase I (Thermo Scientific) for 1 hour, supplemented with RiboLock RNase inhibitor (Thermo Scientific). The RNA underwent additional purification with the same kit. RNA quality was assessed using the Trinean Xpose (Trinean NV, Gentbrugge,

Belgium) and Agilent RNA 6000 Nano Kit on an Agilent 2100 Bioanalyzer (Agilent Technologies, B¨oblingen , Germany). Ribosomal RNA was depleted using the Ribo-Zero rRNA Removal Kit (Illumina, San Diego, CA, USA), and depletion was confirmed with the Agilent RNA 6000 Pico Kit on an Agilent 2100 Bioanalyzer (Agilent Technologies). cDNA libraries were prepared using the TruSeq Stranded mRNA Library Prep Kit (Illumina) and sequenced on an Illumina HiSeq 1500 platform (2 × 75 bp paired-end reads). Reads were aligned to the S. explomaris 4N24 genome (CP110836.1) using Bowtie2 (Langmead and Salzberg, 2012), with an adjusted maximum read pairing distance of 600 bases. ReadXplorer 2.2.3 (Hilker et al., 2014) was used for read visualization and count calculations. Differential gene expression (DGE) was analyzed with DESeq2 (Love et al., 2014). The raw sequencing reads and processed datasets (input matrix and normalized read counts) are publicly available on GEO (GSE291039). For statistical analysis, Student's t-test was applied, selecting genes with $\log_2$ FC ≥ 1 and $p \leq 0.05$. Hierarchical clustering was performed using the gplots package in R (RCoreTeam, 2020; Warnes et al., 2020). All RNA extractions and sequencing were performed in biological triplicates.

4 Results and Discussion

4.1 Taxonomical and biochemical investigation of the promising isolate *S. explomaris*

As an important producers of secondary metabolites, *Streptomyces* contributing nearly half of all known microbial natural products (Bilyk and Luzhetskyy, 2016) . Therefore, as a superstar producer of bioactive substances, isolate new species of *Streptomyces* has attracted much attention (Goodfellow et al., 2017). Marine ecosystems have emerged as promising habitats for *Streptomyces* (Yang et al., 2019), offering unique environmental conditions, such as high salinity, oligotrophy, high hydrostatic pressure, and extreme temperature (Genilloud, 2017). These factors drive distinct physiological adaptations and the production of structurally diverse bioactive metabolites, highlighting the potential of marine-derived *Streptomyces* for novel drug discovery (Barakat and Beltagy, 2015; Lee et al., 2014; Li et al., 2011). Recent examples of *Streptomyces* isolated from marine ecosystems include *Streptomyces bathyalis* (Risdian et al., 2021), *Streptomyces lydicamycinicus* (Komaki et al., 2020), *S. fradiae* MM456M-mF7 (Takehana et al., 2017), *Streptomyces oceani* (Tian et al., 2012), and *Streptomyces bohaiensis* (Pan et al., 2015).

In the present study, strain Je 1-4^T was isolated from the coastal rhizosphere soil of *Juniperus excelsa* M. Bieb. on the Crimean Peninsula. 16S rRNA gene sequence similarity studies revealed that Je 1-4^T is phylogenetically close to *S. libani* subsp. *libani* NBRC 13452^T (JCM 4322) and *S. nigrescens* NBRC 12894^T (DSM 40276). Based on a detailed investigation of its taxonomic status, strain Je 1-4^T represents a novel species of *Streptomyces*, for which the name *Streptomyces explomaris* sp. nov. is proposed.

4.1.1 Genome sequencing and genome-based phylogeny

The genome of strain Je 1-4 ^{T} was assembled into a single contig, representing a linear chromosome. To assess its phylogenetic relationships, the seven 16S rRNA gene sequences were individually analyzed using the EzBioCloud 16S database (Yoon et al., 2017). The highest similarity scores were observed with *S. nigrescens* NBRC 12894^T (99.86%-99.93%) and *S.*

libani subsp. *libani* NBRC 13452^T (99.86%-99.93%), followed by *Streptomyces angustmyceticus* NRRL B 2347^T (99.79%-99.93%), *Streptomyces tubercidicus* DSM 40261^T (99.79%-99.86%), and *S. lydicamycinicus* NBRC 110027^T (99.72%-99.86%). However, since 16S rRNA gene similarity alone does not provide sufficient taxonomic resolution, a whole-genome-based phylogenetic analysis was conducted using the TYGS (Meier-Kolthoff and Goker, 2019). Since the genome and plasmid sequences of *S. nigrescens* NBRC 12894^T were not available in the TYGS database, they were sequenced using a previously established sequencing workflow and subsequently deposited in GenBank (CP114203, CP114204).

The results of dDDH confirmed that strain Je 1-4 ^{T} is related to *S. libani* subsp. *libani* and *S. nigrescens*, yet remains genetically distinct, with dDDH values of 66.6% and 66.7%, respectively, both below the 70% threshold for species delineation (**Table 9, Figure 7**). Notably, the dDDH analysis indicated a close relationship between *S. libani* subsp. *libani* JCM 4322^T and *S. nigrescens* DSM 40276^T, with a dDDH value of 92.0%, suggesting they likely represent the same species.

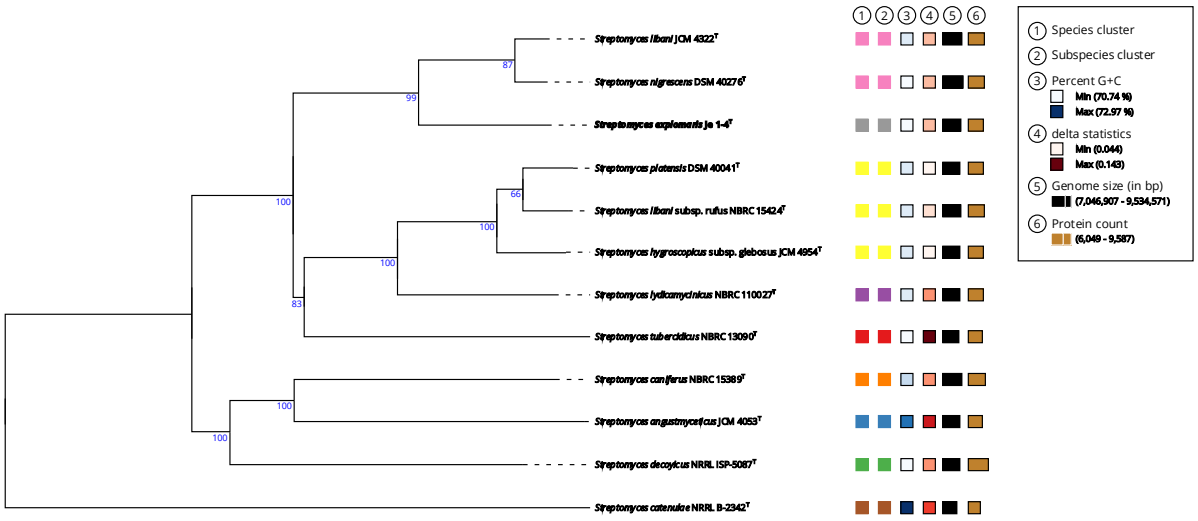

Figure 7: Phylogenetic tree inferred with FastME 2.1.6.1 from GBDP distances calculated from genome sequences. Branch lengths are proportional to distances calculated with the GBDP d5 formula. GBDP pseudo-bootstrap values exceeding 60%, derived from 100 replicates, are indicated above branches, with the average bootstrap support reaching 87.5%. The tree was midpoint-rooted.

Table 9: Pairwise comparison of the genome of strain Je 1-4^T against similar type-strain

genomes. The dDDH values are provided along with their confidence intervals (C.I.).

Strains	dDDH (%)	C.I.	ANI (%)
Streptomyces libani JCM 4322	66.6	75.6-83.0	95.9
Streptomyces nigrescens DSM 40276	66.7	71.6-79.2	95.9
Streptomyces platensis DSM 40041	45.8	59.7-67.1	91.8
Streptomyces libani subsp. *rufus* NBRC 15424	45.9	59.0-66.3	91.9
Streptomyces hygroscopicus subsp. *glebosus* JCM 4954	45.7	59.1-66.5	91.7
Streptomyces lydicamycinicus NBRC 110027	46.8	63.2-70.7	92.1
Streptomyces tubercidicus NBRC 13090	44.2	52.3-59.3	91.3
Streptomyces caniferus NBRC 15389	37.4	44.9-51.8	88.8
Streptomyces angustmyceticus JCM 4053	36.0	46.0-52.9	88.4
Streptomyces decoyicus NRRL ISP-5087	39.4	43.4-50.2	89.6
Streptomyces catenulae NRRL B-2342	25.6	23.2-30.2	82.0

Exception for constructing a Minimum-Evolution tree based on dDDH distances, we calculated four additional phylogenetic trees were generated from a multiple sequence alignment of the *atpD, gyrB, recA*, *rpoB*, and *trpB* genes using the CLUSTAL algorithm. The resulting phylogenies were built employing ME, ML, MP, and NJ. Although the MLST analysis utilized a smaller dataset (~2580 bp) compared to the genome-scale dDDH analysis, all phylogenetic trees revealed highly consistent evolutionary relationships (**Figure 7, Appendix Figure A1**). The only notable inconsistency concerned *S. decoyicus* NRRL ISP-5087^T, which aligned with *S. caniferus* NBRC 15389^T and *S. angustmyceticus* JCM 4053^T in the dDDH-based tree, whereas in the MLST derived phylogenies it grouped with *Streptomyces* sp. Je 1-4^T, *S. libani* JCM 4322^T, and *S. nigrescens* DSM 40276^T.

The genome features of strain Je 1-4^T align closely with those typically reported for members of the genus *Streptomyces*. Its linear chromosome spans approximately 8.9 Mbp, exhibiting a G+C content of 70.9%. No plasmids were identified within the genome. Relatively short inverted terminal repeats, each approximately 36.4 kb, were located at the chromosome ends. Genome annotation predicted 7,707 genes, including 7,377 functional protein-coding genes

and 239 pseudogenes. In addition, the genome contains 91 RNA genes: 67 encoding tRNAs, 21 rRNAs arranged in seven operons, and three non-coding RNAs.

Further genomic analysis with ANTISMASH (Blin et al., 2023) identified 35 biosynthetic gene clusters involved in secondary metabolites formation(**Appendix, Figure A2**). These BGCs consisted of 8 terpenes, 3 non-ribosomal peptides, 3 polyketides, 2 hybrid clusters combining non-ribosomal peptide polyketides, and 8 ribosomally synthesized and post-translationally modified peptides (RiPPs). Among these identified clusters, 8 showed 100% similarity to known BGCs for the biosynthesis of antipain, lydicamycin, pseudouridinomycin, ulleungdin, spore pigment, the siderophore desferrioxamine B, the morphogen SapB, and the compatible solute ectoine. Besides, two clusterss exhibited over 50% similarity to gene clusters involved in hopene and caniferolide biosynthesis. Remarkably, more than half of the identified BGCs lack functional characterization, underlining the considerable metabolic versatility and biosynthetic potential of *S. explomaris*.

4.1.2 Growth properties and utilization of carbon sources

All three strains exhibited well growth on ISP 2, ISP 3, ISP 4, ISP 5, and ISP 7 media. On ISP 6 medium, Je 1-4^T displayed limited growth, whereas the other two strains showed no growth. Je 1-4^T formed substrate mycelium on all tested media and aerial mycelium on all media except ISP 6. There is no diffusible pigments detected on all of examined medium. An overview of the morphological characteristics is presented in **Table 10**.

Table 10: Phenotypic strain characteristics. Strains 1: Je 1-4^T; 2: *S. libani* subsp. *libani* NBRC 13452T; 3: *S. nigrescens* NBRC 12894^T. All strains are positive for glucose, mannitol, fructose, xylose, sucrose, inositol, and raffinose, and negative for cellulose, arabinose, and rhamnose. The capability to utilize other carbon sources differs between the strains, indicated as + (positive) and – (negative). Abbreviations: DPG: diphosphatidylglycerol; PE: phosphatidylethanolamine; PG: phosphatidylglycerol; PI: phosphatidylinositol; AGL: aminoglycolipid; APL: aminophospholipid; AL: aminolipid; GL: glycolipid; PL: phospholipid.

Characteristic	Strain 1	Strain 2	Strain 3

Cultivation			
ISP 2 agar			
Growth	Good	Good	Good
Color of colony	Cement grey	Cement grey	Silver grey
ISP 3 agar			
Growth	Good	Good	Good
Color of colony	Moss grey	Silver grey	Silver grey
ISP 4 agar			
Growth	Good	Good	Good
Color of colony	Black grey	Green grey	Green grey
ISP 5 agar			
Growth	Good	Good	Good
Color of colony	Cement grey	Telegrey	Traffic grey
ISP 6 agar			
Growth	Sparse	None	None
Color of colony	Beige		
ISP 7 agar			
Growth	Good	Good	Good
Color of colony	Beige	Traffic white	Green grey
Carbon source utilization			

N-Acetylglucosamine	+	+	-
D-cellobiose	+	-	-
L-fucose	+	+	-
Gentiobiose	+	+	-
Optimum growth (℃)	25-30	25-37	25-37
Optimum growth (pH)	6.0-8.0	6.0-8.0	6.0-8.0
Optimum growth (% NaCl)	0-2.5	0-5.0	0-7.5
Menaquinones			
MK-9(H_4)	+	+	+
MK-9(H_6)	+	+	+
MK-9(H_8)	+	+	+
Fatty acid content (%)			
iso-$C_{14:0}$	2.3	3.3	4.3
iso-$C_{15:0}$	7.0	7.4	6.5
anteiso-$C_{15:0}$	14.3	13.2	11.6
$C_{15:0}$	1.2	-	-
anteiso-$C_{15:0}$ 2OH	1.4	1.1	-
iso-$C_{16:1}$ H	2.3	3.1	3.3
iso-$C_{16:0}$	24.1	28.3	35.4
$C_{16:1}$ ω/7c	4.0	3.8	3.4

$C_{16:0}$	5.8	5.2	6.0
iso-$C_{17:1}$ ω/7c	4.5	4.2	3.1
anteiso-$C_{17:1}$ ω/7c	4.2	3.6	2.8
iso-$C_{17:0}$	5.7	5.3	4.4
anteiso-$C_{17:0}$	15.6	12.5	10.3
$C_{17:0}$ cyclo ω/7c	1.3	1.3	1.3
iso-$C_{18:1}$ H	1.0	1.1	1.1
Polar lipids	DPG, PE, PG, PI, 2APLs, 2PLs, GL	DPG, PE, PG, PI, 2APLs, PL, GL	DPG, PE, PG, PI, 3APLs, PL, GL

Strain Je 1-4^T formed straight to flexuous spore chains, some of which exhibited partial spirals when cultivated on solid media (**Figure 8**). These spores had smooth surfaces, with oval to cylindrical shapes, and formed elongated chains typically including about 10 to over 25 spores (Saurav and Kannabiran, 2010). The mature spores were approximately 0.5-1.0 mm in diameter, with lengths ranging from 0.8 to 1.0 mm.

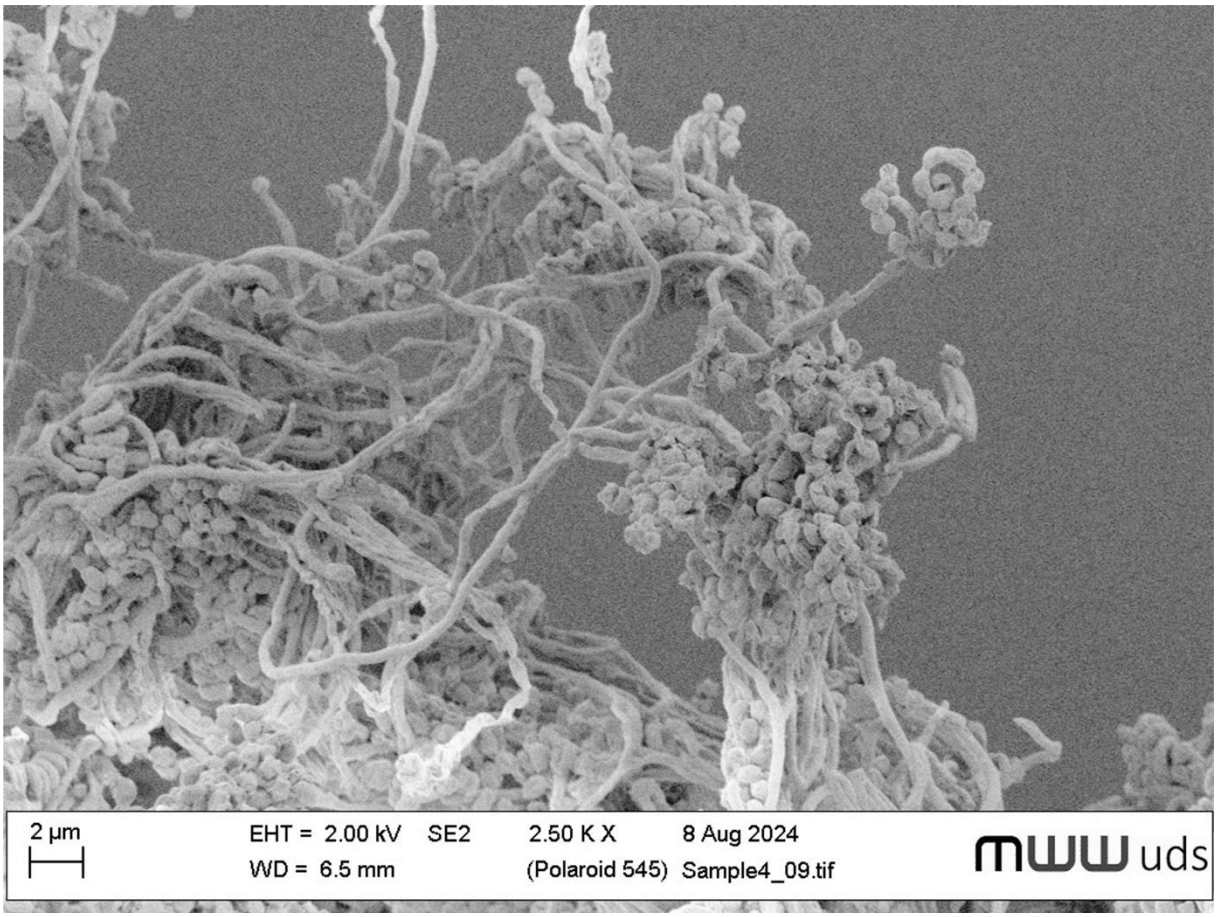

Figure 8: Scanning electron micrograph of strain Je 1-4^T. Prior to analysis, the strain was incubated on ISP 3 agar for 28 days at 30 °C.

The temperature range for growth of Je 1-4^T is 25 to 45°C, with optimal temperature at 25-30°C, while *S. libani* subsp. *libani* and *S. nigrescens* optimally grew between 25 and 37°C. Additionally, Je 1-4^T tolerated pH levels from 6 to 8, with an optimal pH at 7, and was capable of tolerating NaCl concentrations up to 2.5%. The metabolic characteristics of Je 1-4^T compared to those of *S. libani* and *S. nigrescens* are summarized in **Table 10**. Based on the API 50 CH assays, strain Je 1-4^T metabolized glycerol, D-ribose, D-adonitol, D-galactose, D-glucose, D-fructose, D-mannose, inositol, D-mannitol, D-sorbitol, N-acetylglucosamine, D-cellobiose, D-maltose, D-lactose, D-melibiose, D-sucrose, D-trehalose, D-raffinose, starch, glycogen, xylitol, gentiobiose, D-turanose, L-fucose, and D-arabitol. Enzymatic profiles assessed with the API ZYM kit revealed similarities among the three tested strains. Antibiotic susceptibility tests demonstrated that strain Je 1-4^T was sensitive to erythromycin, gentamicin, tetracycline, vancomycin, and rifampicin, while exhibiting resistance to ampicillin, cefotaxime,

and penicillin G, consistent with patterns of closely related species.

4.1.3 Chemotaxonomic characteristics

The chemotaxonomic analysis indicated that strain Je 1-4^T aligns with the typical features of the genus *Streptomyces*. including the detected cell wall LL-diaminopimelic acid composition (Mary P. Lechevalier, 1970) and a predominant menaquinone profile consistent with previous genus descriptions (Grace Alderson, 1985). Whole-cell hydrolysate analysis revealed galactose and ribose as the primary sugars, with glucose and mannose present in smaller amounts. Mycolic acids were absent from the strain. The major menaquinone composition consisted of MK-9(H_6) (66.6%), MK-9(H_8) (16.6%), and MK-9(H_4) (11.9%). Furthermore, fatty acid profiling showed that main fatty acids identified included *iso*-$C_{16:0}$ (24.1 %), *anteiso*-$C_{17:0}$ (15.6%), *anteiso*-$C_{15:0}$ (14.3%), *iso*-$C_{15:0}$ (7%), $C_{16:0}$ (5.8%), and *iso*-$C_{17:0}$ (5.7%). In contrast, the strains *S. libani* and *S. nigrescens* exhibited similar profiles for menaquinone and fatty acid compositions, although their relative abundances differed. Additionally, the primary polar lipids identified were diphosphatidylglycerol, phosphatidylethanolamine, phosphatidylglycerol, aminophospholipids, phosphatidylinositol, and phospholipids. Comprehensive details on these biochemical characteristics are provided in (**Table 10, Figure 9**).

DPG = Diphosphatidylglycerol
PE = Phosphatidylethanolamine
PG = Phosphatidylglycerol
PI = Phosphatidylinositol

AGL = Aminoglycolipid
APL = Aminophospholipid
AL = Aminolipid
GL = Glycolipid
PL = Phospholipid

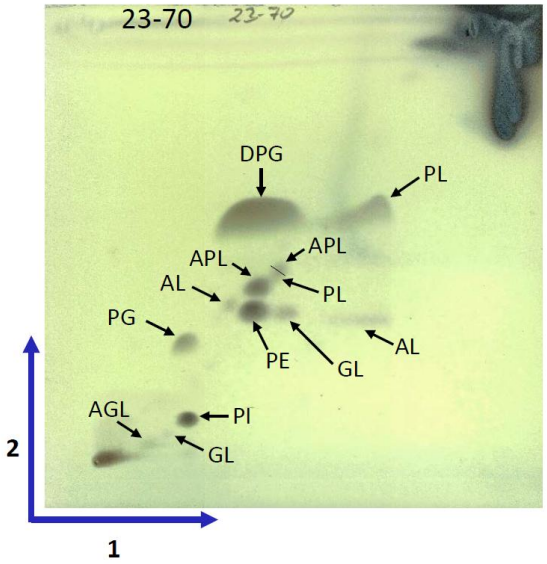

Figure 9: Polar lipid analysis of strain Je 1-4^T (DSMZ Identification Services).

4.1.4 Reclassification of *S. libani*

In this study, *S. libani* subsp. *libani* and *S. nigrescens* demonstrated high genomic similarity, as indicated by a dDDH value of 92.0%, suggesting that these two strains likely represent the same genomospecies. A similar pattern was previously reported among other *Streptomyces* taxa, where *S. libani* subsp. *rufus* and *S. hygroscopicus* subsp. *glebosus* were identified as heterotypic synonyms of the more distantly related *S. platensis* (Komaki and Tamura, 2020). Although minor differences were identified in the chemotaxonomic profiles of these two type strains, these distinctions likely reflect slight genetic variations and are insufficient to justify their classification as separate species.

In this case, Rule 24 of the Bacteriological Code applies, which dictates that name priority is established based on the original publication date. Therefore, we propose that *Streptomyces libani* subsp. *libani* Baldacci and Grein 1966 (Approved Lists 1980) should be recognized as a later heterotypic synonym of *Streptomyces nigrescens* (Sveshnikova 1957) Pridham et al. 1958 (Approved Lists 1980).

4.1.5 Description of *S. explomaris* sp. nov.

Streptomyces explomaris (ex.plo.ma'ris. N.L. gen. n. *explomaris*, derived from EXPLOMARE, named after the publicly funded project which enabled its taxonomic classification). This is a Gram-positive, strictly aerobic actinomycete that develops highly branched substrate mycelia bearing aerial hyphae, which subsequently differentiate into straight to flexuous chains of spores. Optimal growth conditions occur at temperatures between 25 to 30°C, although growth is viable within a broader temperature spectrum of 25-45°C. It grows optimally at pH 7, tolerating a pH range of 6-8 and sodium chloride concentrations up to 2.5% (w/v). Enzymatic activities revealed positive activity for alkaline phosphatase, esterase (C4), esterase lipase (C8), leucine arylamidase, valine arylamidase, cystine arylamidase, acid phosphatase, and Naphthol-AS-BI-phosphohydrolase. It utilizes glucose, mannitol, fructose, xylose, sucrose, inositol, and raffinose, but cannot metabolize cellulose, arabinose, or rhamnose. Chemotaxonomically, the cell peptidoglycan structure is characterized by LL-diaminopimelic acid, and ribose and galactose as predominant sugars within whole-cell hydrolysates. The major cellular fatty acids are *iso*-$C_{16:0}$, *anteiso*-$C_{17:0}$, and *anteiso*-$C_{15:0}$. Principal menaquinones are MK-9(H_6), MK-9(H_8) and MK-9(H_4). The polar lipid composition of *S. explomaris* contains diphosphatidylglycerol, phosphatidylethanolamine, phosphatidylglycerol, aminophospholipid, phospholipid, and phosphatidylinositol. The genome of the type strain is represented by a linear chromosome with a size of 8,866,687 bp, exhibiting G+C content of 70.9%.

The type strain of *S. explomaris* is strain Je 1-4^T, which was initially recovered from coastal rhizosphere soil of *Juniperus excelsa* M. Bieb. (Crimea Peninsula). This strain is stored in the Microbial Culture Collection of Antibiotic Producers of the Ivan Franko National University of Lviv under the collection number Lv 166. Additionally, it is deposited under the number DSM 117375^T at the Leibniz-Institute DSMZ - Deutsche Sammlung von Mikroorganismen und Zellkulturen GmbH (Braunschweig, Germany), and under the number LMG 33490^T at the Belgian Coordinated Collections of Microorganisms (BCCM/LMG, Gent, Belgium). The complete genome sequence, 16S rRNA consensus sequence and the raw sequencing data are publicly accessible in GenBank under accession number CP106840 and OQ740289 as

well as BioProject ID PRJNA883639.

4.2 System metabolic engineering of *S. explomaris* for enhanced production of nybomycin

4.2.1 Screening for high-efficiency nybomycin production hosts

In an initial series of experiments, various *Streptomyces* strains were evaluated for their nybomycin production potential, including the previously engineered *S. albus* 4N24, which has been identified as the most efficient heterologous host for nybomycin biosynthesis (Stegmüller et al., 2024). To facilitate this comparison, the nybomycin BGC was cloned from BAC 4N24 and introduced into six different *Streptomyces* isolates, comprising three terrestrial and three marine strains. All newly engineered mutants, along with *S. albus* 4N24 as a control, were cultivated in DNPM medium for 200 hours.

Nybomycin production was successfully detected in six out of the seven strains (**Figure 10**), though significant variations in yield were observed. Notably, *S. explomaris* 4N24 exhibited the highest production levels, exceeding the nybomycin titer of *S. albus*—the previous benchmark—by nearly sevenfold. In contrast, the marine isolates 94-10 and 94-07 demonstrated minimal and undetectable nybomycin production, respectively, suggesting possible metabolic limitations or regulatory constraints affecting nybomycin biosynthesis in these strains.

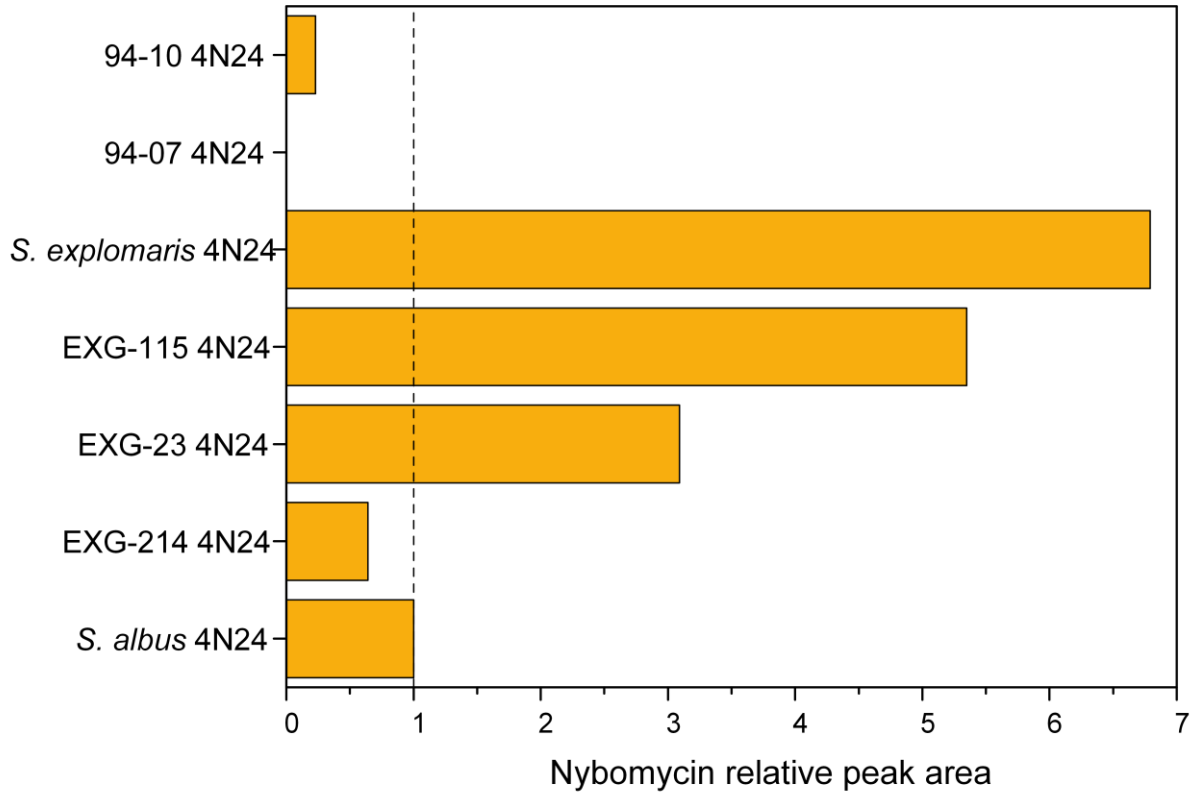

Figure 10: Production of nybomycin by heterologous hosts expressing the 4N24 BCG, relative to *S. albus* 4N24.

4.2.2 Nybomycin production from seaweed sugars using *S. explomaris* 4N24

Due to its superior nybomycin production capacity, *S. explomaris* 4N24 was selected for further investigation and metabolic refinement. To explore the feasibility of seaweed biomass as a sustainable feedstock for nybomycin biosynthesis, its ability to metabolize various sugars and sugar derivatives commonly found in seaweed (Hoffmann et al., 2021; Offei et al., 2018; Poblete-Castro et al., 2020) and seaweed-based hydrolysate feedstocks (Bai et al., 2015; Hoffmann et al., 2021; Hou et al., 2017; Seo et al., 2023) was systematically evaluated. The study evaluated various sugars including hexoses: glucose, mannose, galactose, rhamnose, fucose; pentoses: xylose, arabinose; and the sugar alcohol mannitol. Growth assessments in minimal freshwater medium supplemented with individual sugars demonstrated that *S. explomaris* 4N24 efficiently utilized glucose, mannose, galactose, xylose, and mannitol, whereas it was unable to metabolize arabinose, rhamnose, or fucose (**Figure 11a**).

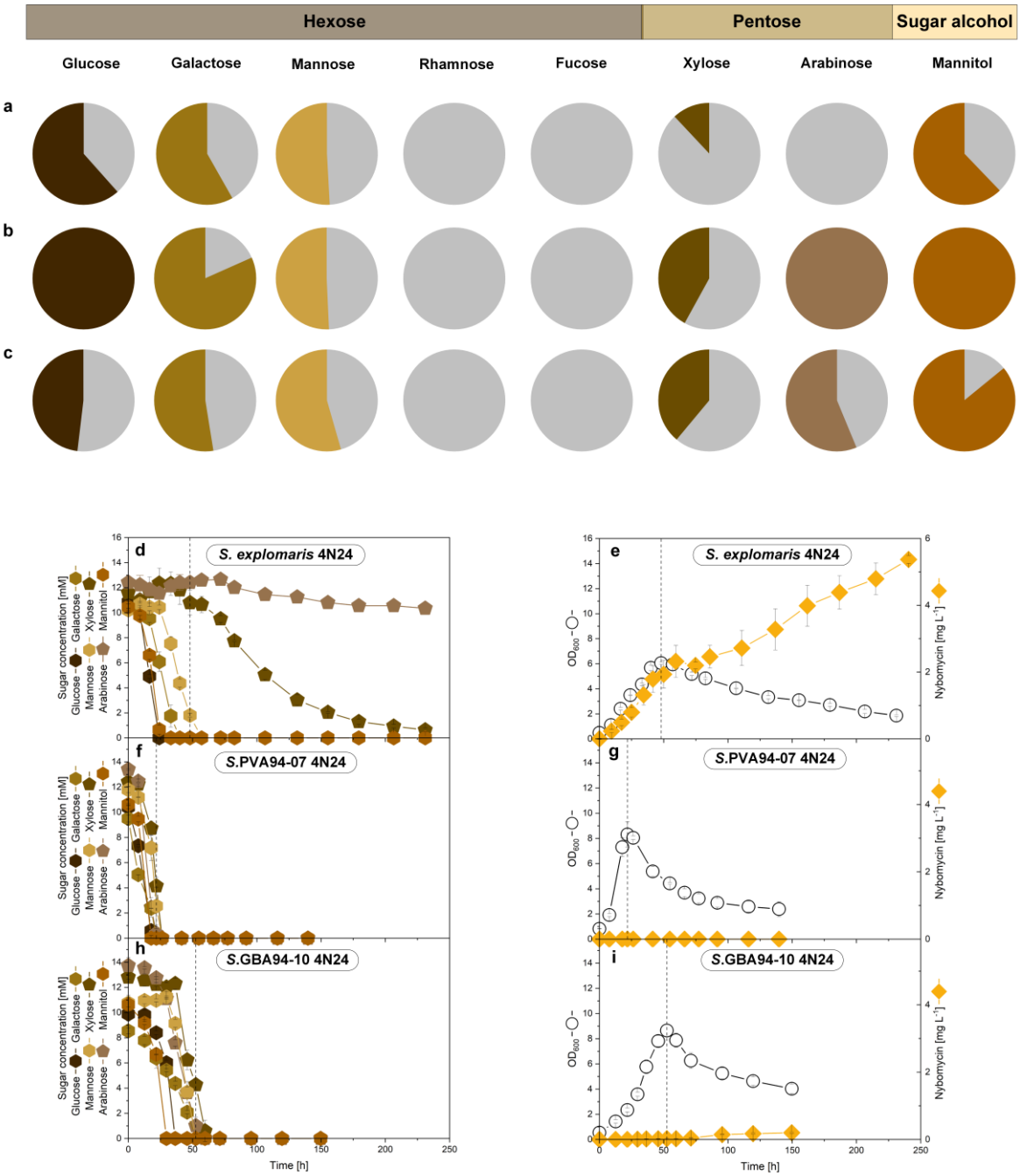

Figure11: Carbon source spectrum test and nybomycin production in mixed sugars with freshwater among different *Streptomyces*. The *S. explomaris* 4N24, *Streptomyces* sp. GBA 94-07 4N24, and *Streptomyces* sp. PVA 94-10 4N24 were cultivated in defined minimal medium with different substrates as sole carbon source in test tube (a-c) and with mixed carbon sources in shake flask (d-i), respectively. Figure a represents *S. explomaris* 4N24, b represents *Streptomyces* sp. GBA 94-07 4N24, and c represents *Streptomyces* sp. PVA 94-10 4N24; grey represents unutilized sugar. Sugar consumption profile of *S. explomaris* 4N24 (d), *Streptomyces* sp. GBA 94-07 4N24 (f), and *Streptomyces* sp. PVA 94-10 4N24 (h); cultivation characteristics of *S. explomaris* 4N24 (e), *Streptomyces* sp. GBA 94-07 4N24 (g), and

Streptomyces sp. PVA 94-10 4N24 (i). n=3.

The inability to process fucose was consistent with prior findings in *S. lividans* (Lee et al., 2013), while the absence of rhamnose catabolism genes corresponded to an incomplete pathway, similar to observations in *S. albidoflavus* J1074 (Yang et al., 2024). For arabinose utilization, *S. explomaris* lacked ability to utilized it. To assess the potential for nybomycin biosynthesis from seaweed-derived carbohydrates, a synthetic hydrolysate was formulated containing six metabolizable carbon sources, mannitol, glucose, galactose, mannose, xylose, along with arabinose. This sugar mixture was incorporated into mineral media, simulating both freshwater and saltwater environments, to evaluate its influence on nybomycin production.

When cultivated in freshwater medium, *S. explomaris* 4N24 exhibited remarkable nybomycin biosynthesis, achieving a titer of 5.4 mg L^{-1} (**Figure 11e**). The strain displayed rapid entry into exponential growth, following a stepwise pattern of sugar metabolism (**Figure 11d**). During the first 24 hours, S. *explomaris* efficiently co-utilized glucose, mannitol, and galactose, suggesting that glucose did not exert strict catabolite repression but was instead metabolized concurrently with other substrates. In numerous microorganisms, glucose modulates the expression of genes involved in the metabolism of alternative sugars, including mannose (Romero-Rodriguez et al., 2017), galactose (Brawner et al., 1997), arabinose (Hodgson, 1982), and xylose (Wong et al., 1991).

Following the depletion of glucose, mannitol, and galactose, the strain transitioned to mannose and xylose metabolism, with mannose being preferentially consumed before xylose. However, when xylose remained the sole carbon source, its metabolism significantly slowed, leading to growth arrest. At the end of the 240-hour cultivation, a portion of xylose remained unutilized. Unlike many *Streptomyces* species, which typically delay secondary metabolite biosynthesis (Lee et al., 2021), *S. explomaris* 4N24 initiated nybomycin production at an early phase and maintained it throughout the later stages of growth. This suggests a distinct regulatory mechanism governs the expression of the biosynthetic pathway. The promoters controlling the nybomycin BGC appeared to function independently of growth phase, resembling observations

reported for *S. albus* 4N24 (Stegmüller et al., 2024). A particularly noteworthy finding was that *S. explomaris* accumulated approximately seven times more nybomycin than the previously used heterologous host, reflecting the huge difference observed in the screening (**Figure 10**). However while the total sugar concentration was identical in both studies (10 g L^{-1}), the prior investigation used only mannitol as the substrate.

Although the other two marine *Streptomyces* strains were less effective in nybomycin biosynthesis, their potential for seaweed-derived biomass utilization deserved further investigation. Both isolates demonstrated the ability to metabolize six out of the eight tested sugars, including arabinose, while rhamnose and fucose remained unutilized (**Figure 11b, 11c**).Under freshwater conditions, *Streptomyces* sp. PVA 94-07 4N24 displayed a rapid carbon consumption rate, distinctively utilizing all available sugars simultaneously rather than sequentially (**Figure 11f**). Within 30 hours, complete sugar depletion was observed. The ability to efficiently co-consume multiple carbon sources suggests that CCR is absent in this strain (Gorke and Stulke, 2008). In many microorganisms, CCR optimizes metabolic efficiency by regulating enzyme synthesis in response to available carbon sources (Romero-Rodriguez et al., 2017). Despite its metabolic versatility, nybomycin production was undetectable in this strain.

Conversely, *Streptomyces* sp. GBA 94-10 4N24 exhibited a slower rate of sugar assimilation and growth but successfully produced nybomycin at 0.2 mg L^{-1} (**Figure 11i**). Unlike PVA 94-07 4N24, this strain followed a sequential sugar utilization pattern, initially depleting mannitol, followed by glucose, while galactose was only partially consumed. The metabolism of mannose, arabinose, and xylose commenced only after glucose depletion. Notably, cell growth peaked at approximately 52 hours, shortly after mannose exhaustion, even though arabinose and xylose were still available. This observation suggests that pentose sugars contribute minimally to biomass accumulation. Nybomycin biosynthesis was initiated during the stationary phase (Kuhl et al., 2020), aligning with the nutrient limitation-induced onset of secondary metabolism commonly reported in *Streptomyces* (Bibb, 2005). A comparable sugar utilization and growth

profile for these three marine *Streptomyces* was observed under saltwater conditions (**Figure 12**). However, nybomycin production was lower in *S. explomaris* 4N24 (3.2 mg L^{-1}), indicating that ionic strength affects metabolite accumulation while still permitting the formation of the desired product

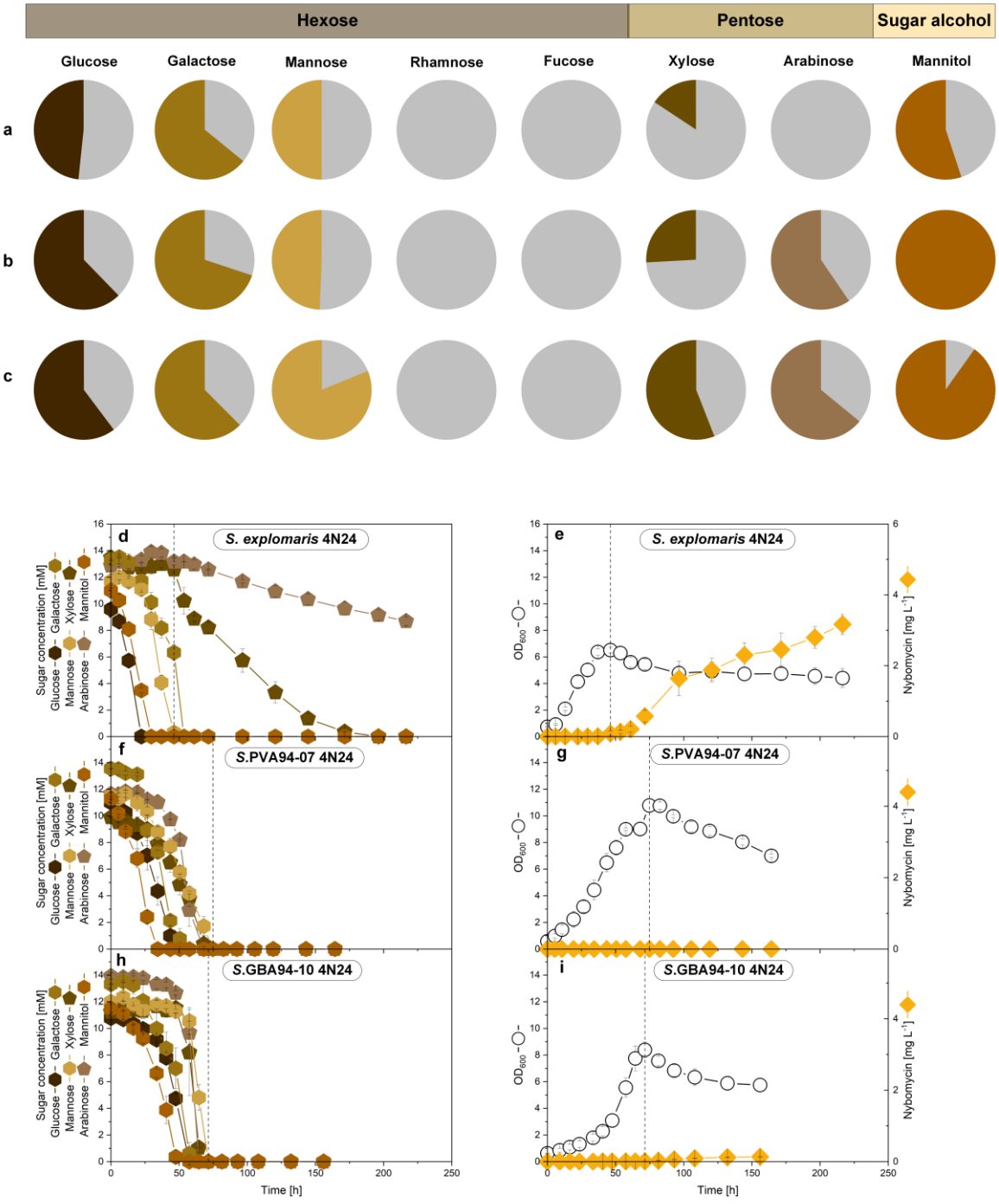

Figure 12: Carbon source spectrum test and nybomycin production in mixed sugars with saltwater among different *Streptomyces*. The *S. explomaris* 4N24, *Streptomyces* sp.

GBA 94-07 4N24, and *Streptomyces* sp. PVA 94-10 4N24 were cultivated in defined minimal medium with different substrates as sole carbon source in test tube (a-c) and with mixed carbon sources in shake flask (d-i), respectively. Figure a represents *S. explomaris* 4N24, b represents *Streptomyces* sp. GBA 94-07 4N24, and c represents *Streptomyces* sp. PVA 94-10 4N24; grey represents unutilized sugar. Sugar consumption profile of *S. explomaris* 4N24 (d), *Streptomyces* sp. GBA 94-07 4N24 (f), and *Streptomyces* sp. PVA 94-10 4N24 (h); cultivation characteristics of *S. explomaris* 4N24 (e), *Streptomyces* sp. GBA 94-07 4N24 (g), and *Streptomyces* sp. PVA 94-10 4N24 (i). n=3.

Following this, we investigated the potential of hydrolysates derived from brown, green, and red seaweed as raw materials for nybomycin production. Ground seaweed *U. lactuca*, *P. palmata*, and *H. elongata* underwent hot water extraction, followed by enzymatic hydrolysis and filtration, resulting in sugar-rich hydrolysates (**Figure 13a**, **13b**, **13c**). The composition of these hydrolysates varied, influenced by the seaweed species and batch-dependent fluctuations, which reflect seasonal and regional variability (Kumar et al., 2021; Mohy El-Din, 2018; Rødde et al., 2004). Green seaweed hydrolysates primarily contained glucose (4.8 g L^{-1}) with minor amounts of xylose (0.6 g L^{-1}). Red seaweed hydrolysates were rich in xylose (3.9 g L^{-1}), while brown seaweed hydrolysates contained predominantly mannitol (4.6 g L^{-1}) alongside glucose (1.5 g L^{-1}).

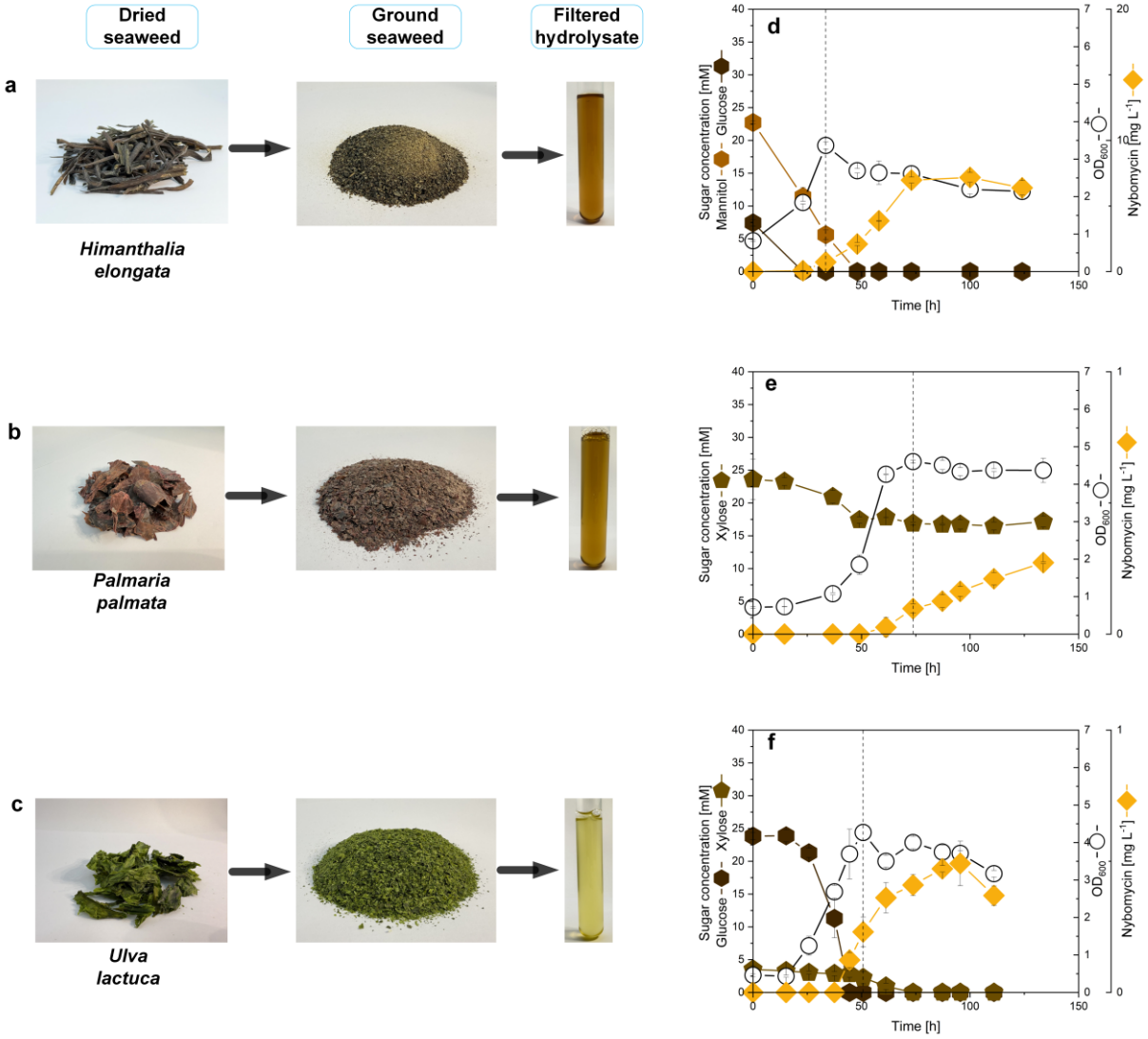

Figure 13: Valorization of different seaweed to fermentable carbon source and cultivation profile in seaweed hydrolysates. The overview indicates the hydrolysate of different type of macroalgae (a-c) and cultivation profile of *S. explomaris* 4N24 in different seaweed hydrolysate (d-f). All cultivations were performed in seaweed hydrolysate supplement with MOPS buffer in shake flask. *S. explomaris* 4N24 grown in brown seaweed hydrolysate (d), red seaweed hydrolysate (e), and green seaweed hydrolysate (f). n=3.

S. explomaris 4N24 exhibited remarkable metabolic adaptability, efficiently utilizing seaweed-derived hydrolysates for nybomycin synthesis, achieving titer of 0.5 mg L^{-1}, 0.3 mg L^{-1}, and 7.2 mg L^{-1} when cultivated in green, red, and brown seaweed hydrolysates, respectively. The results highlight the seaweed potential as a renewable substrate for antibiotic bioproduction. The strain thrived successfully in all three hydrolysates, provided that the pH was buffered to

7, without requiring additional nutrient supplementation (**Figure 13d**, **13e**, **13f**). In green seaweed hydrolysate, both glucose and xylose were fully metabolized, while in brown seaweed hydrolysate, mannitol and glucose were completely consumed. However, red seaweed hydrolysate supported only partial xylose utilization. Notably, *S. explomaris* 4N24 exhibited good growth in seaweed hydrolysates, this may be attributed to bioactive compounds present in seaweed extracts that stimulate cellular metabolism (Torres et al., 2019), highlighting the strain's biotechnological potential.

Next, we explored the option to extend the native spectrum towards more comprehensive metabolization of mixed seaweed hydrolysates. Although not abundant in the examined seaweed species, arabinose is a common sugar in red seaweeds (*Rhodophyta*), where it serves as a structural component of sulfated polysaccharides and xylans. However, *S. explomaris* 4N24 was unable to metabolize this pentose. To overcome this limitation, we used arabinose utilization as a model system for enhancement. To enable the utilization of arabinose, we introduced the corresponding metabolic pathway from the *C. glutamicum* 31831, a strain known for its capability of arabinose metabolism (Kawaguchi et al., 2009) into *S. explomaris* 4N24. The envisioned operon included *araB* (encoding ribulokinase), *araD* (encoding ribulose 5-phosphate 4-epimerase), *araA* (encoding arabinose isomerase), and *araE* which encodes an arabinose transporter, all genes from *C. glutamicum* ATCC 31831 (Accession number AB447371). These genes were placed under the control of the constitute promoter P_{ermEp*} (García-Gutiérrez et al., 2020) and subsequently integrated into chromosome of *S. explomaris* 4N24, generating the new mutant *S. explomaris* P_{ermEp*} *araBDAE*, reflecting both the utilized promoter and the introduced arabinose catabolic genes. Arabinose was successfully co-consumed with glucose, mannitol, and galactose within first 30 h in the new mutant in the mixed sugars medium (**Figure 14**).

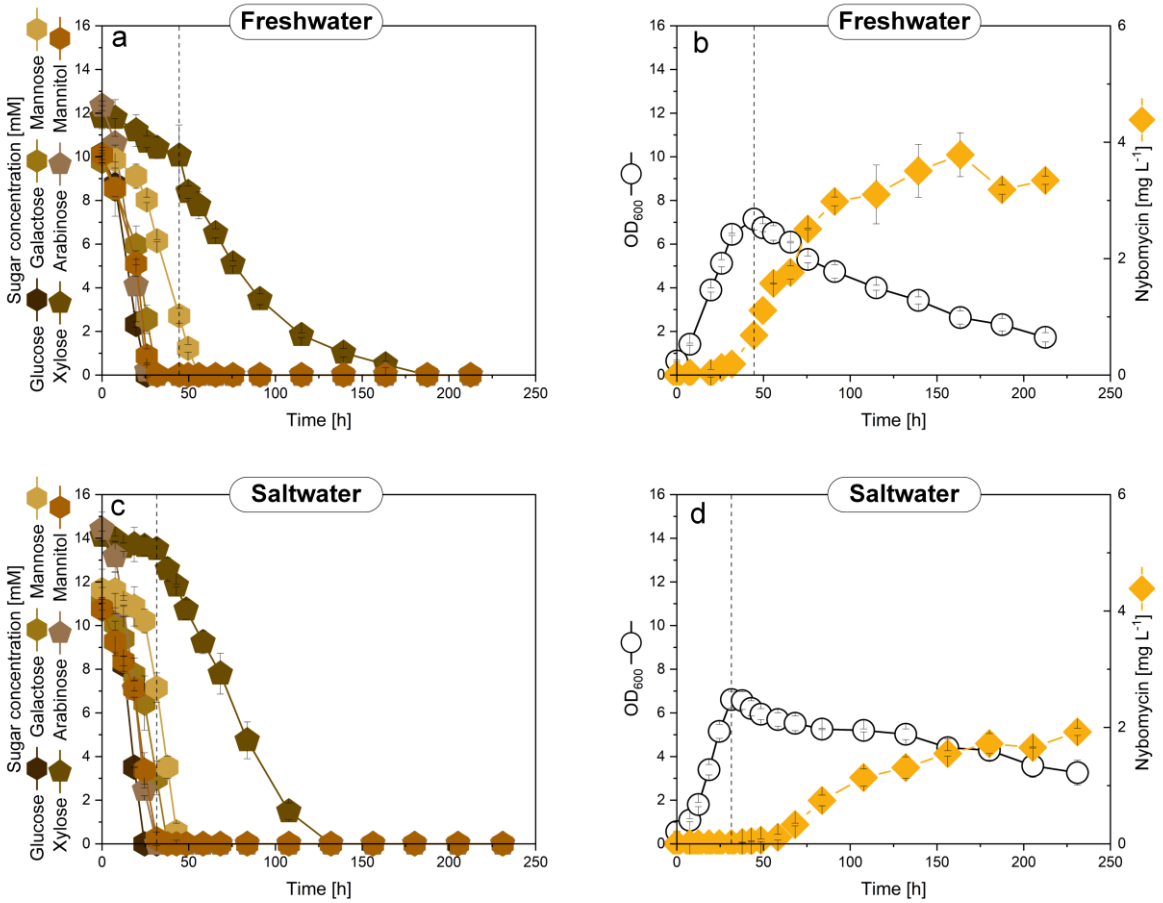

Figure 14: Nybomycin production in mixed sugars in *S. explomaris* P_{ermEp*} *araBDAE* with fresh and salt water. The *S. explomaris* P_{ermEp*} *araBDAE* was cultivated in defined minimal medium with mixed carbon sources containing fresh and salt water in shake flask, respectively. Sugar consumption profile of *S. explomaris* P_{ermEp*} *araBDAE* in fresh water (a) and salt water (c), cultivation characteristics of *S. explomaris* P_{ermEp*} *araBDAE* in fresh water (b) and salt water (d). n=3.

4.2.3 Time-resolved transcriptome analysis to identify potential nybomycin biosynthesis target

Metabolic engineering for natural product formation presents significant challenges due to the complexity of the underlying regulatory networks and metabolic pathways. To identify metabolic bottlenecks and genetic targets for optimizing *S. explomaris* 4N24 for enhanced nybomycin biosynthesis, the transcriptomic profiling was conducted under freshwater and saltwater conditions, providing insights into its metabolic dynamics. RNA sequencing was performed at four critical time points (**Figure 15**): the early exponential phase (17 h), the mid-

exponential phase (33 h) when glucose and mannitol were depleted, the stationary phase (75 h) following the exhaustion of galactose and mannose, and the late phase (175 h). The transcriptomic dataset from the 17-hour time point served as the reference condition.

Notably, substantial changes in gene expression were observed, emphasizing the significant influence of carbon availability on the physiological state of *S. explomaris* 4N24. Under freshwater condition, following glucose and mannitol depletion, 3,193 genes (~41.2% of the genome) were differentially expressed (1,006 upregulated, 2,187 downregulated; adjusted $p \leq 0.05$, $\log_2 FC \geq 1$). By the stationary phase (75 h)—after the exhaustion of galactose and mannose—the number of differentially expressed genes increased to 3,920 (50.6% of the genome). In the late phase (175 h), 3,835 genes (49.5%) exhibited altered expression levels. Given the similarity of transcriptional responses to saltwater (**Appendix Figure A3**), subsequent cultivation experiments and in-depth analysis were conducted under freshwater conditions to streamline further investigations.

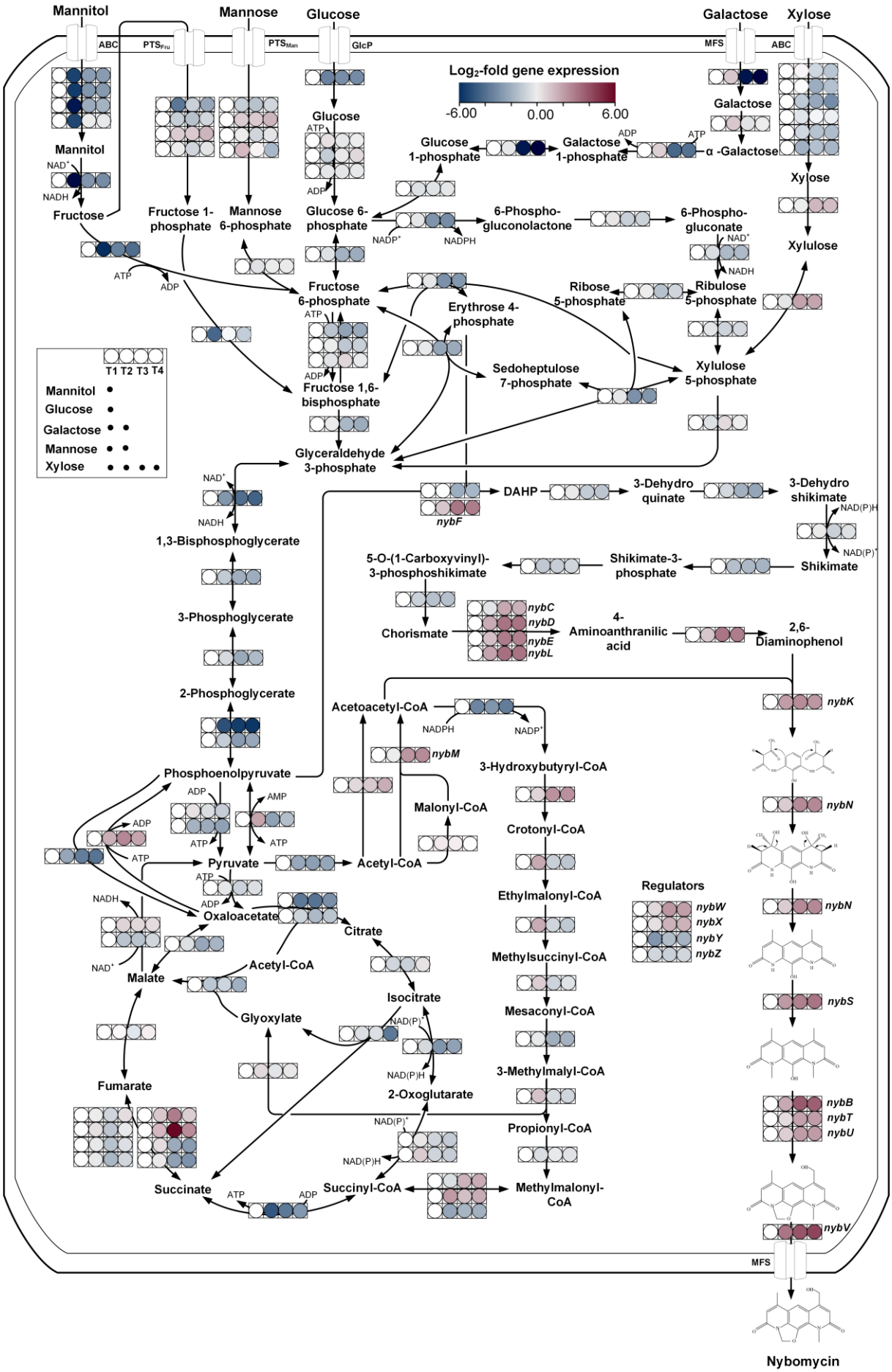
Mannitol
Mannose
Glucose
Galactose
Xylose
ABC
PTS$_{Fru}$
PTS$_{Man}$
GlcP
MFS
ABC
Log$_2$-fold gene expression
-6.00
0.00
6.00
Mannitol
Fructose
Fructose 1-phosphate
Mannose 6-phosphate
Glucose 6-phosphate
Glucose 1-phosphate
Galactose 1-phosphate
α -Galactose
Xylose
Xylulose
6-Phospho-gluconolactone
6-Phospho-gluconate
Ribose 5-phosphate
Ribulose 5-phosphate
Xylulose 5-phosphate
Fructose 6-phosphate
Erythrose 4-phosphate
Sedoheptulose 7-phosphate
Fructose 1,6-bisphosphate
Glyceraldehyde 3-phosphate
T1 T2 T3 T4
Mannitol
Glucose
Galactose
Mannose
Xylose
DAHP
nybF
3-Dehydro quinate
3-Dehydro shikimate
Shikimate
Shikimate-3-phosphate
5-O-(1-Carboxyvinyl)-3-phosphoshikimate
Chorismate
nybC
nybD
nybE
nybL
4-Aminoanthranilic acid
2,6-Diaminophenol
1,3-Bisphosphoglycerate
3-Phosphoglycerate
2-Phosphoglycerate
Phosphoenolpyruvate
Pyruvate
Acetyl-CoA
Malonyl-CoA
nybM
Acetoacetyl-CoA
3-Hydroxybutyryl-CoA
Crotonyl-CoA
Ethylmalonyl-CoA
Methylsuccinyl-CoA
Mesaconyl-CoA
3-Methylmalyl-CoA
Propionyl-CoA
Methylmalonyl-CoA
Succinyl-CoA
Succinate
Fumarate
Malate
Oxaloacetate
Citrate
Isocitrate
2-Oxoglutarate
Glyoxylate
Regulators
nybW
nybX
nybY
nybZ
nybK
nybN
nybN
nybS
nybB
nybT
nybU
nybV
MFS
Nybomycin

Figure 15: Time-resolved transcriptome analysis in *S. explomaris* 4N24 in freshwater. The data display the expression differences between early exponential phase (T1, 12 h, as reference), mid-exponential phase (T2, 36 h), stationary phase (T3, 75 h), and late phase (T4, 175 h). The metabolic network was assembled based on KEGG, including glycolysis, PP pathway, TCA cycle, shikimate pathway and nybomycin biosynthesis pathway. The black dot under each time points represents carbon sources availability at different time points. The circle in square represents gene at different timepoint, expression differences are highlighted by color (blue: down regulated, red: up regulated). n=3.

Analysis on primary metabolism

Investigation of central carbon metabolism and precursor supply pathways uncovered key regulatory factors that significantly impact nybomycin biosynthesis in *S. explomaris* 4N24. These findings highlight the intricate metabolic control networks that dictate precursor availability, influencing the efficiency of secondary metabolite production.

Transcriptomic analysis revealed that genes associated with glycolytic substrate breakdown were generally downregulated during the stationary and death phases, aligning with observations in other *Streptomyces* (Hwang et al., 2019; Stegmüller et al., 2024). This differential gene expression pattern suggests that glycolysis operates more actively in the presence of glucose and mannitol. For instance, significant reductions in the expression of genes 005987 and 000076 were observed. The gene 005987, encoding glyceraldehyde-3-phosphate dehydrogenase, facilitates the phosphorylation of glyceraldehyde 3-phosphate to 1,3-bisphosphoglycerate using NAD^+ as a cofactor (Sprušanský et al., 2001). Expression of this gene was stimulated by glucose and mannitol, exhibiting a pattern similar to gene 000076, which encodes enolase, an enzyme responsible for the reversible conversion of 2-phosphoglycerate (2-PG) to PEP. Conversely, the phosphoenolpyruvate carboxykinase gene (*pepCK*) (002843) was strongly repressed in the presence of these sugars, indicating strict substrate-driven regulation.

Key metabolic enzymes catalyzing irreversible steps often serve as regulatory control points in glycolysis and gluconeogenesis. PEPCK, which catalyzes the conversion of oxaloacetate to PEP and CO_2 in a GTP-dependent manner (Borodina et al., 2005), is a well-documented rate-

limiting enzyme in gluconeogenesis (Delbaere et al., 2004; Lule et al., 2012). Overexpression of PEPCK could result in PEP accumulation, potentially increasing the availability of DAHP, a key precursor in pathway of the nybomycin biosynthesis (Rodríguez Estévez et al., 2018).

As the final oxidative pathway for energy generation, the TCA cycle showed an overall downregulation due to the reduction in pyruvate availability from glycolysis, with most associated genes displaying decreased expression. However, succinate dehydrogenase genes were significantly upregulated when xylose and arabinose remained as the sole carbon sources. Notably, an additional operon regulating succinate dehydrogenase exhibited downregulation, suggesting the presence of multiple succinate dehydrogenase operons operating under distinct regulatory mechanisms in *S. explomaris*.

The succinate dehydrogenase complex, a key enzyme in both the TCA cycle and aerobic electron transport chain, facilitates the conversion of succinate to fumarate while transferring electrons to ubiquinone (Huang and Millar, 2013; Yankovskaya et al., 2003). This enzyme complex is also implicated in cellular protection against oxidative stress, mitigating damage from ROS such as superoxide anion radical and hydrogen peroxide (Beites et al., 2014). The downregulation of fumarate reductase operons, which catalyze the conversion of fumarate to succinate under anaerobic conditions, likely reflects a regulatory adaptation aimed at minimizing ROS formation (Messner and Imlay, 2002).

A particularly noteworthy observation was the differential regulation of malic enzyme (ME) genes, which play a role in connecting glycolysis, gluconeogenesis, and the TCA cycle (Huergo et al., 2020; Sauer and Eikmanns, 2005). In agreement with studies on other antibiotic-producing *Streptomyces* species (Toshiko et al., 2022), the NAD-dependent malic enzyme gene (NAD-ME, 005008) exhibited strong downregulation, whereas the NADP-dependent malic enzyme gene (NADP-ME, 002541) was significantly upregulated. In *S. coelicolor*, NAD-ME deficiency has been linked to a reduction in the conversion of TCA cycle intermediates to acetyl-CoA, consequently leading to a decrease in secondary metabolite synthesis (Rodriguez et al., 2012). The observed downregulation of NAD-ME in this study is likely a response to

diminished TCA cycle flux, which in turn affects precursor availability for secondary metabolism. Conversely, elevated expression of NADP-ME may enhance NADPH production, supporting increased nybomycin biosynthesis, as NADPH is essential for various biosynthetic reactions.

The biosynthesis of nybomycin relies on CoA-derived carbon sources, with acetyl-CoA serving as a key metabolic precursor. Notably, marked upregulation of genes facilitating the synthesis of acetoacetyl-CoA from acetyl-CoA, combined with concurrent downregulation of those genes channeling acetoacetyl-CoA towards further CoA-ester metabolic pathways, effectively enhanced precursor availability, thus promoting nybomycin biosynthesis. Consequently, an adequate availability of acetyl-CoA was highly beneficial for supporting secondary metabolism. However, following the depletion of glucose and mannitol, the expression of pyruvate dehydrogenase (005745)—a key enzyme that converts pyruvate into acetyl-CoA—dropped significantly. This decline may be attributed to a reduction in glycolytic flux, as alternative carbon sources such as mannose and galactose might not provide the same energy yield or metabolic intermediates as glucose or mannitol, ultimately lowering overall metabolic activity.

Interestingly, the genes *nybM* and 004871, both involved in acetoacetyl-CoA formation from acetyl-CoA, were strongly upregulated, particularly after mannose and galactose were exhausted. This suggests that upon entering the stabilization phase, most acetyl-CoA is redirected toward secondary metabolite biosynthesis. Furthermore, the 001919 gene, which encodes 3-hydroxybutyryl-CoA dehydrogenase, exhibited significant downregulation, whereas *nybK*, responsible for incorporating acetoacetyl-CoA into the nybomycin biosynthetic pathway, was notably upregulated. These transcriptional changes indicate that, once glucose and mannitol are depleted, acetoacetyl-CoA is primarily allocated toward nybomycin biosynthesis, reinforcing its role as a crucial building block in antibiotic production.

Transcriptomic analysis revealed a general decline in expression of genes encoding PPP enzymes. Notably, significant downregulation was observed in the gene cluster encoding G6PDH (*zwf2*) (005996), transketolase (*tkt*) (005998), and transaldolase (005997). These genes exhibited strong induction in the presence of glucose, mannitol, galactose, and

mannose, but their expression levels dropped substantially once these sugars were fully consumed, with a $\log_2$ fold change exceeding -2. This gene cluster has been suggested to play a crucial role in NADPH generation, which is integral to secondary metabolite biosynthesis (Challis and Hopwood, 2003).

As the rate-limiting enzyme of the PPP, G6PDH (005996) governs pathway flux, supplying the NADPH required for nybomycin synthesis. Likewise, upregulating transketolase (005998) expression enhances the production of E4P, a fundamental precursor in nybomycin biosynthesis via the shikimate pathway. Therefore, activating the pentose phosphate pathway could simultaneously enhance NADPH availability, thereby improving reducing power for biosynthetic reactions, while also increasing E4P supply, directly supporting nybomycin biosynthesis. Strengthening flux through this pathway presents a promising strategy, particularly by upregulating *zwf2* and *tkt*, has the potential to enhance nybomycin biosynthesis to enhance antibiotic production efficiency.

Three gene clusters (002610, 005807, and 006512–006516) associated with the shikimate pathway exhibited downregulation following depletion of glucose and mannitol. Notably, DAHP synthase (005807), the key entry enzyme of the shikimate pathway, was significantly downregulated ($\log_2$FC = -2.37) with depletion of galactose and mannose, suggesting a potential limitation of precursor supply for nybomycin biosynthesis. Interestingly, the *nybF* (encoding DAHP synthase) within the *nyb* cluster appeared to play an important role in maintaining pathway activity. Expression of *nybF* increased substantially ($\log_2$FC = 3.09) after mannitol and glucose exhaustion, indicating its importance in sustaining metabolic flux. Therefore, enhancing DAHP synthase expression presents a promising strategy.

Previous studies have demonstrated that enhancing the PPP and shikimate pathway activity can lead to higher secondary metabolite yields (Huang et al., 2013; Jin et al., 2017; Perez-Valero et al., 2024; Tang et al., 2011; Thykaer et al., 2010). To further optimize nybomycin production, key metabolic engineering targets include: *nybF* from the shikimate pathway and *zwf2* and *tkt* from the PPP. By modulating these pathways, metabolic flux can be redirected

toward nybomycin biosynthesis, offering a promising approach for strain optimization and yield enhancement.

Analysis on secondary metabolism

The transcriptional analysis of the nybomycin BGC revealed that most genes exhibited a significant increase in expression as carbon sources were depleted. Among them, *nybV*, and *nybB* were the most highly upregulated during the production phase. The enhanced expression of *nybV*, which encodes an MFS transporter, was consistent with the rising nybomycin concentration in the culture medium, confirming its role in secretion. Similarly, *nybB*, responsible for encoding an FAD-binding protein involved in the final hydroxylation step that yields the active structure of nybomycin, was also upregulated, suggesting its contribution to the increased production.

All four cluster-associated transcriptional regulators: *nybW*, *nybX*, *nybY*, and *nybZ* exhibited changes in expression levels, reflecting their involvement in pathway regulation. Based on sequence analysis, *nybW*, *nybX*, and *nybZ* are likely transcriptional regulators controlling the expression of biosynthetic genes (Rodríguez Estévez et al., 2018). Meanwhile, *nybY* which was strongly downregulated, remains functionally uncharacterized, requiring further investigation. The substantial upregulation of *nybW* suggests that it functions as a repressor of *nybQRSTUV*, meaning its increased expression could negatively affect nybomycin biosynthesis. Likewise, *nybX* regulator was also significantly upregulated. Studies on homologous regulators have shown that TetR family members act as negative regulators of antibiotic biosynthesis, as observed in *S. coelicolor* that a TetR regulator strongly suppressed actinorhodin production, morphological differentiation, and sporulation (Xu et al., 2010). This suggests that *nybX* may similarly inhibit nybomycin biosynthesis. Unlike *nybX*, *nybZ* was downregulated, though it also may serve a similar role in repression. These findings indicate that regulatory proteins within the nybomycin cluster influence pathway activation and could act as bottlenecks to production. Given this, modifying transcriptional regulators through genetic engineering may provide an effective strategy for enhancing nybomycin yield.

4.2.4 Optimization of intergenic conjugation method for *S. explomaris*

Intergeneric conjugation between *E. coli* and *Streptomyces* is a widely used and highly efficient transformation approach for introducing plasmids into target strains (Du et al., 2012; Zhou et al., 2012). However, a universal conjugation protocol applicable to all *Streptomyces* strains has not yet been standardized. To facilitate gene expression and genetic manipulation in *S. explomaris* 4N24, an optimized transformation system is required.

The addition of $MgCl_2$ and $CaCl_2$ to conjugation media is known to enhance conjugation efficiency (Choi et al., 2004; Wang and Jin, 2014; Zhang et al., 2019), although the optimal concentrations vary among different *Streptomyces* strains. Therefore, the effects of varying concentrations of $CaCl_2$ and $MgCl_2$, along with different donor-to-recipient ratios, were systematically evaluated.

The results demonstrated that successful conjugation occurred only in media supplemented with $CaCl_2$, with the highest efficiency observed at 20 mM $CaCl_2$ and a 1:1 donor-to-recipient ratio (**Figure 16**). However, increasing the $CaCl_2$ concentration beyond 20 mM led to a sharp decline in conjugation frequency, likely similar to the inhibition of spore formation and mycelial growth by high concentration of $MgCl_2$, a phenomenon also reported in *Strepomyces pristinaespiralis* (Jin et al., 2010). The enhancement of conjugation efficiency is maybe attributed to Ca^{2+}, in neutralizing the negative charges present on both the recipient cell membrane and plasmid DNA (Asif et al., 2017). This charge neutralization mitigates electrostatic repulsion, thereby facilitating closer interaction between the donor DNA and the recipient cell surface, ultimately promoting more efficient DNA transfer during conjugation.

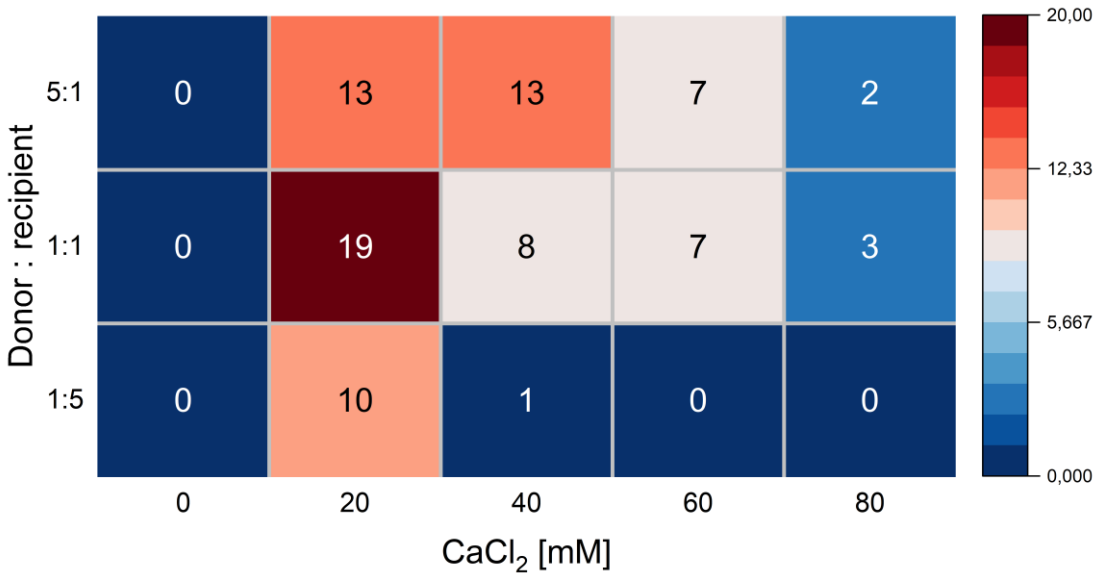

Figure 16: Exconjugants number of intergenic conjugation between *E. coli* ET12567 and *S. explomaris* strain in different conditions. The conjugation was performed with different ratio of donor to recipient on MS plates supplement with different concentration of $CaCl_2$. The number of exconjugants was mean of 3 biological replicates.

In contrast, supplementation with $MgCl_2$ did not result in exconjugant formation, regardless of the donor-to-recipient ratio tested, no exconjugant was observed in different ratio of donor to recipient. The superior effectiveness of Ca^{2+} over Mg^{2+} in enhancing conjugation efficiency aligns with findings in other *Streptomyces* species, including *S. coelicolor*, *Streptomyces. lavendulae*, *S. venezuelae*, and *Streptomyces netropsis* SD-07 (Choi et al., 2004; Wang and Jin, 2014). This suggests that Ca^{2+}-dependent conjugation efficiency may represent a broader trend among *Streptomyces* species, providing valuable insights for optimizing transformation protocols.

4.2.5 Improving Nybomycin production by engineering regulatory factor modules in *nyb* gene cluster

Given its exceptional nybomycin biosynthesis, *S. explomaris* 4N24 was selected for further metabolic optimization to explore its distinctive regulatory mechanisms and its potential as an advanced cell factory for improved yields. Mannitol was identified as the preferred carbon source, as it was metabolized efficiently by the strain and beneficial for nybomycin biosynthesis

among the other sugars (**Figure 17**). Besides, it is abundantly found in seaweed-derived biomass, particularly in brown seaweed (Chades et al., 2018; Groisillier et al., 2014; Tajima et al., 2018). Consequently, it was chosen as the primary substrate for further studies aimed at enhancing nybomycin production.

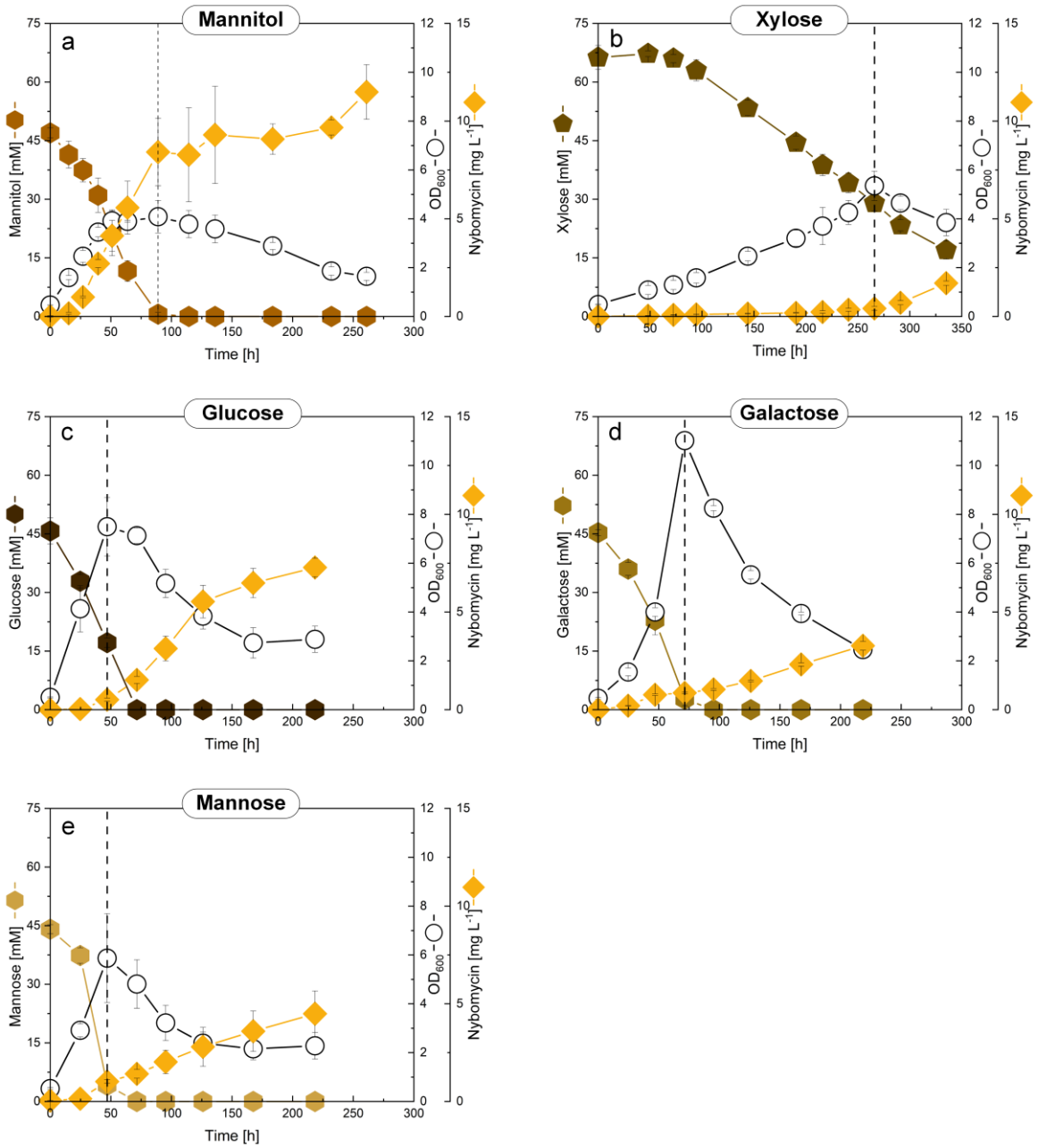

Figure 17: Nybomycin production of *S. explomaris* 4N24 in different substrates. Strain was cultivated in minimal medium with mannitol (a), xylose (b), glucose (c), galactose (d), and mannose (e). n=3.

Antibiotic biosynthesis in *Streptomyces* is tightly regulated by complex genetic control mechanisms, particularly those involving transcriptional regulators embedded within BGCs. These regulators act as key modulators of production, functioning as either activators or repressors. Targeting regulatory elements has proven to be an effective strategy for yield optimization, as demonstrated by *nemR* overexpression, which led to increased nemadectin production (Li et al., 2019) and chromomycin enhancement achieved by disrupting the repressor *srcmRII* while overexpressing SrcmRI (Sun et al., 2018).

Recent studies have identified four transcriptional repressors (*nybW*, *nybX*, *nybY*, and *nybZ*) in nybomycin gene cluster, which play a role in controlling nybomycin biosynthesis (Rodríguez Estévez et al., 2018; Stegmüller et al., 2024). To further enhance nybomycin production, the regulatory elements within the 4N24 cluster were genetically modified. Specifically, two strategies were implemented that deletion repressors mutants were generated: NYB-1 (4N24 Δ*nybWX*) and NYB-2 (4N24 Δ*nybWXYZ*) (**Figure 18a, 18b**). The correctness of these mutants was validated through PCR and sequencing.

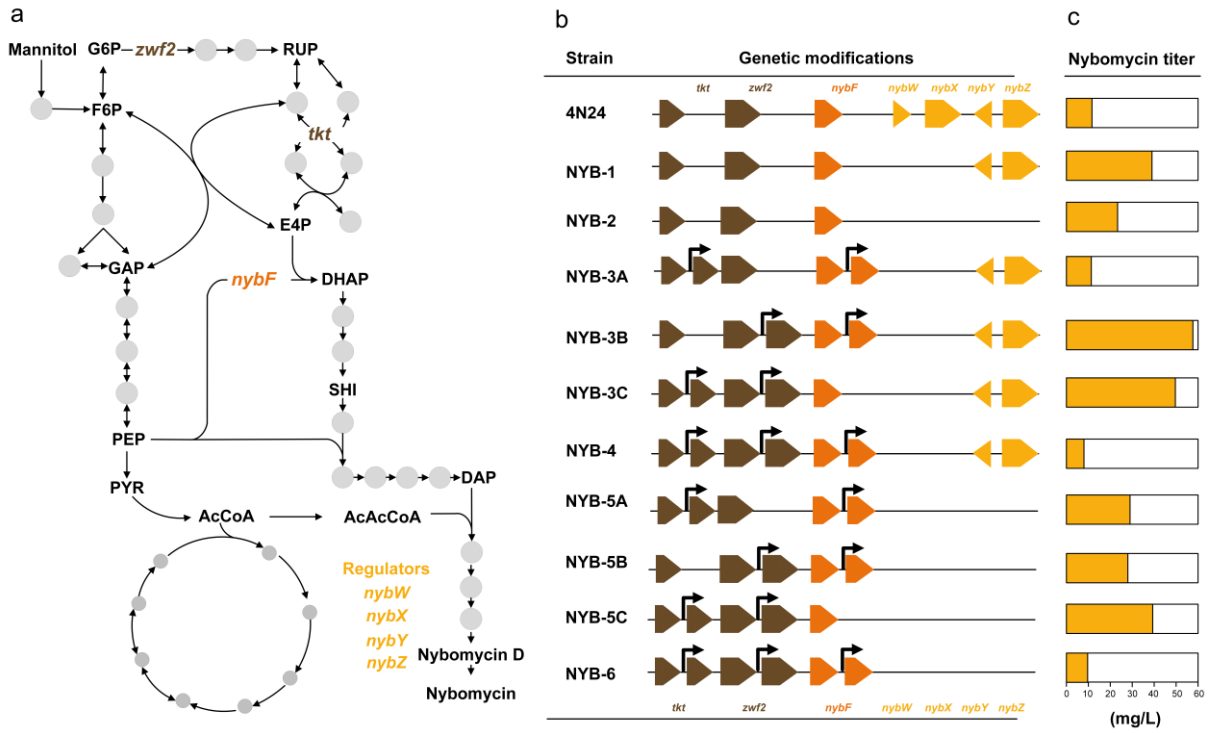

Figure 18: Metabolic pathway design and genetic layout of *S. explomaris* with nybomycin titer. The targets of metabolic engineering in primary and secondary metabolism

(a), genetic layouts of nybomycin producers created in this work (b) and nybomycin titer of each producers (c). The genomic changes were indicated for each producers, including deletion of regulatory factor modules and overexpression of precursor pathway modules under the constitutive promoter.

The antibiotics biosynthesis is often governed by a complex regulatory network involving multiple overlapping transcriptional controls in *Streptomyces* (Pei et al., 2024). As a result, the deletion of a single repressor gene is typically insufficient to fully relieve repression, necessitating the simultaneous disruption of multiple regulatory genes to achieve significant derepression of the cluster. Transcriptomic analysis further supported this regulatory model. During the nybomycin biosynthesis phase, *nybW* and *nybX* were significantly up regulated, while the down regulation of *nybY* and *nybZ* was observed. Based on these findings, double deletion mutants were generated by removing *nybW* plus *nybX* (NYB-1), and *nybW* plus *nybXYZ* (NYB-2) to investigate the impact of multi-repressor knockouts on nybomycin production.

The NYB-1 mutant exhibited a 3.4-fold increase in nybomycin production, accumulating 39.1 mg L^{-1} (**Figure 19a**), compared to 11.5 mg L^{-1}in the parental strain 4N24(**Figure 17a**). In contrast, NYB-2 produced 23.2 mg L^{-1} of nybomycin (**Figure 19b**), reflecting an increase of approximately 102 % over the wild-type strain. The removal of transcriptional repressors led to an enhancement in nybomycin titers, with NYB-1 showing an increase of 2.4-fold and NYB-2 achieving a 1.1-fold improvement.

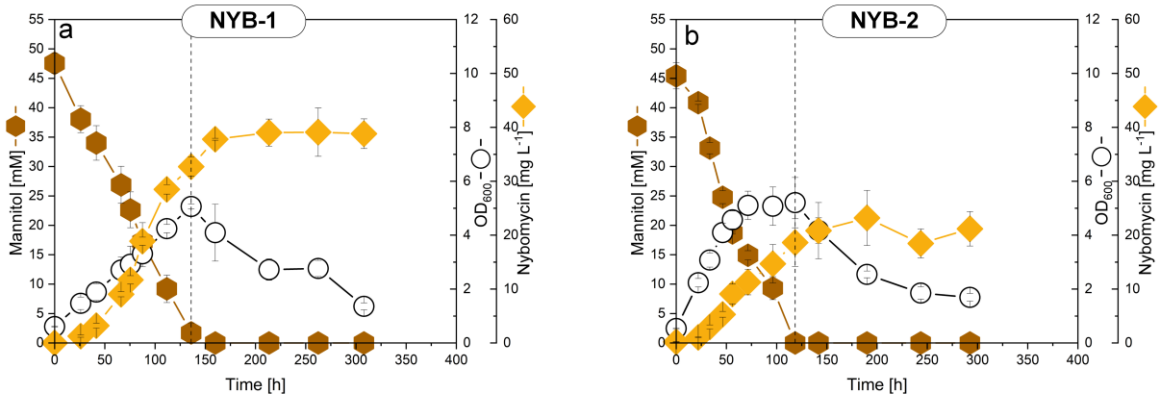

Figure 19: Growth profile and nybomycin production from mannitol in recombinant nybomycin producers. The data includes the cultivation profile of NYB-1 (a) and NYB-2 (b). All strains were grown in shake flask with mannitol based minimal medium, the corresponding genetic layouts are shown in Figure 18. n=3.

These findings suggest that eliminating *nybWX* might alleviates repression within the core biosynthetic pathway, thereby redirecting metabolic flux toward nybomycin synthesis. However, this modification may also influence strain growth, potentially impacting overall productivity. More notably, the combined deletion of *nybWX* indicated revealed that multiple regulators act synergistically in controlling gene cluster expression. A similar phenomenon has been observed in *S. coelicolor* A3(2), where the double deletion of regulators significantly enhanced actinorhodin production (Kim et al., 2018).

Interestingly, despite removing additional transcriptional repressors, NYB-2 did not exhibit a proportionally greater increase in nybomycin yield. This suggests that the simultaneous deletion of multiple regulatory factors may not always have additive effects and, in some cases, may introduce competition or interference between regulatory pathways, leading to diminished improvements in production. Further deletion of *nybY* and *nybZ* may potentially relieve upstream gene clusters from inhibition, prioritizing metabolic resources for cellular growth over secondary metabolism. The excessive release of metabolic flux may thus create competition between rapid growth and nybomycin biosynthesis, ultimately restricting further yield enhancement. A comparable effect was reported in *S. clavuligerus* NRRL3585, where simultaneous expression of three regulatory genes led to only a modest enhancement in

clavulanic acid yield. (Hung et al., 2006). This indicates that an unbalanced distribution of metabolic resources can limit improvements in final product yield when regulatory modifications do not align with optimal metabolic flux allocation.

4.2.6 Combination of regulators with tailored increase of pentose pathway and shikimate pathway fluxes

Transcriptomic analysis identified the overexpression of *zwf2* and *tkt* (**Figure 18a**) as a promising target for improving precursor availability in nybomycin biosynthesis. Since the shikimate pathway provides the carbon backbone for 2,6-diaminophenol, the key precursor of nybomycin, efforts were also directed toward increasing metabolic flux through this pathway. One of the critical enzymes in this pathway, the enzyme DAHP synthase, initiates shikimic acid biosynthesis by catalyzing the condensation of PEP and E4P to form DAHP. Given its role in precursor supply, this enzyme was selected as a target for further pathway optimization. Previous studies have demonstrated that enhancing precursor pathways via overexpression of primary metabolism genes is an effective strategy to increase secondary metabolite yields. Examples include the improvement of daptomycin production in *S. roseosporus* (Huang et al., 2012), ascomycin in *S. hygroscopicus* (Wang et al., 2019), FK506 in *S. tsukubaensis* (Huang et al., 2013), and mithramycin in *Streptomyces argillaceus* (Zabala et al., 2013).

To implement this precursor optimization strategy, four operons contain the *zwf2*, *tkt*, and *nybF* were constructed under the control of strong constitutive promoter P_{kasOP*} (Bai et al., 2015) (**Figure 18b**).The designed constructs included: P_{kasOP*} *nybF-tkt*, P_{kasOP*} *nybF-zwf2*, P_{kasOP*} *tkt-zwf2*, and P_{kasOP*} *nybF-tkt-zwf2*. To further enhance the production of nybomycin, a modular metabolic engineering approach was applied, integrating both primary metabolism and regulatory pathway modules. This involved combining different operons with an optimized nybomycin biosynthetic pathway layout. These operons were subsequently introduced into the regulatory-engineered strains NYB-1 and NYB-2. As a result, eight combinatorial engineered strains were developed to assess the impact of different gene expression patterns and pathway configurations on nybomycin biosynthesis (**Figure 18b**): NYB-3A (4N24 *ΔnybWX* P_{kasOP*} *nybF-tkt*), NYB-3B (4N24 *ΔnybWX* P_{kasOP*} *nybF-zwf2*), NYB-3C (4N24 *ΔnybWX* P_{kasOP*} *tkt-zwf2*), and

NYB-4 (4N24 *ΔnybWX* P_{kasOP*} *nybF-tkt-zwf2*); NYB-5A (4N24 *ΔnybWXYZ* P_{kasOP*} *nybF-tkt*), NYB-5B (4N24 *ΔnybWXYZ* P_{kasOP*} *nybF-zwf2*), NYB-5C (4N24 *ΔnybWXYZ* P_{kasOP*} *tkt-zwf2*), and NYB-6 (4N24 *ΔnybWXYZ* P_{kasOP*} *nybF-tkt-zwf2*).

The engineered mutants were cultivated in the minimal medium with mannitol as the primary carbon source, revealing that dual-gene combinations led to significant improvements in nybomycin yield. Co-expressing *zwf2* alongside other genes resulted in enhanced production, as observed in NYB-3B (57.6 mg L^{-1}) (**Figure 20b**), NYB-3C(49.9 mg L^{-1}) (**Figure 20c**), NYB-5B(27.5 mg L^{-1}) (**Figure 20f**), and NYB-5C(37.0 mg L^{-1}) (**Figure 20g**). The improved *zwf2* expression likely contributed to increased NADPH availability by stimulating the PP pathway, which in turn may have facilitated higher flux toward nybomycin. Elevated NADPH levels have been known to support secondary metabolites production, as seen in chloramphenicol in *S. avermitilis* (Doi et al., 2020), actinorhodin in *S. coelicolor* (Borodina et al., 2008), rapamycin in *S. hygroscopicus* (Dang et al., 2017), and thaxtomins in *S. albus* (Kallifidas et al., 2018).

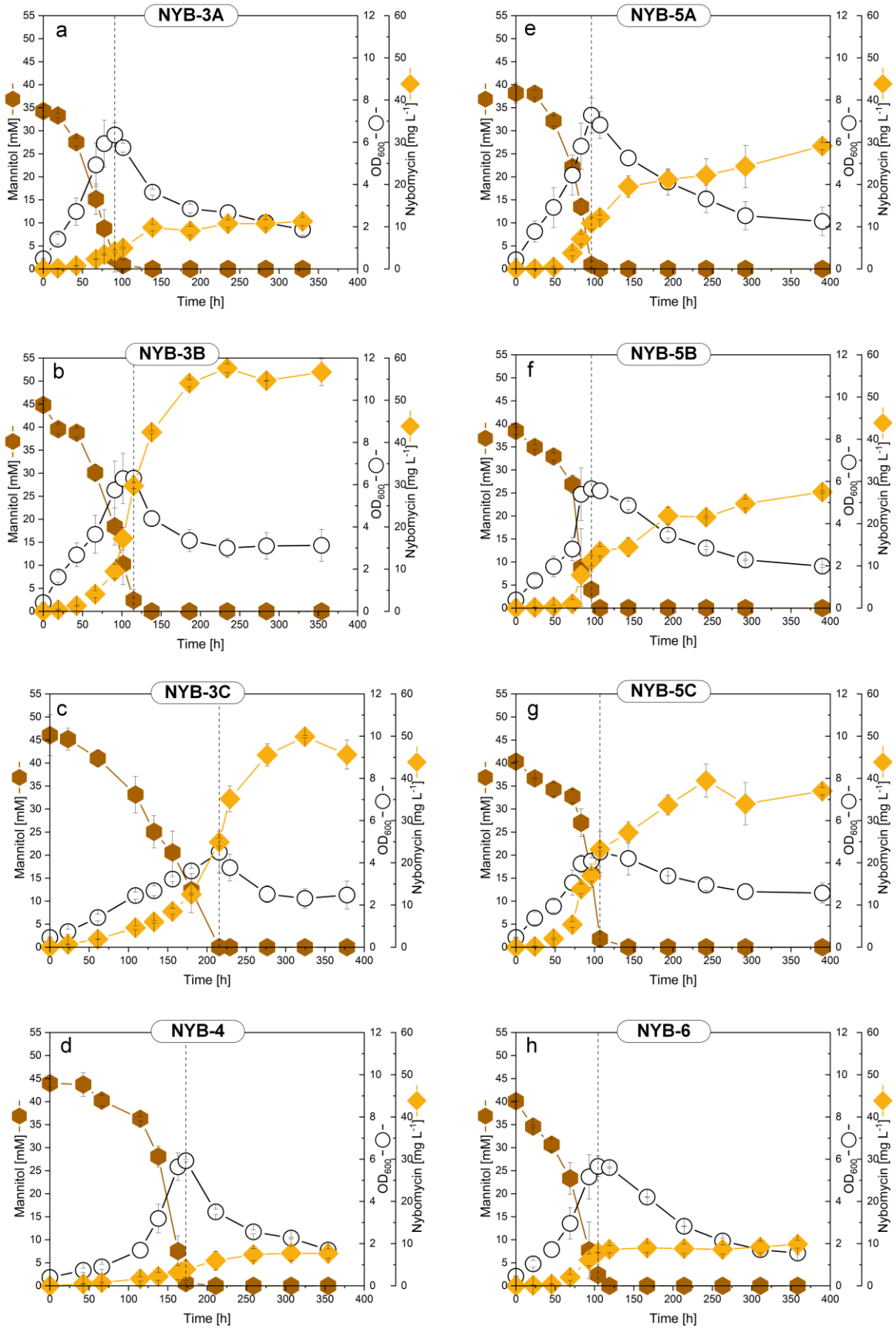

Figure 20: Growth profile and nybomycin production from mannitol in recombinant

nybomycin producers. The data includes the cultivation profile of NYB-3A (a), NYB-3B (b), NYB-3C (c), NYB-4 (d), NYB-5A (e), NYB-5B (f), NYB-5C (g), and NYB-6 (h). All strains were cultivated in shake flask with mannitol based minimal medium, the corresponding genetic layouts are shown in Figure 18. n=3.

The most notable improvement was observed in NYB-3B (**Figure 20b**), where co-expression of *nybF* and *zwf2* in combination with *nybWX* deletion resulted in a more than 5-fold enhancement in nybomycin production, reaching 57.6 mg L^{-1} titer, compared to the baseline strain *S. explomaris* 4N24(**Figure 17a**). This indicates the potential of *zwf2* overexpression, when paired with targeted regulatory modifications, to effectively optimize metabolic flux toward nybomycin biosynthesis.

Unexpectedly, the mutants (NYB-4 and NYB-6) introducing triple-gene combinations of *nybF*, *tkt* and *zwf2* exhibited reduced production (**Figure 20d** and **20h**), with nybomycin titer even lower than the parental strain. This outcome suggests that excessive precursor pathway activation may disrupt intracellular metabolic balance, leading to inefficiencies in biosynthesis. A similar phenomenon has been observed in *S. coelicolor*, the declined oviedomycin production resulted from overexpression of multiple metabolic genes (Gu et al., 2023). This discrepancy could be attributed to the complexity of secondary metabolites biosynthesis, which relies on finely tuned regulatory networks rather than linear metabolic amplification (Ceroni et al., 2015; Dahl et al., 2013; Ji et al., 2019).

To evaluate the nybomycin production capacity of strain NYB-3B, cultivation was conducted using a fed-batch system (**Figure 21**). During the initial batch phase, the strain exhibited exponential growth, reaching a nybomycin concentration of 25.3 mg L^{-1}. At 115 hours, the initial mannitol (10 g L^{-1}) supply was depleted. Following mannitol supplementation to restore the concentration to 10 g L^{-1}, exponential growth resumed, accompanied by the accumulation of an unknown red pigment in the cultural broth (**Appendix Figure A4**). Despite the renewed growth phase, nybomycin production increased only slightly, with the final concentration reaching 29.8 mg L^{-1}. This limited improvement suggests that an elevated mannitol concentration may have triggered a metabolic shift, diverting precursor flux away from

nybomycin biosynthesis toward alternative unidentified pathways. The exact regulatory mechanisms responsible for this metabolic redirection remain unclear and require further investigation to optimize nybomycin yield in fed-batch systems.

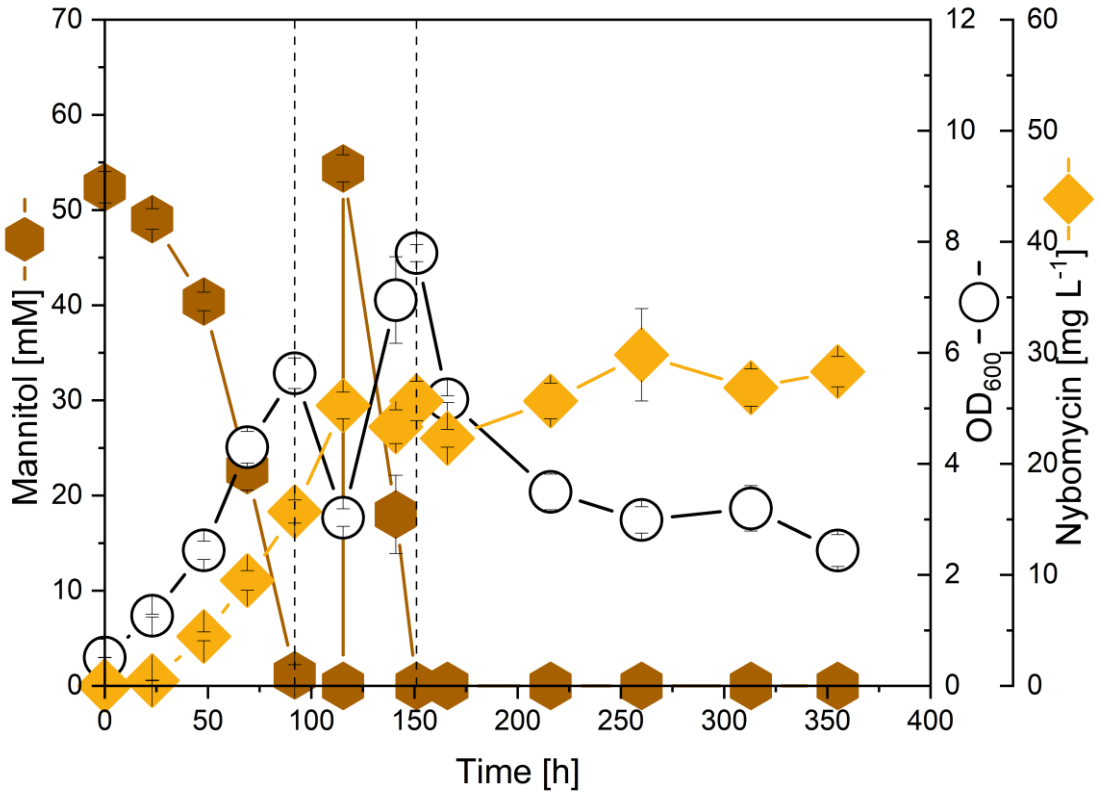

Figure 21: Cultivation profiles of NYB-3B in fed-batch. The NYB-3B was cultivated in 10 g L^{-1} of mannitol minimal medium feeding with 10 g L^{-1} of mannitol. n=3.

By applying systems metabolic engineering, nybomycin production was increased nearly fivefold, with *S. explomaris* mutant NYB-3B yielding the highest reported titer to date. These findings emphasize the crucial role of balancing precursor availability and regulatory control in maximizing secondary metabolite biosynthesis.

4.3 Production of nybomycin from seaweed sugars

Having previously optimized antibiotic biosynthesis pathways at the product level in *S. explomaris*, we now expand our metabolic engineering strategy to include substrate-level improvements in carbon-source utilization. Recognizing that the economic sustainability of antibiotic production strongly depends on the utilize efficiency of abundant renewable carbohydrates such as xylose and arabinose, we selected *S. albus* as an ideal host due to its genetic tractability and identical antibiotic product profile. Employing our established synthetic biology methodologies, and metabolic insights into arabinose metabolism in *S. explomaris*, we aim to systematically engineer arabinose and xylose metabolism pathways in *S. albus* 4N24. Such targeted metabolic engineering is anticipated to enhance nybomycin production efficiency from sustainable substrates, particularly seaweed-derived hydrolysates.

4.3.1 Transfer xylose and arabinose utilization to *S. albus*

Xylose and arabinose are renewable pentose sugars that can be sustainably sourced from seaweed, a rapidly growing marine biomass. Seaweed-derived xylose and arabinose have taken significant part in some microalgae such as *P: palmata* (Maribu et al., 2024), *Ulva linza* (Turner et al., 2022), *Porphyra umbilicalis* (Greetham et al., 2020), and *Rugulopteryx okamurae* (Agabo-Garcia et al., 2023). However, seaweed hydrolysates hydrolysates remain underutilized, largely due to the inability of many industrially relevant microorganisms to efficiently metabolize pentose sugars. Metabolic engineering strategies aimed at enhancing pentose utilization have been successfully implemented in well-established microbial hosts such as *Saccharomyces cerevisiae*, expanding their substrate spectrum and improving bioconversion efficiency (Hoang Nguyen Tran et al., 2020; Ruchala and Sibirny, 2021) and *C. glutamicum* (Buschke et al., 2013; Meiswinkel et al., 2013). The research of these sustainable sugars consumption in *Streptomyces* is still limited.

S. albus J1074 is recognized as one of the fastest-growing heterologous hosts for secondary metabolite production, which contains the smallest linear chromosome among frequently utilized *Streptomyces* spp. host strains (Myronovskyi and Luzhetskyy, 2019; Zaburannyi et al.,

2014). Further minimized genome results in strain *S. albus* Del14 (Myronovskyi et al., 2018), whose highly streamlined metabolic background significantly facilitates the identification and isolation of heterologous expressed compounds. In this regard, nybomycin cluster 4N24 was successfully transferred into this promising host, leading to the creation of *S. albus* 4N24 (Rodríguez Estévez et al., 2018), the first reported example of heterologous nybomycin production. Traditionally, *Streptomyces* species are known for their versatile sugar metabolism, supported by an extensive array of carbohydrate transport systems (Bertram et al., 2004), and the production of a wide variety of extracellular enzymes capable of degrading complex biopolymers in their natural environment (Prakash et al., 2013). However, with inefficient xylose and arabinose utilization capabilities of *S. albus* 4N24, hindered the efficient production of nybomycin using seaweed extracts because of the abundance of arabinose and xylose in seaweed hydrolysate. Hence, metabolic engineering was harnessed to enable efficient xylose and arabinose utilization in *S. albus* 4N24.

Naturally, xylose typically undergoes initial isomerization to xylulose, catalyzed by xylose isomerase (encoded by *xylA*), followed by phosphorylation to xylulose 5-phosphate via xylulose kinase (encoded by *xylB*), and is subsequently channeled into the PP pathway in bacterial (**Figure 22a**) (Wong et al., 1991). In addition, transporters also are essential in xylose utilization, as the initial uptake of substrates is the first key step in the whole metabolism system during the conversion from sugars to products. Therefore, heterologous expression of xylose isomerase, xylulose kinase and xylose transporter could establish the xylose utilization system in *Streptomyces*. For this purpose, we selected the *xylA* gene derived from *X. campestris* pv. *Campestris* ATCC 33913 (Meiswinkel et al., 2013), placing it at the upstream region of our expression module. This was followed downstream by the *xylB* gene from *C. glutamicum* ATCC 13032 (Meiswinkel et al., 2013), and finally by the *xylE* from *E. coli* MG 1655 (Yim et al., 2016) (**Figure 22b**).

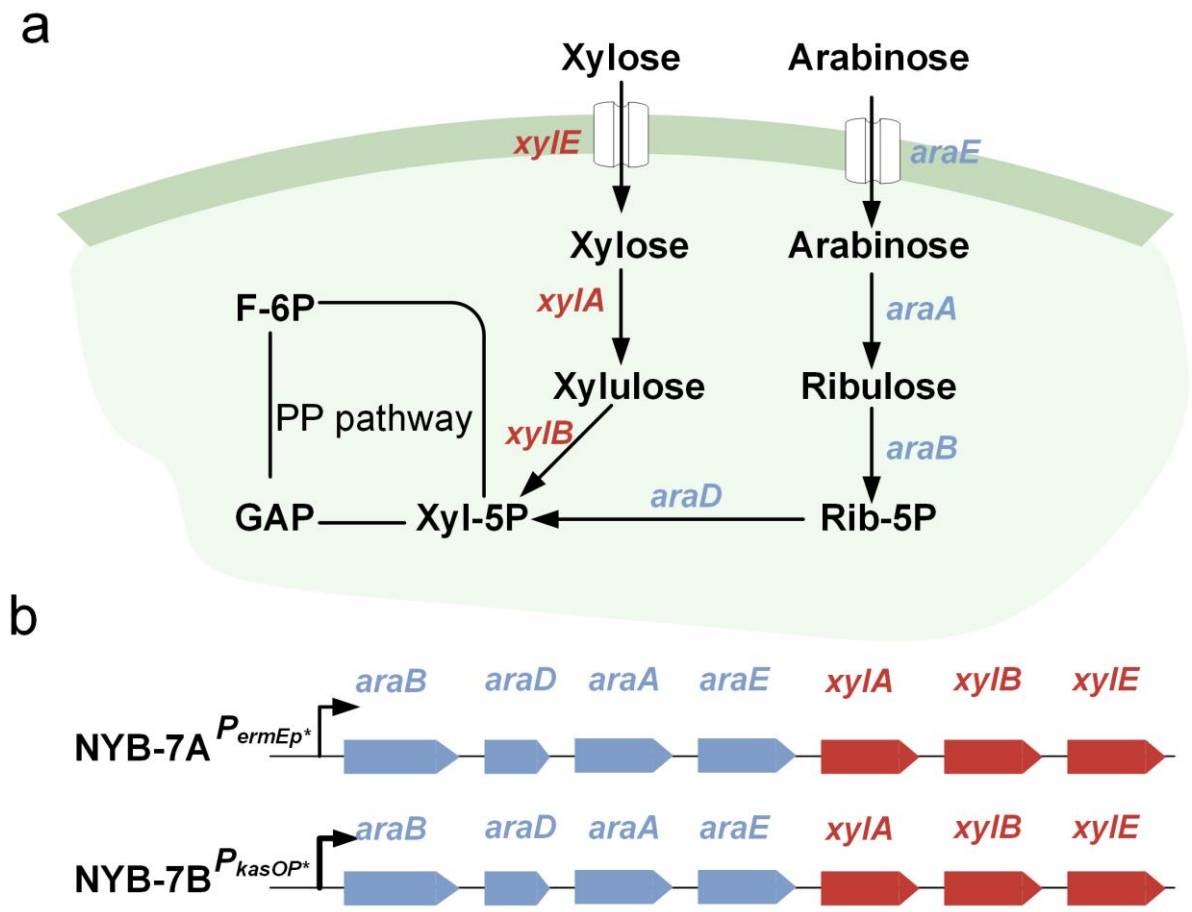

Figure 22: Metabolic pathway design to produce nybomycin in *S. albus* 4N24. The overview illustrates the targets of the pathway for metabolic engineering (a) and the genetic layout of the NYB strain family created in this work (b). Designations and abbreviations: *xylA*, xylose isomerase; *xylB*, xylulose kinase; *xylE*, xylose transporter; *araA*, arabinose isomerase; *araB*, ribulokinase; *araD*, ribulose-5-phosphate 4-epimerase; F-6P, fructose 6-phosphate; GAP, glyceraldehyde 3-phosphate; Rib-5P, ribulose 5-phosphate; Xyl-5P, xylulose 5-phosphate.

The arabinose displayed another sugar relevance, which is contained in some seaweed hydrolysates and the second most abundant pentose in lignocellulosic biomass after xylose (Jacob et al., 2023; Kumar et al., 2023), also represents a significant target. Efficient use these sustainable pentose is crucial for the commercial success of valorization of seaweed extracts. Although *S. albus* 4N24 can metabolize arabinose naturally (**Figure 23c**), further improvements were pursued by overexpressing the complete arabinose metabolic pathway along with a dedicated transporter (Kawaguchi et al., 2009) into the genome of *S. albus*. This involved genomic integration of genes encoding arabinose isomerase (*araA*), ribulokinase

(*araB*), ribulose-5-phosphate 4-epimerase (*araD*), as well as transporter (*araE*) module into genome of *S. albus*. Additionally, *araE* was specifically selected due to its demonstrated capability for xylose transport, providing an advantageous dual benefit for both pentoses (Chen et al., 2017; Sasaki et al., 2009).

Therefore, a synthetic operon (**Figure 22b**) enabling arabinose and xylose utilization was constructed under the control of constitutive P_{ermEp*} promoter (Myronovskyi and Luzhetskyy, 2016), containing *araA*, *araB*, *araD*, *araE*, *xylA*, *xylB*, and *xylE* genes, a 25 bp ribosomal binding site (RBS) (Horbal et al., 2018) as intergenic region between each genes. After intergenic conjugation, the mutant NYB-7A (P_{ermEp*}-*araBDAE-xylABE*) was established.

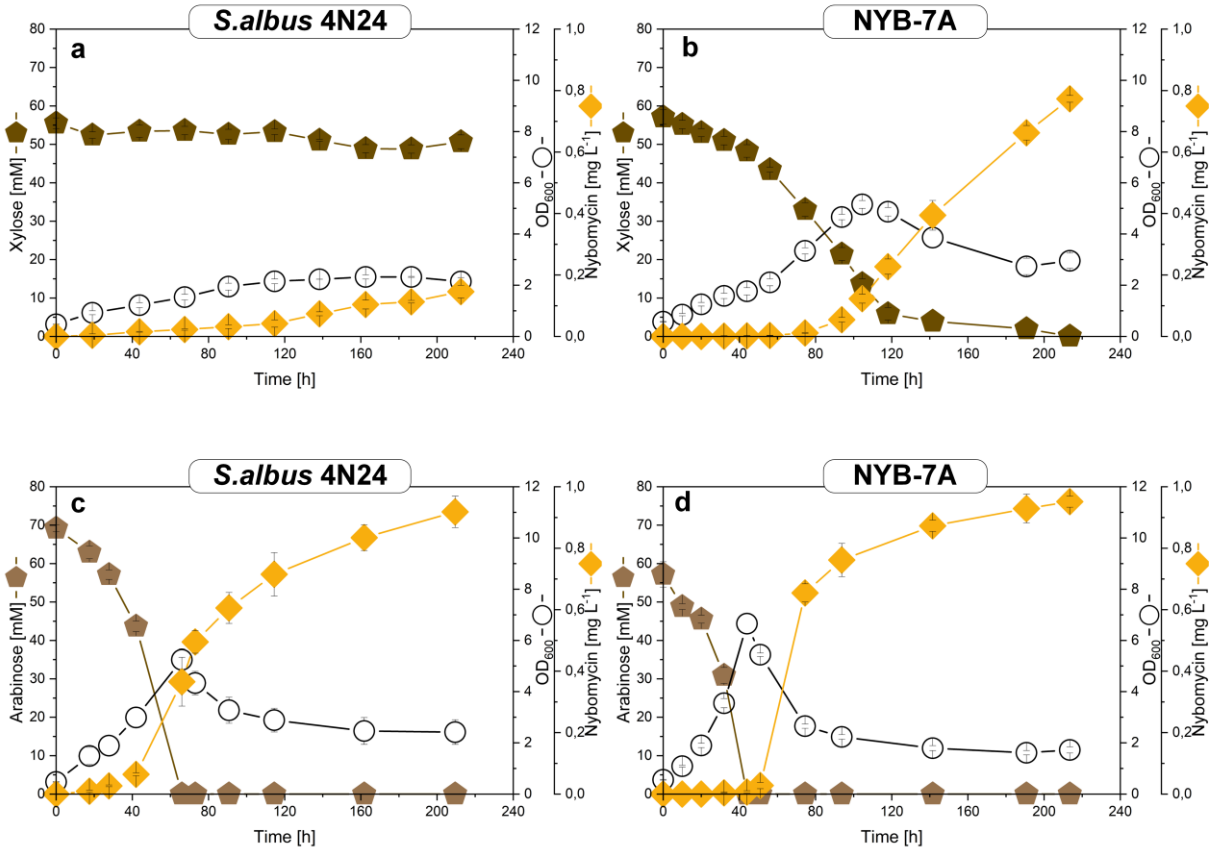

Figure 23: Growth profile of *S. albus* 4N24 and mutant NYB-7A in xylose and arabinose as sole carbon source, respectively. Cultivation of *S. albus* 4N24 in xylose (a), Cultivation of NYB-7A in xylose (b), Cultivation of *S. albus* 4N24 in arabinose (c), Cultivation of NYB-7A in arabinose (d). n=3.

The strain *S. albus* 4N24 and mutant NYB-7A were cultivated on the minimal medium with

xylose and arabinose as sole substrate, respectively. The genetic design enable the efficient xylose and arabinose utilization (**Figure 23b** and **23d**). Xylose was completely consumed during the cultivation process, accumulating 0.77 mg L^{-1} of nybomycin, which improved 5.1-fold compared to *S. albus* 4N24. The high yield of nybomycin in mutant obtained from xylose indicated its significantly contribution to nybomycin production. The fully assimilation of xylose leading to higher biomass yield suggests that xylose metabolism is no longer a bottleneck for cell growth, an increased cell density allows more cells to enter the production phase, thereby boosting nybomycin accumulation. Xylose was efficiently utilized for nybomycin biosynthesis, highlighting its potential as a valuable carbon source. This observation can be attributed to the adequate supply of the key precursor E4P and NADPH, resulting from xylose metabolism via the PP pathway. This finding aligns well with previous reports indicating that xylose positively influenced actinorhodin production in *S. coelicolor* (Świątek et al., 2013) and enhanced validamycin A production in *S. hygroscopicus* 5008 (Zhou and Zhong, 2015).

Although the nybomycin titer of NYB-7A in arabinose was similar to *S. albus* 4N24, the consumption rate of arabinose was improved around 33% (**Figure 23c** and **23d**). These findings indicate that the introduction of the arabinose operon substantially enhances carbon utilization efficiency, leading to faster growth and higher biomass accumulation. The improved arabinose metabolism in the engineered strain can be attributed to the heterologous overexpression of essential enzymes within the arabinose degradation pathway, which facilitate the conversion of arabinose into intermediates of the PP pathway, thereby increasing carbon flux toward central metabolism. The accelerated sugar uptake and conversion efficiency likely contributed to the shortened sugar consumption time and the higher final OD. Similar trends have been reported in engineered *Streptomyces* strains where enhanced sugar catabolism resulted in higher biomass yields and improved metabolic performance (Jin et al., 2020).

Despite the substantial improvement in growth and sugar utilization efficiency, the increase in nybomycin production was relatively modest. This suggests that while enhanced carbon

metabolism supports biomass accumulation, secondary metabolism may be limited by additional regulatory factors rather than by carbon availability alone.

In *Streptomyces*, the biosynthesis of secondary metabolites is often dependent on the growth phase, typically beginning as cells transition from exponential to stationary phase. A faster growth rate of the engineered strain may have altered the timing of secondary metabolism activation, potentially leading to a dilution effect, where the increased biomass does not proportionally contribute to nybomycin biosynthesis. A similar phenomenon has been observed in previous studies, where increased precursor supply did not always translate to higher antibiotic yields due to rate-limiting enzymatic steps (Chen et al., 2020) or transcriptional regulation of nybomycin BGC (Stegmüller et al., 2024). Further transcriptomic or metabolomic analyses would be necessary to elucidate these regulatory mechanisms.

4.3.2 Efficient utilization of xylose and arabinose through expression balance

Promoters are specific DNA regions located upstream of structural genes, essential for RNA polymerase binding and transcription initiation, playing a central role in gene expression regulation. Enhanced gene expression can be achieved by increasing gene copy number or by substituting native promoters with stronger, heterologous ones (Sekurova et al., 2004; Stratigopoulos et al., 2004; Wu et al., 2014). Among these, the constitutive promoter P_{ermEp^*} , derived from the erythromycin resistance gene (*ermE*) of *Saccharopolyspora erythraea*, and characterized by a point mutation, is the most widely employed promoter for heterologous gene expression in *Streptomyces* species (Gomez-Escribano et al., 2014). P_{kasOP^*} promoter is one of the strongest synthetic promoters developed for actinomycetes and therefore is frequently used for gene overexpression (Bai et al., 2015), which shows much strengthened active in contrast to P_{ermEp^*} in *S. albus* 4N24 (Stegmüller et al., 2024).

Although the xylose and arabinose operon with P_{ermEp^*} enable *S. albus* could utilize sugars effectively, the xylose exhausted time was more than 200 h. To make it use xylose more efficient, we decided to use a stronger promoter P_{kasOP^*} to replace P_{ermEp^*} within this operon.

The engineered strain NYB-7B (*P*$_{kasOP*}$-*araBDAE-xylABE*) was constructed afterwards. To investigate the *P*$_{kasOP*}$ promoter impacts on *S. albus*, the cultivation on xylose (10 g L^{-1}) and arabinose (10 g L^{-1}) as sole carbohydrate in the minimal medium were conducted, respectively.

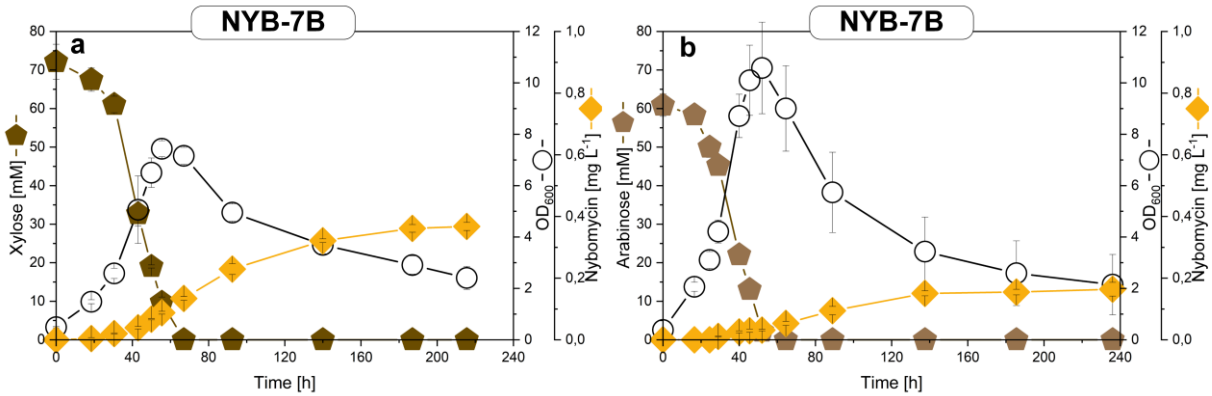

Figure 24: Growth profile of mutant NYB-7B in xylose and arabinose as sole carbon source, respectively. NYB-7B growth on 10 g L^{-1} xylose (a) and 10 g L^{-1} arabinose (b). n=3.

When cultivated in sole xylose medium (**Figure 24a**), the new mutant strain exhibited faster xylose utilization, fully consuming xylose in 67 h, compared to 210 h for the strain with *P*$_{ermEp*}$ promoter. This acceleration in sugar metabolism was accompanied by an increase in maximum OD to 7.4, indicating enhanced biomass accumulation.

In arabinose medium (**Figure 24b**), however, NYB-7B showed an unexpected trend, the time required to fully consume arabinose increased from 44 h to 55 h. Despite this extended consumption period, the strain achieved a higher OD of 10.6, suggesting that a larger fraction of the carbon flux was directed toward biomass formation. The slower arabinose consumption may indicate metabolic burden or regulatory constraints introduced by the stronger promoter, leading to potential inefficiencies in sugar utilization despite an overall increase in cell density.

These results confirm that promoter strength plays a crucial role in optimizing sugar metabolism in *Streptomyces*, affecting both carbon flux distribution and cellular growth dynamics. Despite improved growth, nybomycin production decreased significantly in both xylose and arabinose conditions. In xylose medium, nybomycin titer increased from 0.77 mg

L^{-1} to 0.37 mg L^{-1}, while in arabinose medium, it dropped from 0.95 mg L^{-1} to 0.16 mg L^{-1}. This suggests that stronger sugar metabolism enhances biomass accumulation but negatively impacts secondary metabolism, likely due to metabolic and regulatory trade-offs. In *Streptomyces*, secondary metabolite biosynthesis is typically activated in the change of log phase to stationary phase. The higher biomass accumulation P_{kasOP*} promoter strain suggests that cells likely remained in the active growth phase for a longer period, delaying the metabolic shift toward nybomycin production. This effect was particularly pronounced in arabinose medium, where the higher OD was correlated with the lowest nybomycin production. This phenomenon is well documented in antibiotic-producing *Streptomyces*, where rapid cell proliferation diverts metabolic resources away from secondary metabolism. The increased sugar metabolism in NYB-7B may have caused a redistribution of intracellular carbon flux, favoring primary metabolism over secondary metabolism. Xylose and arabinose are both metabolized through the PP pathway, generating precursors for nucleotide biosynthesis and cofactor regeneration for cell biomass synthesis. Similar metabolic shifts have been observed in engineered *Streptomyces* strains that reduced carbon flux through pp pathway would lead to increased secondary metabolites production (Rossa et al., 2002; Ryu et al., 2006). A detailed transcriptomic and metabolic flux analysis would be necessary to determine whether these differences arise from regulatory effects, metabolic inefficiencies, or differential resource allocation between sugar metabolism and antibiotic biosynthesis.

4.3.3 Engineered *S. explomaris* demonstrates efficient nybomycin production from green, red, and brown seaweed

Given the superior nybomycin yield, NYB-3B was chosen for further fermentation in seaweed hydrolysates(**Figure 25**). However, due to batch variability, the sugar composition in the hydrolysates differed from those used in the cultivation of *S. explomaris* 4N24. The brown seaweed hydrolysate contained 4.1 g L^{-1} of mannitol and 1.9 g L^{-1} of glucose, while the green seaweed hydrolysate had 6.2 g L^{-1} of glucose and 0.8 g L^{-1} of xylose. The red seaweed hydrolysate primarily consisted of 4.5 g L^{-1} of xylose.

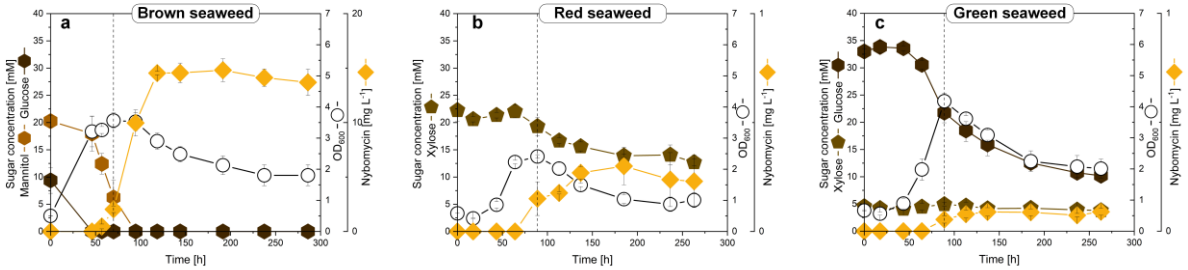

Figure 25: Cultivation profile of *S. explomaris* 4N24 in seaweed hydrolysates. The overview indicates cultivation profile of *S. explomaris* 4N24 in different seaweed hydrolysate (a-c). All cultivations were performed in seaweed hydrolysate supplement with MOPS buffer in shake flask. *S. explomaris* 4N24 grown in brown seaweed hydrolysate (a), red seaweed hydrolysate (b), and green seaweed hydrolysate (c). n=3

In the early phase of brown seaweed hydrolysate cultivation, glucose metabolism supported biomass accumulation, while subsequent mannitol utilization was closely associated with enhanced nybomycin synthesis, ultimately reaching 14.8 mg L^{-1}; nearly twice the yield observed in *S. explomaris* 4N24. The nybomycin yield of NYB-3B remained unchanged when cultivated in red algae hydrolysate and even less in green seaweed extracts, suggesting that these extracts may lack key compounds necessary for optimal biosynthesis. The absence of essential precursors or cofactors might have limited metabolic flux toward nybomycin production, preventing further enhancement. These findings highlight potential of mannitol-rich seaweed hydrolysate as an economical and renewable feedstock for nybomycin biosynthesis. This study establishes a sustainable bioprocess for high-value antibiotic production, demonstrating the industrial viability of renewable raw materials in biopharmaceutical applications.

5 Conclusion and Outlook

This study identified a new isolate Je 1-4^T from coastal rhizosphere soil of *Juniperus excelsa* M. Bieb. (Crimea Peninsula). Phylogenetic studies based on the 16S rRNA gene sequence revealed that Je 1-4^T is phylogenetically close to *S. libani* subsp. *libani* NBRC 13452^T (JCM 4322) and *S. nigrescens* NBRC 12894^T (DSM 40276) with sequence similarities of 99.86 % to 99.93 %. Digital DNA-DNA hybridization (dDDH) analysis showed that Je 1-4^T is distinct from both *S. libani* subsp. *libani* and *S. nigrescens* (dDDH values of 66.6% and 66.7%, respectively), while the latter two strains likely represent the same species (dDDH value of 92.0%). The predominant fatty acids in the strains were *iso*-$C_{16:0}$, *anteiso*-$C_{17:0}$, and *anteiso*-$C_{15:0}$, and the major menaquinones were MK-9(H_6) and MK-9(H_8). Based on these genomic and phenotypic data, strain Je 1-4^T represents a novel species of *Streptomyces*, for which the name *Streptomyces explomaris* sp. nov. is proposed. The type strain is Je 1-4^T (= DSM 117375^T = LMG 33490^T). Additionally, we propose that *Streptomyces libani* subsp. *libani* Baldacci and Grein 1966 (Approved Lists 1980) is a later heterotypic synonym of *Streptomyces nigrescens* (Sveshnikova 1957) Pridham et al. 1958 (Approved Lists 1980).

The new marine isolate *S. explomaris* revealed promising performance as heterologous producer of nybomycin when compared to other hosts. The global transcriptomic analysis indicates that unfavorably downregulation of genes, related to precursors supply including the PP pathway (*zwf2*, *tkt*) and shikimate pathway (DAHP synthase gene). In contrast, the regulatory genes *nybW* and *nybX* were found up-regulated, while *nybY* and *nybZ* were down-regulated significantly. The changed expression pattern then guided metabolic engineering of the microbe. The deletion of the two regulatory genes and four regulatory genes leading to 3.5 fold and 1 fold increasement of nybomycin yield. The deletion of repressors may release the genes in nybomycin biosynthetic pathway from repression and reallocate more carbon flux into this pathway.

In different combination with the overexpression of key metabolic genes *zwf2*, *tkt*, and *nybF*, enhancing the precursor availability. Notably, the highest reported nybomycin titer of 57 mg L$^-$

[1] was achieved in strain NYB-3B, the combined deletion of regulatory repressors (*nybWX*) with overexpression of *nybF* and *zwf2*. It can efficiently utilize untreated brown, red, and green seaweed hydrolysate for nybomycin production, yielding approximately 15 mg L^{-1} nybomycin in brown seaweed hydrolysate, which demonstrates the potential of marine biomass as an alternative feedstock, reducing reliance on traditional agricultural sugars. By integrating improved xylose and arabinose utilization pathways in *S. albus* 4N24, we achieved enhanced antibiotic production from sustainable seaweed sugars. Our findings establish a scalable bioprocess for nybomycin production using renewable marine resources.

The next step should involve the fine-tuning and adaptation of production systems to particular hydrolysates, addressing substrate variability. A question remaining is elucidating the mechanisms underlying nybomycin-substrates interactions, particularly in addressing the production limitations observed at high substrate concentrations. The global regulatory mechanism of nybomycin formation will be important in this regard. Combination with global transcription analysis would be a potential tool to tackle this problem. Future efforts should also focus on optimizing fermentation conditions, paving the way to explore and develop nybomycin for medical treatment.

6 Appendix

6.1 Supplementary data: tables

Primers used in this work are listed in **Table A1**.

Table A1: Specific primers and sequence used for this work

Primers	Sequence
$P_{Ara\_araB\_F}$	GTTGGAGGCAAACACATTACATGTTAGCGATAACACCAATAC
$P_{Ara\_araB\_R}$	CTCTTTGTCGATGTTGTCATATGTGTTTGCCTCCAACGGTTCATTTTA GTTCTCAATTGGCAGGG
$P_{Ara\_araD\_F}$	ACCGTTGGAGGCAAACACATATGACAACATCGACAAAGAG
$P_{Ara\_araD\_R}$	TCGAACGGGTTCTTCATCATATGTGTTTGCCTCCAACGGTTCATTTTA CTGACCGTAGACGTTCTG
$P_{Ara\_araA\_F}$	ACCGTTGGAGGCAAACACATATGATGAAGAACCCGTTCGAAG
$P_{Ara\_araA\_R}$	CGGATGATGTGCCCTGCCATATGTGTTTGCCTCCAACGGTTCATTCT AGAGCTGCTGGGCGAC
$P_{Ara\_araE\_F}$	ACCGTTGGAGGCAAACACATATGGCAGGGCACATCATCCG
$P_{Ara\_araE\_R}$	GCTGAAACTGTTGAAAGTACTCAGACCCTGGCCTTGGTGC
$P_{BT1HP\text{-}Ara\text{-}Xyl1\text{-}F}$	CCGGTTGGTAGGATCCAGCGAATGAACCGTTGGAGGCAAACACATT ACATGTTAGCGATAACACCAATAC
$P_{BT1HP\text{-}Ara\text{-}Xyl2\text{-}R}$	GAGGTTCATGAAGTCCATGTCGATCGAAGACCAGGGCAGC
$P_{BT1HP\text{-}Ara\text{-}Xyl3\text{-}F}$	GCTGCCCTGGTCTTCGATCGACATGGACTTCATGAACCTC
$P_{BT1HP\text{-}Ara\text{-}Xyl1\text{-}R}$	GATGAAAACGGTGTTGCTCATATGTGTTTGCCTCCAACGGTTCATTTC AGACCCTGGCCTTGGTG
$P_{BT1HP\text{-}Ara\text{-}Xyl4\text{-}F}$	GCACCAAGGCCAGGGTCTGAAATGAACCGTTGGAGGCAAACACATA TGAGCAACACCGTTTTCATC
$P_{Ara\_Xyl4\_R}$	ATTCCAAGAACCAAAGCCATATGTGTTTGCCTCCAACGGTTCATTTCA ACGCGTCAGGTACTGATTG
$P_{Ara\_Xyl5\_F}$	CAATCAGTACCTGACGCGTTGAAATGAACCGTTGGAGGCAAACACAT ATGGCTTTGGTTCTTGGAATCG
$P_{Ara\_Xyl5\_R}$	GAATTATACTGGGTATTCATATGTGTTTGCCTCCAACGGTTCATTCTAG TACCAACCCTGCGTTG
$P_{Ara\_Xyl6\_F}$	CAACGCAGGGTTGGTACTAGAATGAACCGTTGGAGGCAAACACATAT GAATACCCAGTATAATTCCAG
$P_{BT1HP\text{-}Ara\text{-}Xyl6\text{-}R}$	TCCGCTGAAACTGTTGAAAGTACTTACAGCGTAGCAGTTTGTTG
$P_{kasOP\text{-}Ara\text{-}Xyl\text{-}F}$	TGGCCGATTCATTAATGCAGTGTTCACATTCGAACGGTCTCTGCTTTG ACAACATGCTGTGCGGTGTTGTAAAGTCGTGGCCAATGAACCGTTG GAGGCAAACACATTACATGTTAGCGA

$P_{kasOP*\text{-}nybF\text{-}zwf\_1}$	AGCGGGTTCGCTCCGTGCAGATGTGTTTGCCTCCAACGGTTCATTTC AGCCCCCCGCCGCCTGCC
$P_{kasOP*\text{-}nybF\text{-}zwf\_2}$	GGCAGGCGGCGGGGGGCTGAAATGAACCGTTGGAGGCAAACACAT CTGCACGGAGCGAACCCGC
$P_{kasOP*\text{-}nybF\text{-}tkt\_1}$	GTGGTCGGCTTGGTGCTCACATGTGTTTGCCTCCAACGGTTCATTTC AGCCCCCCGCCGCCTGCC
$P_{kasOP*\text{-}nybF\text{-}tkt\_2}$	GGCAGGCGGCGGGGGGCTGAAATGAACCGTTGGAGGCAAACACAT GTGAGCACCAAGCCGACCAC
$P_{kasOP*\text{-}tkt\text{-}zwf\_1}$	AGCGGGTTCGCTCCGTGCAGATGTGTTTGCCTCCAACGGTTCATTTC AGCGCTGAGCGGCGGCGA
$P_{kasOP*\text{-}tkt\text{-}zwf\_2}$	TCGCCGCCGCTCAGCGCTGAAATGAACCGTTGGAGGCAAACACATC TGCACGGAGCGAACCCGC
$P_{DnybWXYZ\_Kan\_F}$	ATTTCGGAGGTGAACGTCATCGCAGACAAAGAGCGCACGAAGAGCC GTTTGCTAAAGGAAGCGGAACACG
$P_{DnybWX\_Kan\_R}$	GTCCGCTCGGCGCAGTCCCGCGATGAGGAGAGCGACCAGCCGGC GGGCGTCGCCTGATGCGGTATTTTC
$P_{DnybWXYZ\_Kan\_F}$	ATTTCGGAGGTGAACGTCATCGCAGACAAAGAGCGCACGAAGAGCC GTTTGCTAAAGGAAGCGGAACACG
$P_{DnybWXYZ\_Kan\_R}$	GTCTCCCCCGGGCGCGGTGTGCCGCAGCAGAGGGCCGGTGTGGC GCTGGAGGGCGCCTGATGCGGTATTTTC

Table A2: clustal_align_nucleotide.mao

[MEGAinfo]	
ver	= 10200331-x86_64 MS Windows
[DataSettings]	
datatype	= snNucleotide
containsCodingNuc	= False
missingBaseSymbol	= ?
identicalBaseSymbol	= .
gapSymbol	= -
[ProcessTypes]	
ppAlign	= true
ppClustalW	= true
[AnalysisSettings]	
Pairwise Alignment	= ====================
DNAPWGapOpeningPenalty	= 15.00
DNAPWGapExtensionPenalty	= 6.66
Multiple Alignment	= ====================
DNAMAGapOpeningPenalty	= 15.00
DNAMAGapExtensionPenalty	= 6.66
Global Options	= ====================
DNA Weight Matrix	= IUB
TransitionWeightNEdit	= 0.50
UseNegativeMatrix	= ON
DelayDivergentCutoff	= 30
KeepPredefinedGaps	= True

Table A3: infer_ME_nucleotide.mao

[MEGAinfo]	
ver	= 10200331-x86_64 MS Windows
[DataSettings]	
datatype	= snNucleotide
containsCodingNuc	= False
MissingBaseSymbol	= ?
IdenticalBaseSymbol	= .
GapSymbol	= -
Labelled Sites	= All Sites
Labels to Include	=
[ProcessTypes]	
ppInfer	= true
ppME	= true
[AnalysisSettings]	
Analysis	= Phylogeny Reconstruction
Scope	= All Selected Taxa
Statistical Method	= Minimum Evolution method
Phylogeny Test	= ==========
Test of Phylogeny	= None
No. of Bootstrap Replications	= Not Applicable
Substitution Model	= ==========
Substitutions Type	= Nucleotide
Model/Method	= Maximum Composite Likelihood
Substitutions to Include	= d: Transitions + Transversions
Rates and Patterns	= ==========
Rates among Sites	= Uniform Rates
Gamma Parameter	= Not Applicable
Pattern among Lineages	= Same (Homogeneous)
Data Subset to Use	= ==========
Gaps/Missing Data Treatment	= Pairwise deletion
Site Coverage Cutoff (%)	= Not Applicable
Tree Inference Options	= ==========
ME Heuristic Method	= Close-Neighbor-Interchange (CNI)
Initial Tree for ME	= Obtain initial tree by Neighbor-Joining

ME Search Level	= 1
System Resource Usage	= ==========
Number of Threads	= 1
Has Time Limit	= False
Maximum Execution Time	= -1

Table A4: infer_ML_nucleotide.mao

[MEGAinfo]	
ver	= 10200331-x86_64 MS Windows
[DataSettings]	
datatype	= snNucleotide
containsCodingNuc	= False
MissingBaseSymbol	= ?
IdenticalBaseSymbol	= .
GapSymbol	= -
Labelled Sites	= All Sites
Labels to Include	=
[ProcessTypes]	
ppInfer	= true
ppML	= true
[AnalysisSettings]	
Analysis	= Phylogeny Reconstruction
Statistical Method	= Maximum Likelihood
Phylogeny Test	= ==========
Test of Phylogeny	= Bootstrap method
No. of Bootstrap Replications	= 100
Substitution Model	= ==========
Substitutions Type	= Nucleotide
Model/Method	= Tamura-Nei model
Rates and Patterns	= ==========
Rates among Sites	= Gamma Distributed With Invariant Sites (G+I)
No of Discrete Gamma Categories	= 5
Data Subset to Use	= ==========
Gaps/Missing Data Treatment	= Use all sites
Site Coverage Cutoff (%)	= Not Applicable
Tree Inference Options	= ==========
ML Heuristic Method	= Nearest-Neighbor-Interchange (NNI)
Initial Tree for ML	= Make initial tree automatically (Default - NJ/BioNJ)
Branch Swap Filter	= None
System Resource Usage	= ==========
Number of Threads	= 8
Has Time Limit	= False
Maximum Execution Time	= -1

Table A5: infer_MP_nucleotide.mao

MEGAinfo]	
ver	= 10200331-x86_64 MS Windows
[DataSettings]	
datatype	= snNucleotide
containsCodingNuc	= False
MissingBaseSymbol	= ?
IdenticalBaseSymbol	= .
GapSymbol	= -
Labelled Sites	= All Sites
Labels to Include	=
[ProcessTypes]	
ppInfer	= true
ppMP	= true
[AnalysisSettings]	
Analysis	= Phylogeny Reconstruction
Statistical Method	= Maximum Parsimony
Phylogeny Test	= ==========
Test of Phylogeny	= Bootstrap method
No. of Bootstrap Replications	= 100
Substitution Model	= ==========
Substitutions Type	= Nucleotide
Data Subset to Use	= ==========
Gaps/Missing Data Treatment	= Use all sites
Site Coverage Cutoff (%)	= Not Applicable
Tree Inference Options	= ==========
MP Search Method	= Subtree-Pruning-Regrafting (SPR)
No. of Initial Trees (random addition)	= 10
MP Search level	= 1
Max No. of Trees to Retain	= 100
System Resource Usage	= ==========
Number of Threads	= 8
Has Time Limit	= False
Maximum Execution Time	= -1

Table A6: infer_NJ_nucleotide.mao

[MEGAinfo]	
ver	= 10200331-x86_64 MS Windows
[DataSettings]	
datatype	= snNucleotide
containsCodingNuc	= False
MissingBaseSymbol	= ?
IdenticalBaseSymbol	= .
GapSymbol	= -
Labelled Sites	= All Sites
Labels to Include	=
[ProcessTypes]	
ppInfer	= true
ppNJ	= true
[AnalysisSettings]	
Analysis	= Phylogeny Reconstruction
Scope	= All Selected Taxa
Statistical Method	= Neighbor-joining
Phylogeny Test	= ==========
Test of Phylogeny	= None
No. of Bootstrap Replications	= Not Applicable
Substitution Model	= ==========
Substitutions Type	= Nucleotide
Model/Method	= Maximum Composite Likelihood
Substitutions to Include	= d: Transitions + Transversions
Rates and Patterns	= ==========
Rates among Sites	= Uniform Rates
Gamma Parameter	= Not Applicable
Pattern among Lineages	= Same (Homogeneous)
Data Subset to Use	= ==========
Gaps/Missing Data Treatment	= Pairwise deletion
Site Coverage Cutoff (%)	= Not Applicable
System Resource Usage	= ==========
Number of Threads	= 1
Has Time Limit	= False

```
Maximum Execution Time              = -1
```

6.2 Supplementary data: figures

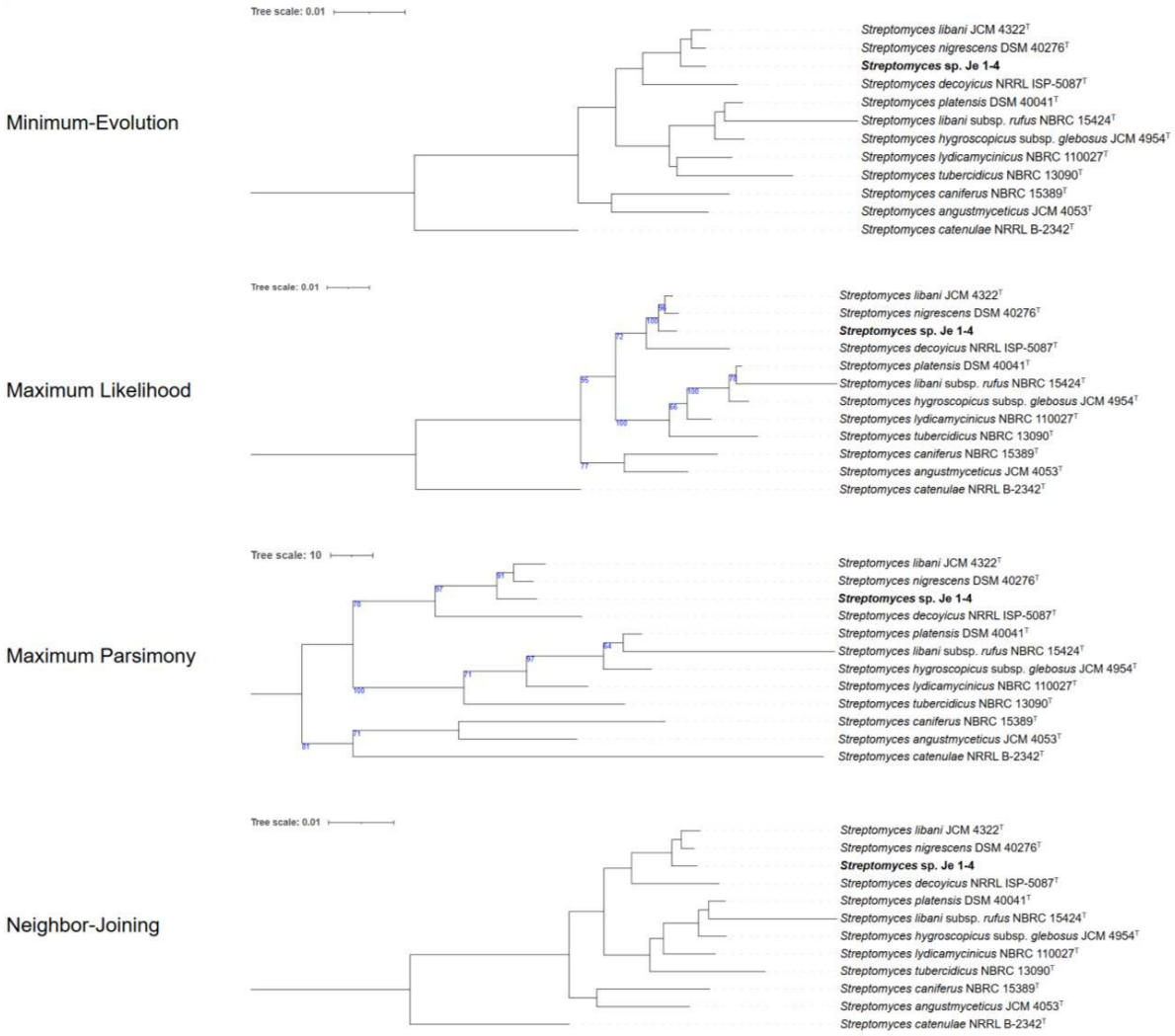

Figure A1: Calculation of four phylogenetic trees based on a CLUSTAL alignment of the *atpD, gyrB, recA*, *rpoB*, and *trpB* genes. The algorithms employed were Minimum-Evolution (ME), Maximum Likelihood (ML), Maximum Parsimony (MP), and Neighbor-Joining (NJ).

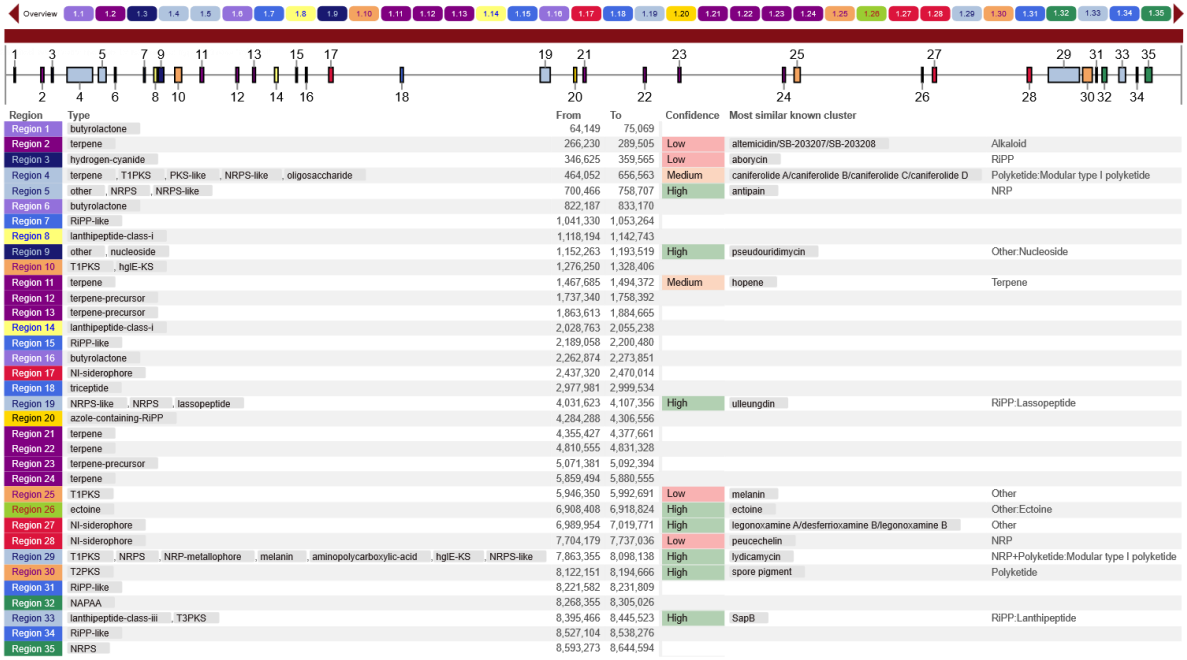

Region	Type	From	To	Confidence	Most similar known cluster	
Region 1	butyrolactone	64,149	75,069			
Region 2	terpene	266,230	289,505	Low	altemicidin/SB-203207/SB-203208	Alkaloid
Region 3	hydrogen-cyanide	346,625	359,565	Low	aborycin	RiPP
Region 4	terpene, T1PKS, PKS-like, NRPS-like, oligosaccharide	464,052	656,563	Medium	caniferolide A/caniferolide B/caniferolide C/caniferolide D	Polyketide:Modular type I polyketide
Region 5	other, NRPS, NRPS-like	700,466	758,707	High	antipain	NRP
Region 6	butyrolactone	822,187	833,170			
Region 7	RiPP-like	1,041,330	1,053,264			
Region 8	lanthipeptide-class-i	1,118,194	1,142,743			
Region 9	other, nucleoside	1,152,263	1,193,519	High	pseudouridimycin	Other:Nucleoside
Region 10	T1PKS, hglE-KS	1,276,250	1,328,406			
Region 11	terpene	1,467,685	1,494,372	Medium	hopene	Terpene
Region 12	terpene-precursor	1,737,340	1,758,392			
Region 13	terpene-precursor	1,863,613	1,884,665			
Region 14	lanthipeptide-class-i	2,028,763	2,055,238			
Region 15	RiPP-like	2,189,058	2,200,480			
Region 16	butyrolactone	2,262,874	2,273,851			
Region 17	NI-siderophore	2,437,320	2,470,014			
Region 18	triceptide	2,977,981	2,999,534			
Region 19	NRPS-like, NRPS, lassopeptide	4,031,623	4,107,356	High	ulleungdin	RiPP:Lassopeptide
Region 20	azole-containing-RiPP	4,284,288	4,306,556			
Region 21	terpene	4,355,427	4,377,661			
Region 22	terpene	4,810,555	4,831,328			
Region 23	terpene-precursor	5,071,381	5,092,394			
Region 24	terpene	5,859,494	5,880,555			
Region 25	T1PKS	5,946,350	5,992,691	Low	melanin	Other
Region 26	ectoine	6,908,408	6,918,824	High	ectoine	Other:Ectoine
Region 27	NI-siderophore	6,989,954	7,019,771	High	legonoxamine A/desferrioxamine B/legonoxamine B	Other
Region 28	NI-siderophore	7,704,179	7,737,036	Low	peucechelin	NRP
Region 29	T1PKS, NRPS, NRP-metallophore, melanin, aminopolycarboxylic-acid, hglE-KS, NRPS-like	7,863,355	8,098,138	High	lydicamycin	NRP+Polyketide:Modular type I polyketide
Region 30	T2PKS	8,122,151	8,194,666	High	spore pigment	Polyketide
Region 31	RiPP-like	8,221,582	8,231,809			
Region 32	NAPAA	8,268,355	8,305,026			
Region 33	lanthipeptide-class-iii, T3PKS	8,395,466	8,445,523	High	SapB	RiPP:Lanthipeptide
Region 34	RiPP-like	8,527,104	8,538,276			
Region 35	NRPS	8,593,273	8,644,594			

Figure A2: Biosynthetic gene clusters (BGCs) encoded in the genome strain Je 1-4^T as revealed by ANTISMASH analysis.

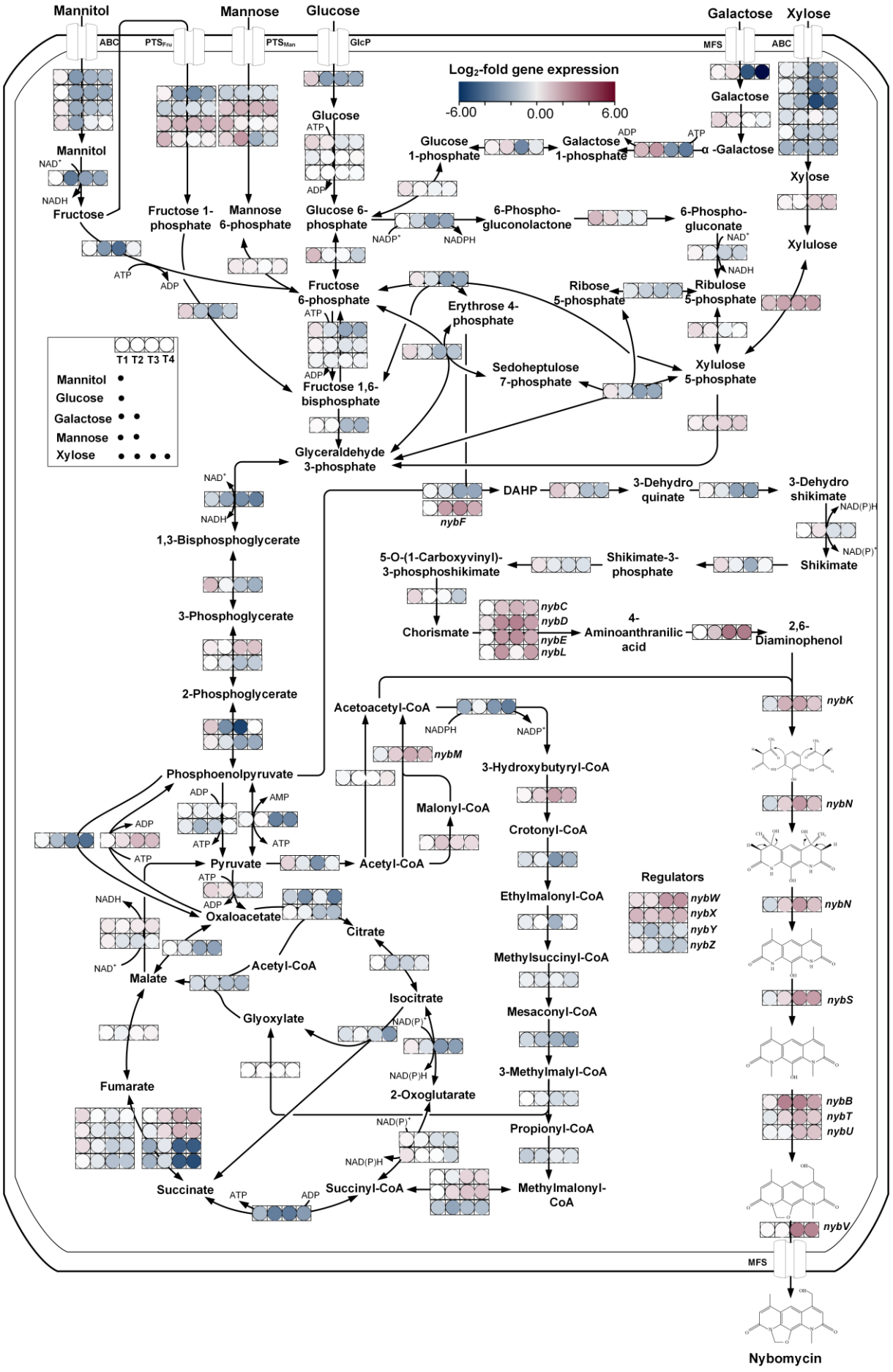
Mannitol
Mannose
Glucose
Galactose
Xylose
ABC
PTS$_{Fru}$
PTS$_{Man}$
GlcP
MFS
ABC
Log$_2$-fold gene expression
-6.00
0.00
6.00
Mannitol
Fructose
Fructose 1-phosphate
Mannose 6-phosphate
Glucose
Glucose 6-phosphate
Glucose 1-phosphate
Galactose 1-phosphate
α -Galactose
Galactose
Xylose
Xylulose
6-Phospho-gluconolactone
6-Phospho-gluconate
Ribose 5-phosphate
Ribulose 5-phosphate
Xylulose 5-phosphate
Fructose 6-phosphate
Erythrose 4-phosphate
Sedoheptulose 7-phosphate
Fructose 1,6-bisphosphate
Glyceraldehyde 3-phosphate
T1 T2 T3 T4
Mannitol
Glucose
Galactose
Mannose
Xylose
DAHP
nybF
3-Dehydro quinate
3-Dehydro shikimate
Shikimate
Shikimate-3-phosphate
5-O-(1-Carboxyvinyl)-3-phosphoshikimate
Chorismate
nybC
nybD
nybE
nybL
4-Aminoanthranilic acid
2,6-Diaminophenol
1,3-Bisphosphoglycerate
3-Phosphoglycerate
2-Phosphoglycerate
Phosphoenolpyruvate
Pyruvate
Acetyl-CoA
Acetoacetyl-CoA
nybM
Malonyl-CoA
3-Hydroxybutyryl-CoA
Crotonyl-CoA
Ethylmalonyl-CoA
Methylsuccinyl-CoA
Mesaconyl-CoA
3-Methylmalyl-CoA
Propionyl-CoA
Methylmalonyl-CoA
Succinyl-CoA
Succinate
Fumarate
Malate
Oxaloacetate
Citrate
Isocitrate
2-Oxoglutarate
Glyoxylate
Regulators
nybW
nybX
nybY
nybZ
nybK
nybN
nybN
nybS
nybB
nybT
nybU
nybV
MFS
Nybomycin

Figure A3: Time-resolved transcriptome analysis in *S. explomaris* 4N24 in saltwater. The data display the expression differences between early exponential phase (T1, 12 h, as reference), mid-exponential phase (T2, 36 h), stationary phase (T3, 75 h), and late phase (T4, 175 h). The metabolic network was assembled based on KEGG, including glycolysis, PP pathway, TCA cycle, shikimate pathway and nybomycin biosynthesis pathway. The black dot under each time points represents carbon sources availability at different time points. The circle in square represents gene at different timepoint, expression differences are highlighted by color (blue: down regulated, red: up regulated). n=3.

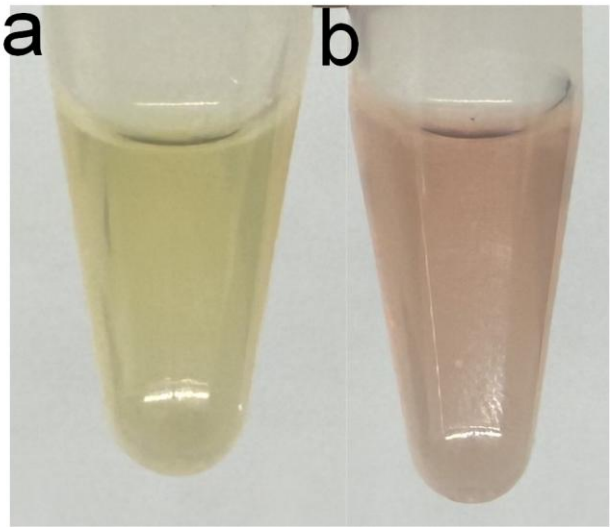

Figure A4: Broth color of cultivation in *S. explomaris* NYB-3B. Cultivation broth color of NYB-3B with 10 g L^{-1} of mannitol (a), and cultivation broth color of NYB 3B in fed-batch (b).

7 References

Agabo-Garcia, C., Romero-Garcia, L.I., Alvarez-Gallego, C.J., Blandino, A. 2023. Valorisation of the invasive alga *Rugulopteryx okamurae* through the production of monomeric sugars. *Appl Microbiol Biotechnol*, **107**(5-6), 1971-1982.

Agtarap, A., Chamberlin, J.W., Pinkerton, M., Steinrauf, L.K. 1967. Structure of monensic acid, a new biologically active compound. *J Am Chem Soc*, **89**(22), 5737-5739.

Alam, K., Mazumder, A., Sikdar, S., Zhao, Y.M., Hao, J., Song, C., Wang, Y., Sarkar, R., Islam, S., Zhang, Y., Li, A. 2022. *Streptomyces*: The biofactory of secondary metabolites. *Front Microbiol*, **13**, 968053.

Alam, M.T., Merlo, M.E., Takano, E., Breitling, R. 2010. Genome-based phylogenetic analysis of *Streptomyces* and its relatives. *Mol Phylogenet Evol*, **54**(3), 763-72.

Alderson, G., Goodfellow, M., Minnikin, D.E. 1985. Menaquinone Composition in the Classification of *Streptomyces* and Other *Sporoactinomycetes*. *Microbiol*, **131**, 1671-1679.

Aldred, K.J., McPherson, S.A., Turnbough, C.L., Jr., Kerns, R.J., Osheroff, N. 2013. Topoisomerase IV-quinolone interactions are mediated through a water-metal ion bridge: mechanistic basis of quinolone resistance. *Nucleic Acids Res*, **41**(8), 4628-39.

Anderson, A.S., Wellington, E.M. 2001. The taxonomy of *Streptomyces* and related genera. *Int J Syst Evol Microbiol*, **51**(3), 797-814.

Andersson, M.I., MacGowan, A.P. 2003. Development of the quinolones. *J Antimicrob Chemother*, **51**(suppl_1), 1-11.

Anne, J., Maldonado, B., Van Impe, J., Van Mellaert, L., Bernaerts, K. 2012. Recombinant protein production and *Streptomycetes*. *J Biotechnol*, **158**(4), 159-67.

Antony-Babu, S., Stien, D., Eparvier, V., Parrot, D., Tomasi, S., Suzuki, M.T. 2017. Multiple *Streptomyces* species with distinct secondary metabolomes have identical 16S rRNA gene sequences. *Sci Rep*, **7**(1), 11089.

Arai, M., Kamiya, K., Pruksakorn, P., Sumii, Y., Kotoku, N., Joubert, J.P., Moodley, P., Han, C., Shin, D., Kobayashi, M. 2015. Anti-dormant mycobacterial activity and target analysis of nybomycin produced by a marine-derived *Streptomyces* sp. *Bioorg Med Chem*, **23**(13), 3534-41.

Asif, A., Mohsin, H., Tanvir, R., Rehman, Y. 2017. Revisiting the Mechanisms Involved in Calcium Chloride Induced Bacterial Transformation. *Front Microbiol*, **8**.

Aslam, B., Wang, W., Arshad, M.I., Khurshid, M., Muzammil, S., Rasool, M.H., Nisar, M.A., Alvi, R.F., Aslam, M.A., Qamar, M.U., Salamat, M.K.F., Baloch, Z. 2018. Antibiotic resistance: a rundown of a global crisis. *Infect Drug Resist*, **11**, 1645-1658.

Bai, B., Zhou, J.M., Yang, M.H., Liu, Y.L., Xu, X.H., Xing, J.M. 2015. Efficient production of

succinic acid from macroalgae hydrolysate by metabolically engineered *Escherichia coli*. *Bioresour Technol*, **185**, 56-61.

Bai, C., Zhang, Y., Zhao, X., Hu, Y., Xiang, S., Miao, J., Lou, C., Zhang, L. 2015. Exploiting a precise design of universal synthetic modular regulatory elements to unlock the microbial natural products in *Streptomyces*. *Proc Natl Acad Sci U S A*, **112**(39), 12181-12186.

Baltz, R.H. 2010. *Streptomyces* and *Saccharopolyspora* hosts for heterologous expression of secondary metabolite gene clusters. *J Ind Microbiol Biotechnol*, **37**(8), 759-72.

Banos, S., Perez-Redondo, R., Koekman, B., Liras, P. 2009. Glycerol utilization gene cluster in *Streptomyces clavuligerus*. *Appl Environ Microbiol*, **75**(9), 2991-5.

Barakat, K.M., Beltagy, E.A. 2015. Bioactive phthalate from marine *Streptomyces ruber* EKH2 against virulent fish pathogens. *Egyptian Journal of Aquatic Research*, **41**(1), 49-56.

Bardell-Cox, O.A., White, A.J.P., Aragón, L., Fuchter, M.J. 2019. Synthetic studies on the reverse antibiotic natural products, the nybomycins. *MedChemComm*, **10**(8), 1438-1444.

Barka, E.A., Vatsa, P., Sanchez, L., Gaveau-Vaillant, N., Jacquard, C., Meier-Kolthoff, J.P., Klenk, H.P., Clement, C., Ouhdouch, Y., van Wezel, G.P. 2016. Taxonomy, Physiology, and Natural Products of Actinobacteria. *Microbiol Mol Biol Rev*, **80**(1), 1-43.

Barkei, J.J., Kevany, B.M., Felnagle, E.A., Thomas, M.G. 2009. Investigations into viomycin biosynthesis by using heterologous production in *Streptomyces lividans*. *Chembiochem*, **10**(2), 366-76.

Bauer, A.W., Kirby, W.M.M., Sherris, J.C., Turck, M. 1966. Antibiotic Susceptibility Testing by a Standardized Single Disk Method. *Am J Clin Pathol*, **45**(4_ts), 493-496.

Beganovic, S., Ruckert-Reed, C., Sucipto, H., Shu, W., Glaser, L., Patschkowski, T., Struck, B., Kalinowski, J., Luzhetskyy, A., Wittmann, C. 2023. Systems biology of industrial oxytetracycline production in *Streptomyces rimosus*: the secrets of a mutagenized hyperproducer. *Microb Cell Fact*, **22**(1), 222.

Beites, T., Rodriguez-Garcia, A., Santos-Beneit, F., Moradas-Ferreira, P., Aparicio, J.F., Mendes, M.V. 2014. Genome-wide analysis of the regulation of pimaricin production in *Streptomyces natalensis* by reactive oxygen species. *Appl Microbiol Biotechnol*, **98**(5), 2231-41.

Bennani, H., Mateus, A., Mays, N., Eastmure, E., Stark, K.D.C., Hasler, B. 2020. Overview of Evidence of Antimicrobial Use and Antimicrobial Resistance in the Food Chain. *Antibiotics (Basel)*, **9**(2).

Bentley, S.D., Chater, K.F., Cerdeño-Tárraga, A.M., Challis, G.L., Thomson, N.R., James, K.D., Harris, D.E., Quail, M.A., Kieser, H., Harper, D., Bateman, A., Brown, S., Chandra, G., Chen, C.W., Collins, M., Cronin, A., Fraser, A., Goble, A., Hidalgo, J., Hornsby, T.,

Howarth, S., Huang, C.H., Kieser, T., Larke, L., Murphy, L., Oliver, K., O'Neil, S., Rabbinowitsch, E., Rajandream, M.A., Rutherford, K., Rutter, S., Seeger, K., Saunders, D., Sharp, S., Squares, R., Squares, S., Taylor, K., Warren, T., Wietzorrek, A., Woodward, J., Barrell, B.G., Parkhill, J., Hopwood, D.A. 2002. Complete genome sequence of the model actinomycete *Streptomyces coelicolor* A3(2). *Nature*, **417**(6885), 141-147.

Bergy, M.E., Eble, T.E., Herr, R.R. 1961. Actinospec-tacin, a New Antibiotic: IV. Isolation, Purification, and Chemical Properties. *Antibiot Chemother (Northfield)*, **11**, 661-664.

Bertram, R., Schlicht, M., Mahr, K., Nothaft, H., Saier, M.H., Jr., Titgemeyer, F. 2004. In silico and transcriptional analysis of carbohydrate uptake systems of *Streptomyces coelicolor* A3(2). *J Bacteriol*, **186**(5), 1362-73.

Bibb, M.J. 2005. Regulation of secondary metabolism in *Streptomycetes*. *Curr Opin Microbiol*, **8**(2), 208-15.

Bilyk, O., Luzhetskyy, A. 2016. Metabolic engineering of natural product biosynthesis in actinobacteria. *Curr Opin Biotechnol*, **42**, 98-107.

Bilyk, O., Sekurova, O.N., Zotchev, S.B., Luzhetskyy, A. 2016. Cloning and Heterologous Expression of the Grecocycline Biosynthetic Gene Cluster. *PLoS One*, **11**(7), e0158682.

Blin, K., Shaw, S., Augustijn, H.E., Reitz, Z.L., Biermann, F., Alanjary, M., Fetter, A., Terlouw, B.R., Metcalf, W.W., Helfrich, E.J.N., van Wezel, G.P., Medema, M.H., Weber, T. 2023. antiSMASH 7.0: new and improved predictions for detection, regulation, chemical structures and visualisation. *Nucleic Acids Res*, **51**(W1), W46-w50.

Bonadonna, G., Monfardini, S., de Lena, M., Fossati-Bellani, F. 1969. Clinical evaluation of adriamycin, a new antitumour antibiotic. *Br Med J*, **3**(5669), 503-506.

Borodina, I., Preben, K., Nielsen, J. 2005. Genome-scale analysis of *Streptomyces coelicolor* A3(2) metabolism. *Genome Res*, **15**(6), 820-829.

Borodina, I., Siebring, J., Zhang, J., Smith, C.P., van Keulen, G., Dijkhuizen, L., Nielsen, J. 2008. Antibiotic overproduction in *Streptomyces coelicolor* A3 2 mediated by phosphofructokinase deletion. *J Biol Chem*, **283**(37), 25186-25199.

Brawner, M.E., Mattern, S.G., Babcock, M.J., Westpheling, J. 1997. The *Streptomyces galP1* promoter has a novel RNA polymerase recognition sequence and is transcribed by a new form of RNA polymerase in vitro. *J Bacteriol*, **179**(10), 3222-3231.

Bruce J. Walker, T.A., Terrance Shea, Margaret Priest, Amr Abouelliel, Sharadha Sakthikumar, Christina A. Cuomo, Qiandong Zeng, Jennifer Wortman, Sarah K. Young, Ashlee M. Earl. 2014. Pilon: An Integrated Tool for Comprehensive Microbial Variant Detection and Genome Assembly Improvement. *PLoS One*, **9**(11).

Burg, R.W., Miller, B.M., Baker, E.E., Birnbaum, J., Currie, S.A., Hartman, R., Kong, Y.-L., Monaghan, R.L., Olson, G., Putter, I., Tunac, J.B., Wallick, H., Stapley, E.O., Oiwa, R.,

Ōmura, S. 1979. Avermectins, New Family of Potent Anthelmintic Agents: Producing Organism and Fermentation. *Antimicrob Agents Chemother*, **15**(3), 361-367.

Buschke, N., Becker, J., Schäfer, R., Kiefer, P., Biedendieck, R., Wittmann, C. 2013. Systems metabolic engineering of xylose-utilizing *Corynebacterium glutamicum* for production of 1,5-diaminopentane. *Biotechnol J*, **8**(5), 557-570.

Butler, M.J., Bruheim, P., Jovetic, S., Marinelli, F., Postma, P.W., Bibb, M.J. 2002. Engineering of primary carbon metabolism for improved antibiotic production in *Streptomyces lividans*. *Appl Environ Microbiol*, **68**(10), 4731-9.

Camacho, C., Coulouris, G., Avagyan, V., Ma, N., Papadopoulos, J., Bealer, K., Madden, T.L. 2009. BLAST+: architecture and applications. *BMC Bioinformatics*, **10**(1), 421.

Campbell, W.C. 1985. Ivermectin: an update. *Parasitol Today*, **1**(1), 10-6.

Carere, C.R., Sparling, R., Cicek, N., Levin, D.B. 2008. Third generation biofuels via direct cellulose fermentation. *Int J Mol Sci*, **9**(7), 1342-60.

Ceroni, F., Algar, R., Stan, G.B., Ellis, T. 2015. Quantifying cellular capacity identifies gene expression designs with reduced burden. *Nat Methods*, **12**(5), 415-8.

Chades, T., Scully, S.M., Ingvadottir, E.M., Orlygsson, J. 2018. Fermentation of Mannitol Extracts From Brown Macro Algae by *Thermophilic Clostridia*. *Front Microbiol*, **9**, 1931.

Challis, G.L., Hopwood, D.A. 2003. Synergy and contingency as driving forces for the evolution of multiple secondary metabolite production by *Streptomyces* species. *Proc Natl Acad Sci U S A*, **100**(Suppl 2), 14555-61.

Chater, K.F. 1972. A Morphological and Genetic Mapping Study of White Colony Mutants of *Streptomyces coelicolor*. *Microbiol*, **72**(1), 9-28.

Chen, H., Cui, J., Wang, P., Wang, X., Wen, J. 2020. Enhancement of bleomycin production in *Streptomyces verticillus* through global metabolic regulation of N-acetylglucosamine and assisted metabolic profiling analysis. *Microb Cell Fact*, **19**(1), 32.

Chen, Y., Wendt-Pienkowski, E., Shen, B. 2008. Identification and utility of FdmR1 as a *Streptomyces* antibiotic regulatory protein activator for fredericamycin production in *Streptomyces griseus* ATCC 49344 and heterologous hosts. *J Bacteriol*, **190**(16), 5587-96.

Chen, Z., Huang, J., Wu, Y., Wu, W., Zhang, Y., Liu, D. 2017. Metabolic engineering of *Corynebacterium glutamicum* for the production of 3-hydroxypropionic acid from glucose and xylose. *Metab Eng*, **39**, 151-158.

Choi, S.U., Lee, C.K., Hwang, Y.I., Kinoshita, H., Nihira, T. 2004. Intergeneric conjugal transfer of plasmid DNA from *Escherichia coli* to *Kitasatospora setae*, a bafilomycin B1 producer. *Arch Microbiol*, **181**(4), 294-8.

Chun, J., Rainey, F.A. 2014. Integrating genomics into the taxonomy and systematics of the Bacteria and Archaea. *Int J Syst Evol Microbiol*, **64**(Pt 2), 316-324.

Claessen, D., Rozen, D.E., Kuipers, O.P., Sogaard-Andersen, L., van Wezel, G.P. 2014. Bacterial solutions to multicellularity: a tale of biofilms, filaments and fruiting bodies. *Nat Rev Microbiol*, **12**(2), 115-24.

Coenye, T., Gevers, D., Van de Peer, Y., Vandamme, P., Swings, J. 2005. Towards a prokaryotic genomic taxonomy. *FEMS Microbiol Rev*, **29**(2), 147-67.

Cozzarelli, N.R. 1980. DNA Gyrase and the Supercoiling of DNA. *Science*, **207**(4434), 953-960.

Dahl, R.H., Zhang, F., Alonso-Gutierrez, J., Baidoo, E., Batth, T.S., Redding-Johanson, A.M., Petzold, C.J., Mukhopadhyay, A., Lee, T.S., Adams, P.D., Keasling, J.D. 2013. Engineering dynamic pathway regulation using stress-response promoters. *Nat Biotechnol*, **31**(11), 1039-46.

Dang, L., Liu, J., Wang, C., Liu, H., Wen, J. 2017. Enhancement of rapamycin production by metabolic engineering in *Streptomyces hygroscopicus* based on genome-scale metabolic model. *J Ind Microbiol Biotechnol*, **44**(2), 259-270.

Daquioag, J.E.L., Penuliar, G.M. 2021. Isolation of *Actinomycetes* with Cellulolytic and Antimicrobial Activities from Soils Collected from an Urban Green Space in the Philippines. *Int J Microbiol*, **2021**, 6699430.

Debono, M., Abbott, B.J., Molloy, R.M., Fukuda, D.S., HUNT, A.H., Daupert, V.M., Counter, F.T., Ott, J.L., Carrell, C.B., Howard, L.C. 1988. Enzymatic and chemical modifications of ipopeptide antibiotic A21978c: the synthesis and evaluation of daptomycin (Ly146032). *J Antibiot*, **41**(8), 1093-1105.

Delbaere, L.T., Sudom, A.M., Prasad, L., Leduc, Y., Goldie, H. 2004. Structure/function studies of phosphoryl transfer by phosphoenolpyruvate carboxykinase. *Biochim Biophys Acta*, **1697**(1-2), 271-8.

Deng, Q., Zhou, L., Luo, M., Deng, Z., Zhao, C. 2017. Heterologous expression of Avermectins biosynthetic gene cluster by construction of a Bacterial Artificial Chromosome library of the producers. *Synth Syst Biotechnol*, **2**(1), 59-64.

Dhakal, D., Rayamajhi, V., Mishra, R., Sohng, J.K. 2019. Bioactive molecules from Nocardia: diversity, bioactivities and biosynthesis. *J Ind Microbiol Biotechnol*, **46**(3-4), 385-407.

Doi, S., Komatsu, M., Ikeda, H. 2020. Modifications to central carbon metabolism in an engineered *Streptomyces* host to enhance secondary metabolite production. *J Biosci Bioeng*, **130**(6), 563-570.

Du, L., Liu, R.H., Ying, L., Zhao, G.R. 2012. An efficient intergeneric conjugation of DNA from Escherichia coli to mycelia of the lincomycin-producer *Streptomyces lincolnensis*. *Int J Mol Sci*, **13**(4), 4797-4806.

El-Tayeb, T.S., Abdelhafez, A.A., Ali, S.H., Ramadan, E.M. 2012. Effect of acid hydrolysis and fungal biotreatment on agro-industrial wastes for obtainment of free sugars for

bioethanol production. *Braz J Microbio*, **43**, 1523-1535.

Embley, T., O'Donnell, A., Rostron, J., Goodfellow, M. 1988. Chemotaxonomy of Wall Type IV *Actinomycetes* Which Lack Mycolic Acids. *J Gen Microbiol*, **134**, 953-960.

Enquist-Newman, M., Faust, A.M.E., Bravo, D.D., Santos, C.N.S., Raisner, R.M., Hanel, A., Sarvabhowman, P., Le, C., Regitsky, D.D., Cooper, S.R., Peereboom, L., Clark, A., Martinez, Y., Goldsmith, J., Cho, M.Y., Donohoue, P.D., Luo, L., Lamberson, B., Tamrakar, P., Kim, E.J., Villari, J.L., Gill, A., Tripathi, S.A., Karamchedu, P., Paredes, C.J., Rajgarhia, V., Kotlar, H.K., Bailey, R.B., Miller, D.J., Ohler, N.L., Swimmer, C., Yoshikuni, Y. 2013. Efficient ethanol production from brown macroalgae sugars by a synthetic yeast platform. *Nature*, **505**(7482), 239-243.

Fang, C., Thomsen, M.H., Brudecki, G.P., Cybulska, I., Frankaer, C.G., Bastidas-Oyanedel, J.R., Schmidt, J.E. 2015. Seawater as Alternative to Freshwater in Pretreatment of Date Palm Residues for Bioethanol Production in Coastal and/or Arid Areas. *ChemSusChem*, **8**(22), 3823-31.

Fang, Q., Maglangit, F., Mugat, M., Urwald, C., Kyeremeh, K., Deng, H. 2020. Targeted Isolation of Indole Alkaloids from *Streptomyces* sp. CT37. *Molecules*, **25**(5).

Farris, J.S. 1972. Estimating Phylogenetic Trees from Distance Matrices. *Am Nat*, **106**(951), 645-668.

Felnagle, E.A., Rondon, M.R., Berti, A.D., Crosby, H.A., Thomas, M.G. 2007. Identification of the biosynthetic gene cluster and an additional gene for resistance to the antituberculosis drug capreomycin. *Appl Environ Microbiol*, **73**(13), 4162-70.

Feng, Z., Wang, L., Rajski, S.R., Xu, Z., Coeffet-LeGal, M.F., Shen, B. 2009. Engineered production of iso-migrastatin in heterologous *Streptomyces* hosts. *Bioorg Med Chem*, **17**(6), 2147-53.

Flardh, K., Buttner, M.J. 2009. *Streptomyces* morphogenetics: dissecting differentiation in a filamentous bacterium. *Nat rev Microbiol*, **7**(1), 36-49.

Forster, J., Radulovich, R. 2015. Chapter 11 - Seaweed and food security. in: *Seaweed Sustainability*, (Eds.) B.K. Tiwari, D.J. Troy, Academic Press. San Diego, pp. 289-313.

Fukuda, H., Hori, S., Hiramatsu, K. 1998. Antibacterial Activity of Gatifloxacin (AM-1155, CG5501, BMS-206584), a Newly Developed Fluoroquinolone, against Sequentially Acquired Quinolone-Resistant Mutants and thenorA Transformant of *Staphylococcus aureus*. *Antimicrob Agents Chemother*, **42**(8), 1917-1922.

García-Gutiérrez, C., Aparicio, T., Torres-Sánchez, L., Martínez-García, E., de Lorenzo, V., Villar, C.J., Lombó, F. 2020. Multifunctional SEVA shuttle vectors for actinomycetes and Gram-negative bacteria. *Microbiologyopen*, **9**(6), e1024.

Garrity, G.M. 2016. A New Genomics-Driven Taxonomy of Bacteria and Archaea: Are We There Yet?. *J Clin Microbiol* **54**(8), 1955-1963.

Gellert, M., Mizuuchi, K., O'Dea, M.H., Itoh, T., Tomizawa, J.-I. 1977. Nalidixic Acid Resistance: A Second Genetic Character Involved in DNA Gyrase Activity. *Proc Natl Acad Sci U S A*, **74**(11), 4772-4776.

Genilloud, O. 2017. Actinomycetes: still a source of novel antibiotics. *Nat Prod Rep*, **34**(10), 1203-1232.

Gibson, D.G., Young, L., Chuang, R.-Y., Venter, J.C., Hutchison, C.A., Smith, H.O. 2009. Enzymatic assembly of DNA molecules up to several hundred kilobases. *Nat Methods*, **6**(5), 343-345.

Github. nanoporetech/medaka: Sequence correction provided by ONT Research. [accessed].

Glaeser, S.P., Kampfer, P. 2015. Multilocus sequence analysis (MLSA) in prokaryotic taxonomy. *Syst Appl Microbiol*, **38**(4), 237-45.

Gläser, L., Kuhl, M., Stegmüller, J., Rückert, C., Myronovskyi, M., Kalinowski, J., Luzhetskyy, A., Wittmann, C. 2021. Superior production of heavy pamamycin derivatives using a bkdR deletion mutant of *Streptomyces albus* J1074/R2. *Microb Cell Fact*, **20**(1), 111.

Goh, C.S., Lee, K.T. 2010. A visionary and conceptual macroalgae-based third-generation bioethanol (TGB) biorefinery in Sabah, Malaysia as an underlay for renewable and sustainable development. *Renew Sustain Energy Rev*, **14**(2), 842-848.

Gomez-Escribano, Pablo, J., Bibb, M.J. 2014. Heterologous expression of natural product biosynthetic gene clusters in *Streptomyces coelicolor*: from genome mining to manipulation of biosynthetic pathways. *J Ind Microbiol Biotechnol*, **41**(2), 425-431.

Goodfellow, M., Busarakam, K., Idris, H., Labeda, D.P., Nouioui, I., Brown, R., Kim, B.-Y., del Carmen Montero-Calasanz, M., Andrews, B.A., Bull, A.T. 2017. *Streptomyces asenjonii* sp. nov., isolated from hyper-arid Atacama Desert soils and emended description of *Streptomyces viridosporus* Pridham et al. 1958. *Antonie Van Leeuwenhoek*, **110**(9), 1133-1148.

Goodfellow, M., Minnikin, D.E. 1985. *Society for Applied Bacteriology*. Orlando: Academic Press.

Goodfellow, M., Williams, S.T., Mordarski, M. 1988. *Actinomycetes in Biotechnology*. Academic Press.

Gordon, D., Abajian, C., Green, P. 1998. Consed: a graphical tool for sequence finishing. *Genome Res*, **8**(3), 195-202.

Gorke, B., Stulke, J. 2008. Carbon catabolite repression in bacteria: many ways to make the most out of nutrients. *Nat Rev Microbiol*, **6**(8), 613-24.

Goto, T., Kino, T., Hatanaka, H., Nishiyama, M., Okuhara, M., Kohsaka, M., Aoki, H., Imanaka, H. 1987. Discovery of FK-506, a novel immunosuppressant isolated from *Streptomyces tsukubaensis*. *Transplant Proc* **19**, 4-8.

Grace Alderson, M.G., David E Minnikin. 1985. Menaquinone Composition in the Classification

of *Streptomyces* and Other *Sporoactinomycetes*. *J Gen Microbiol*, **131**, 1671-1679.

Greetham, D., Adams, J.M., Du, C. 2020. The utilization of seawater for the hydrolysis of macroalgae and subsequent bioethanol fermentation. *Sci Rep*, **10**(1), 9728.

Groisillier, A., Shao, Z., Michel, G., Goulitquer, S., Bonin, P., Krahulec, S., Nidetzky, B., Duan, D., Boyen, C., Tonon, T. 2014. Mannitol metabolism in brown algae involves a new phosphatase family. *J Exp Bot*, **65**(2), 559-70.

Gu, B., Kim, D.G., Kim, D.K., Kim, M., Kim, H.U., Oh, M.K. 2023. Heterologous overproduction of oviedomycin by refactoring biosynthetic gene cluster and metabolic engineering of host strain *Streptomyces coelicolor*. *Microb Cell Fact*, **22**(1), 212.

Gupta, R.S. 2021. Microbial Taxonomy: How and Why Name Changes Occur and Their Significance for (Clinical) Microbiology. *Clin Chem*, **68**(1), 134-137.

Han, J.H., Cho, M.H., Kim, S.B. 2012. Ribosomal and protein coding gene based multigene phylogeny on the family *Streptomycetaceae*. *Syst Appl Microbiol*, **35**(1), 1-6.

Hargreaves, P.I., Barcelos, C.A., da Costa, A.C.A., Pereira, N. 2013. Production of ethanol 3G from *Kappaphycus alvarezii*: Evaluation of different process strategies. *Bioresour Technol*, **134**, 257-263.

Harrison, J., Studholme, D.J. 2014. Recently published *Streptomyces* genome sequences. *Microb Biotechnol*, **7**(5), 373-80.

Hata, T., Sano, Y., Sugawara, R., Matsumae, A., Kanamori, K., Shima, T., Hoshi, T. 1956. Mitomycin, a new antibiotic from *Streptomyces*. I. *J Antibiot, Series A*, **9**(4), 141-146.

Hilker, R., Stadermann, K.B., Doppmeier, D., Kalinowski, J., Stoye, J., Straube, J., Winnebald, J., Goesmann, A. 2014. ReadXplorer--visualization and analysis of mapped sequences. *Bioinformatics*, **30**(16), 2247-54.

Hiramatsu, K., Igarashi, M., Morimoto, Y., Baba, T., Umekita, M., Akamatsu, Y. 2012. Curing bacteria of antibiotic resistance: reverse antibiotics, a novel class of antibiotics in nature. *Int J Antimicrob Agents*, **39**(6), 478-85.

Hiramatsu, K., Sasaki, T., Morimoto, Y.U.H. 2015. Future Chemotherapy Preventing Emergence of Multi-Antibiotic Resistance. *Juntendo Med J*, **61**(3), 249-256.

Hoang Nguyen Tran, P., Ko, J.K., Gong, G., Um, Y., Lee, S.-M. 2020. Improved simultaneous co-fermentation of glucose and xylose by *Saccharomyces cerevisiae* for efficient lignocellulosic biorefinery. *Biotechnol biofuels*, **13**(1), 12.

Hodgson, D.A. 1982. Glucose Repression of Carbon Source Uptake and Metabolism in *Streptomyces coelicolor* A3(2) and its Perturbation in Mutants Resistant to 2-Deoxyglucose. *Microbiol*, **128**(10), 2417-2430.

Hoffmann, S.L., Kohlstedt, M., Jungmann, L., Hutter, M., Poblete-Castro, I., Becker, J., Wittmann, C. 2021. Cascaded valorization of brown seaweed to produce l-lysine and value-added products using *Corynebacterium glutamicum* streamlined by systems

metabolic engineering. *Metab Eng*, **67**, 293-307.

Hooper, D.C. 1999. Mode of Action of Fluoroquinolones. *Drugs*, **58**(2), 6-10.

Hopwood, D.A. 2019. Highlights of *Streptomyces* genetics. *Heredity (Edinb)*, **123**(1), 23-32.

Hopwood, D.A. 2006. Soil to genomics: the *Streptomyces* chromosome. *Annu Rev Genet*, **40**, 1-23.

Horbal, L., Marques, F., Nadmid, S., Mendes, M.V., Luzhetskyy, A. 2018. Secondary metabolites overproduction through transcriptional gene cluster refactoring. *Metab Eng*, **49**, 299-315.

Horbal, L., Siegl, T., Luzhetskyy, A. 2018. A set of synthetic versatile genetic control elements for the efficient expression of genes in Actinobacteria. *Sci Rep*, **8**(1), 491.

Hou, X., From, N., Angelidaki, I., Huijgen, W.J.J., Bjerre, A.B. 2017. Butanol fermentation of the brown seaweed *Laminaria digitata* by *Clostridium beijerinckii* DSM-6422. *Bioresour Technol*, **238**, 16-21.

Huang, D., Li, S., Xia, M., Wen, J., Jia, X. 2013. Genome-scale metabolic network guided engineering of *Streptomyces tsukubaensis* for FK506 production improvement. *Microb Cell Fact*, **12**(1), 52.

Huang, D., Wen, J., Wang, G., Yu, G., Jia, X., Chen, Y. 2012. In silico aided metabolic engineering of *Streptomyces roseosporus* for daptomycin yield improvement. *Appl Microbiol Biotechnol*, **94**(3), 637-49.

Huang, S., Millar, A.H. 2013. Succinate dehydrogenase: the complex roles of a simple enzyme. *Curr Opin Plant Biol*, **16**(3), 344-349.

Huang, X., Ma, T., Tian, J., Shen, L., Zuo, H., Hu, C., Liao, G. 2017. wblA, a pleiotropic regulatory gene modulating morphogenesis and daptomycin production in *Streptomyces roseosporus*. *J Appl Microbiol*, **123**(3), 669-677.

Huergo, L.F., Araujo, G.A.T., Santos, A.S.R., Gerhardt, E.C.M., Pedrosa, F.O., Souza, E.M., Forchhammer, K. 2020. The NADP-dependent malic enzyme MaeB is a central metabolic hub controlled by the acetyl-CoA to CoASH ratio. *Biochim Biophys Acta Proteins Proteom*, **1868**(9), 140462.

Hugenholtz, P., Chuvochina, M., Oren, A., Parks, D.H., Soo, R.M. 2021. Prokaryotic taxonomy and nomenclature in the age of big sequence data. *Isme J*, **15**(7), 1879-1892.

Hung, T.V., Ishida, K., Parajuli, N., Liou, K., Lee, H.C., Sohng, J.K. 2006. Enhanced clavulanic acid production in *Streptomyces clavuligerus* NRRL3585 by overexpression of regulatory genes. *Biotechnol Bioprocess Eng*, **11**(2), 116-120.

Hwang, K.S., Kim, H.U., Charusanti, P., Palsson, B.O., Lee, S.Y. 2014. Systems biology and biotechnology of *Streptomyces* species for the production of secondary metabolites. *Biotechnol Adv*, **32**(2), 255-68.

Hwang, S., Lee, N., Jeong, Y., Lee, Y., Kim, W., Cho, S., Palsson, B.O., Cho, B.K. 2019.

Primary transcriptome and translatome analysis determines transcriptional and translational regulatory elements encoded in the *Streptomyces clavuligerus* genome. *Nucleic Acids Res*, **47**(12), 6114-6129.

Ian, E., Malko, D.B., Sekurova, O.N., Bredholt, H., Ruckert, C., Borisova, M.E., Albersmeier, A., Kalinowski, J., Gelfand, M.S., Zotchev, S.B. 2014. Genomics of sponge-associated *Streptomyces* spp. closely related to *Streptomyces albus* J1074: insights into marine adaptation and secondary metabolite biosynthesis potential. *PLoS One*, **9**(5), e96719.

Ikeda, H., Kazuo, S.Y., Omura, S. 2014. Genome mining of the *Streptomyces avermitilis* genome and development of genome-minimized hosts for heterologous expression of biosynthetic gene clusters. *J Ind Microbiol Biotechnol*, **41**(2), 233-50.

Ivana Charousová, S.J., Joachim Wink. 2015. Isolation and characterization of *Streptomyces rishiriensis* (VY31) with antibiotic activity against various pathogenic microorganisms. *J Microbiol Biotechnol Food Sci* **4**, 23-27.

Jacob, S., Dilshani, A., Rishivanthi, S., Khaitan, P., Vamsidhar, A., Rajeswari, G., Kumar, V., Rajak, R., Din, M., Zambare, V. 2023. Lignocellulose-Derived Arabinose for Energy and Chemicals Synthesis through Microbial Cell Factories: A Review. *Processes*, **11**(5), 1516.

Ji, C.H., Kim, H., Kang, H.S. 2019. Synthetic Inducible Regulatory Systems Optimized for the Modulation of Secondary Metabolite Production in *Streptomyces*. *ACS Synth Biol*, **8**(3), 577-586.

Jin, P., Li, S., Zhang, Y., Chu, L., He, H., Dong, Z., Xiang, W. 2020. Mining and fine-tuning sugar uptake system for titer improvement of milbemycins in *Streptomyces bingchenggensis*. *Synth Syst Biotechnol*, **5**(3), 214-221.

Jin, X.M., Chang, Y.K., Lee, J.H., Hong, S.K. 2017. Effects of Increased NADPH Concentration by Metabolic Engineering of the Pentose Phosphate Pathway on Antibiotic Production and Sporulation in *Streptomyces lividans* TK24. *J Microbiol Biotechnol*, **27**(10), 1867-1876.

Jin, Z., Jin, X., Jin, Q. 2010. Conjugal transferring of resistance gene ptr for improvement of pristinamycin-producing *Streptomyces pristinaespiralis*. *Appl Biochem Biotechnol*, **160**(6), 1853-64.

John Ehrlich, Quentin R. Bartz, Robert M. Smith, Dwight A. Joslyn, Burkholder, P.R. 1947. Chloromycetin, a New Antibiotic From a Soil Actinomycete. *Science*, **106**(2757), 417.

Jolley, K.A., Bray, J.E., Maiden, M.C.J. 2018. Open-access bacterial population genomics: BIGSdb software, the PubMLST.org website and their applications. *Wellcome Open Res*, **3**, 124.

Jung, W.S., Kim, E., Yoo, Y.J., Ban, Y.H., Kim, E.J., Yoon, Y.J. 2014. Characterization and engineering of the ethylmalonyl-CoA pathway towards the improved heterologous

production of polyketides in *Streptomyces venezuelae*. *Appl Microbiol Biotechnol*, **98**(8), 3701-13.

Kallifidas, D., Jiang, G., Ding, Y., Luesch, H. 2018. Rational engineering of *Streptomyces albus* J1074 for the overexpression of secondary metabolite gene clusters. *Microb Cell Fact*, **17**(1), 25.

Kang, H.S., Kim, E.S. 2021. Recent advances in heterologous expression of natural product biosynthetic gene clusters in *Streptomyces* hosts. *Curr Opin Biotechnol*, **69**, 118-127.

Kawaguchi, H., Sasaki, M., Vertes, A.A., Inui, M., Yukawa, H. 2009. Identification and functional analysis of the gene cluster for L-arabinose utilization in *Corynebacterium glutamicum*. *Appl Environ Microbiol*, **75**(11), 3419-29.

Kenneth, L., Rinehart, J., Leadbetter, G., Larson, R.A., Forbis, R.M. 1970. Nybomycin. III. Revised structure. *J Am Chem Soc*, **92**(23), 6994-6995.

Kepplinger, B., Morton-Laing, S., Seistrup, K.H., Marrs, E.C.L., Hopkins, A.P., Perry, J.D., Strahl, H., Hall, M.J., Errington, J., Allenby, N.E.E. 2018. Mode of Action and Heterologous Expression of the Natural Product Antibiotic Vancoresmycin. *ACS Chem Biol*, **13**(1), 207-214.

Kern, A., Tilley, E., Hunter, I.S., Legisa, M., Glieder, A. 2007. Engineering primary metabolic pathways of industrial micro-organisms. *J Biotechnol*, **129**(1), 6-29.

Kiefer, P., Heinzle, E., Zelder, O., Wittmann, C. 2004. Comparative Metabolic Flux Analysis of Lysine-Producing *Corynebacterium glutamicum* Cultured on Glucose or Fructose. *Appl Environ Microbiol*, **70**(1), 229-239.

Kieser, T., Bibb, M.J., Buttner, M.J., Chater, K.F., Hopwood, D.A. 2000. *Practical Streptomyces genetics*. The John Innes Foundation, Norwich.

Kim, J.H., Feng, Z., Bauer, J.D., Kallifidas, D., Calle, P.Y., Brady, S.F. 2010. Cloning large natural product gene clusters from the environment: piecing environmental DNA gene clusters back together with TAR. *Biopolymers*, **93**(9), 833-44.

Kim, M.W., Lee, B.R., You, S., Kim, E.J., Kim, J.N., Song, E., Yang, Y.H., Hwang, D., Kim, B.G. 2018. Transcriptome analysis of wild-type and afsS deletion mutant strains identifies synergistic transcriptional regulator of afsS for a high antibiotic-producing strain of *Streptomyces coelicolor* A3(2). *Appl Microbiol Biotechnol*, **102**(7), 3243-3253.

Kim, N.J., Li, H., Jung, K., Chang, H.N., Lee, P.C. 2011. Ethanol production from marine algal hydrolysates using *Escherichia coli* KO11. *Bioresour Technol*, **102**(16), 7466-9.

Knoell, W.M.J., Huxtable, R.J., Rinehart, K.L. 1973. Nybomycin. VI. Incorporation of carbon-13-labeled acetate, carbon-14-labeled acetate, and carbon-14-labeled methionine. *J Am Chem Soc*, **95**(8), 2703-2705.

Kolmogorov, M., Yuan, J., Lin, Y., Pevzner, P.A. 2019. Assembly of long, error-prone reads using repeat graphs. *Nat Biotechnol*, **37**(5), 540-546.

Komaki, H. 2023. Recent Progress of Reclassification of the Genus *Streptomyces*. *Microorganisms*, **11**(4).

Komaki, H., Hosoyama, A., Igarashi, Y., Tamura, T. 2020. *Streptomyces lydicamycinicus* sp. nov. and itssecondary metabolite biosynthetic gene clusters for polyketide and nonribosomal peptide compounds. *Microorganisms*, **8**(3).

Komaki, H., Tamura, T. 2020. Reclassification of *Streptomyces hygroscopicus* subsp. *glebosus* and *Streptomyces libani* subsp. *rufus* as later heterotypic synonyms of *Streptomyces platensis*. *Int J Syst Evol Microbiol*, **70**(7), 4398-4405.

Komaki, H., Tamura, T. 2019. Reclassification of *Streptomyces rimosus* subsp. *paromomycinus* as *Streptomyces paromomycinus* sp. nov. *Int J Syst Evol Microbiol*, **69**(8), 2577-2583.

Kraan, S. 2010. Mass-cultivation of carbohydrate rich macroalgae, a possible solution for sustainable biofuel production. *Mitig Adapt Strateg Glob Change*, **18**(1), 27-46.

Kreft, Ł., Botzki, A., Coppens, F., Vandepoele, K., Van Bel, M. 2017. PhyD3: a phylogenetic tree viewer with extended phyloXML support for functional genomics data visualization. *Bioinformatics*, **33**(18), 2946-2947.

Kuhl, M., Glaser, L., Rebets, Y., Ruckert, C., Sarkar, N., Hartsch, T., Kalinowski, J., Luzhetskyy, A., Wittmann, C. 2020. Microparticles globally reprogram *Streptomyces albus* toward accelerated morphogenesis, streamlined carbon core metabolism, and enhanced production of the antituberculosis polyketide pamamycin. *Biotechnol Bioeng*, **117**(12), 3858-3875.

Kumar, K.S., Kumari, S., Singh, K., Kushwaha, P. 2021. Influence of Seasonal Variation on Chemical Composition and Nutritional Profiles of Macro- and Microalgae. in: *Recent Advances in Micro and Macroalgal Processing*, pp. 14-71.

Kumar, V., Agrawal, D., Bommareddy, R.R., Islam, M.A., Jacob, S., Balan, V., Singh, V., Thakur, V.K., Navani, N.K., Scrutton, N.S. 2023. Arabinose as an overlooked sugar for microbial bioproduction of chemical building blocks. *Crit Rev Biotechnol*, **44**(6), 1103-1120.

Labeda, D.P., Goodfellow, M., Brown, R., Ward, A.C., Lanoot, B., Vanncanneyt, M., Swings, J., Kim, S.B., Liu, Z., Chun, J., Tamura, T., Oguchi, A., Kikuchi, T., Kikuchi, H., Nishii, T., Tsuji, K., Yamaguchi, Y., Tase, A., Takahashi, M., Sakane, T., Suzuki, K.I., Hatano, K. 2012. Phylogenetic study of the species within the family *Streptomycetaceae*. *Antonie Van Leeuwenhoek*, **101**(1), 73-104.

Lagesen, K., Hallin, P., Rødland, E.A., Stærfeldt, H.-H., Rognes, T., Ussery, D.W. 2007. RNAmmer: consistent and rapid annotation of ribosomal RNA genes. *Nucleic Acids Res*, **35**(9), 3100-3108.

Landwehr, W., Kampfer, P., Glaeser, S.P., Ruckert, C., Kalinowski, J., Blom, J., Goesmann, A., Mack, M., Schumann, P., Atasayar, E., Hahnke, R.L., Rohde, M., Martin, K., Stadler,

M., Wink, J. 2018. Taxonomic analyses of members of the *Streptomyces cinnabarinus* cluster, description of *Streptomyces cinnabarigriseus* sp. nov. and *Streptomyces davaonensis* sp. nov. *Int J Syst Evol Microbiol*, **68**(1), 382-393.

Langmead, B., Salzberg, S.L. 2012. Fast gapped-read alignment with Bowtie 2. *Nat Methods*, **9**(4), 357-9.

Lee, H.Y., Parkinson, E.I., Granchi, C., Paterni, I., Panigrahy, D., Seth, P., Minutolo, F., Hergenrother, P.J. 2017. Reactive Oxygen Species Synergize To Potently and Selectively Induce Cancer Cell Death. *ACS Chem Biol*, **12**(5), 1416-1424.

Lee, J.S., Chi, W.J., Hong, S.K., Yang, J.W., Chang, Y.K. 2013. Bioethanol production by heterologous expression of Pdc and AdhII in *Streptomyces lividans*. *Appl Microbiol Biotechnol*, **97**(13), 6089-97.

Lee, N., Hwang, S., Kim, W., Lee, Y., Kim, J.H., Cho, S., Kim, H.U., Yoon, Y.J., Oh, M.-K., Palsson, B.O., Cho, B.-K. 2021. Systems and synthetic biology to elucidate secondary metabolite biosynthetic gene clusters encoded in *Streptomyces* genomes. *Nat Prod Rep*, **38**(7), 1330-1361.

Lee, S.H., Moon, K., Kim, H., Shin, J., Oh, D.C., Oh, K.B. 2014. Bahamaolide A from the marine-derived *Streptomyces* sp. CNQ343 inhibits isocitrate lyase in *Candida albicans*. *Bioorg Med Chem Lett*, **24**(17), 4291-3.

Lefort, V., Desper, R., Gascuel, O. 2015. FastME 2.0: A Comprehensive, Accurate, and Fast Distance-Based Phylogeny Inference Program. *Mol Biol Evol*, **32**(10), 2798-800.

Leipoldt, F., Santos-Aberturas, J., Stegmann, D.P., Wolf, F., Kulik, A., Lacret, R., Popadic, D., Keinhorster, D., Kirchner, N., Bekiesch, P., Gross, H., Truman, A.W., Kaysser, L. 2017. Warhead biosynthesis and the origin of structural diversity in hydroxamate metalloproteinase inhibitors. *Nat Commun*, **8**(1), 1965.

Li, C., He, H., Wang, J., Liu, H., Wang, H., Zhu, Y., Wang, X., Zhang, Y., Xiang, W. 2019. Characterization of a LAL-type regulator NemR in nemadectin biosynthesis and its application for increasing nemadectin production in *Streptomyces cyaneogriseus*. *Sci China Life Sci*, **62**(3), 394-405.

Li, F., Jiang, P., Zheng, H., Wang, S., Zhao, G., Qin, S., Liu, Z. 2011. Draft genome sequence of the marine bacterium *Streptomyces griseoaurantiacus* M045, which produces novel manumycin-type antibiotics with a pABA core component. *J Bacteriol*, **193**(13), 3417-8.

Li, M., Chen, Z., Zhang, X., Song, Y., Wen, Y., Li, J. 2010. Enhancement of avermectin and ivermectin production by overexpression of the maltose ATP-binding cassette transporter in *Streptomyces avermitilis*. *Bioresour Technol*, **101**(23), 9228-35.

Li, Q., Woods, K.W., Claiborne, A., Gwaltney, I.I.S.L., Barr, K.J., Liu, G., Gehrke, L., Credo, R.B., Hui, Y.H., Lee, J., Warner, R.B., Kovar, P., Nukkala, M.A., Zielinski, N.A., Tahir,

S.K., Fitzgerald, M., Kim, K.H., Marsh, K., Frost, D., Ng, S.-C., Rosenberg, S., Sham, H.L. 2002. Synthesis and Biological Evaluation of 2-Indolyloxazolines as a New Class of Tubulin Polymerization Inhibitors. Discovery of A-289099 as an Orally Active Antitumor Agent. *Bioorg Med Chem Lett*, **12**(3), 465-469.

Li, R., Townsend, C.A. 2006. Rational strain improvement for enhanced clavulanic acid production by genetic engineering of the glycolytic pathway in *Streptomyces clavuligerus*. *Metab Eng*, **8**(3), 240-252.

Li, W., O'Neill, K.R., Haft, D.H., DiCuccio, M., Chetvernin, V., Badretdin, A., Coulouris, G., Chitsaz, F., Derbyshire, M.K., Durkin, A.S., Gonzales, N.R., Gwadz, M., Lanczycki, C.J., Song, J.S., Thanki, N., Wang, J., Yamashita, R.A., Yang, M., Zheng, C., Marchler-Bauer, A., Thibaud-Nissen, F. 2021. RefSeq: expanding the Prokaryotic Genome Annotation Pipeline reach with protein family model curation. *Nucleic Acids Res*, **49**(D1), D1020-D1028.

Liu, K., Zhang, J., Zhang, G., Zhang, L., Meng, Z., Ma, L., Zhang, W., Xiong, W., Zhu, Y., Wang, B., Zhang, C. 2023. Deciphering Deoxynybomycin Biosynthesis Reveals Fe(II)/alpha-Ketoglutarate-Dependent Dioxygenase-Catalyzed Oxazoline Ring Formation and Decomposition. *J Am Chem Soc*, **145**(50), 27886-27899.

Liu, R., Deng, Z., Liu, T. 2018. *Streptomyces* species: Ideal chassis for natural product discovery and overproduction. *Metab Eng*, **50**, 74-84.

Love, M.I., Huber, W., Anders, S. 2014. Moderated estimation of fold change and dispersion for RNA-seq data with DESeq2. *Genome Biol*, **15**(12), 550.

Lule, I., Maldonado, B., D'Huys, P.J., Van Mellaert, L., Van Impe, J., Bernaerts, K., Anne, J. 2012. On the influence of overexpression of phosphoenolpyruvate carboxykinase in *Streptomyces lividans* on growth and production of human tumour necrosis factor-alpha. *Appl Microbiol Biotechnol*, **96**(2), 367-72.

Lyu, M., Cheng, Y., Han, X., Wen, Y., Song, Y., Li, J., Chen, Z. 2020. AccR, a TetR Family Transcriptional Repressor, Coordinates Short-Chain Acyl Coenzyme A Homeostasis in *Streptomyces avermitilis*. *Appl Environ Microbiol*, **86**(12), e00508-20.

MacLeod, A.J., Ross, H.B., Ozere, R.L., Digout, G., Van Rooyen, C.E. 1964. Lincomycin: a new antibiotic active against *Staphylococci* and other gram-positive cocci: clinical and laboratory studies. *Can Med Assoc J*, **91**(20), 1056.

Mann, R.L., Bromer, W. 1958. The isolation of a second antibiotic from *Streptomyces hygroscopicus*. *J Am Chem Soc*, **80**(11), 2714-2716.

Manni, M., Berkeley, M.R., Seppey, M., Zdobnov, E.M. 2021. BUSCO: Assessing genomic data quality and beyond. *Curr Protoc*, **1**, e323.

Mao, D., Okada, B.K., Wu, Y., Xu, F., Seyedsayamdost, M.R. 2018. Recent advances in activating silent biosynthetic gene clusters in bacteria. *Curr Opin Microbiol*, **45**, 156-

163.

Maribu, I., Blikra, M.J., Eilertsen, K.E., Elvevold, K. 2024. Protein enrichment of the red macroalga *Palmaria palmata* using pulsed electric field and enzymatic processing. *J Appl Phycol*, **36**(6), 3665-3673.

Marjorie A Darken, Herman Berenson, Richard J Shirk, Sjolander, N.O. 1960. Production of Tetracycline by *Streptomyces aureofaciens* in Synthetic Media. *Appl Microbiol*, **8**(1), 46-51.

Martin-Sanchez, L., Singh, K.S., Avalos, M., van Wezel, G.P., Dickschat, J.S., Garbeva, P. 2019. Phylogenomic analyses and distribution of terpene synthases among *Streptomyces*. *Beilstein J Org Chem*, **15**, 1181-1193.

Mary P. Lechevalier, H.L. 1970. Chemical composition as a criterion in the classification of aerobic Actinomycetes. *Int J Syst Evol Microbiol*, **20**(4), 435-443.

Mazumdar, S., Bang, J., Oh, M.K. 2014. L-lactate production from seaweed hydrolysate of *Laminaria japonica* using metabolically engineered *Escherichia coli*. *Appl Biochem Biotechnol*, **172**(4), 1938-52.

Mazumdar, S., Lee, J., Oh, M.K. 2013. Microbial production of 2,3 butanediol from seaweed hydrolysate using metabolically engineered *Escherichia coli*. *Bioresour Technol*, **136**, 329-36.

McCulloch, K.M., McCranie, E.K., Smith, J.A., Sarwar, M., Mathieu, J.L., Gitschlag, B.L., Du, Y., Bachmann, B.O., Iverson, T.M. 2015. Oxidative cyclizations in orthosomycin biosynthesis expand the known chemistry of an oxygenase superfamily. *Proc Natl Acad Sci U S A*, **112**(37), 11547-52.

McKerrow, J., Vagg, S., McKinney, T., Seviour, E.M., Maszenan, A.M., Brooks, P., Seviour, R.J. 2000. A simple HPLC method for analysing diaminopimelic acid diastereomers in cell walls of Gram-positive bacteria. *Lett Appl Microbiol*, **30**(3), 178-82.

Medema, M.H., Kottmann, R., Yilmaz, P., Cummings, M., Biggins, J.B., Blin, K., de Bruijn, I., Chooi, Y.H., Claesen, J., Coates, R.C., Cruz-Morales, P., Duddela, S., Dusterhus, S., Edwards, D.J., Fewer, D.P., Garg, N., Geiger, C., Gomez-Escribano, J.P., Greule, A., Hadjithomas, M., Haines, A.S., Helfrich, E.J., Hillwig, M.L., Ishida, K., Jones, A.C., Jones, C.S., Jungmann, K., Kegler, C., Kim, H.U., Kotter, P., Krug, D., Masschelein, J., Melnik, A.V., Mantovani, S.M., Monroe, E.A., Moore, M., Moss, N., Nutzmann, H.W., Pan, G., Pati, A., Petras, D., Reen, F.J., Rosconi, F., Rui, Z., Tian, Z., Tobias, N.J., Tsunematsu, Y., Wiemann, P., Wyckoff, E., Yan, X., Yim, G., Yu, F., Xie, Y., Aigle, B., Apel, A.K., Balibar, C.J., Balskus, E.P., Barona-Gomez, F., Bechthold, A., Bode, H.B., Borriss, R., Brady, S.F., Brakhage, A.A., Caffrey, P., Cheng, Y.Q., Clardy, J., Cox, R.J., De Mot, R., Donadio, S., Donia, M.S., van der Donk, W.A., Dorrestein, P.C., Doyle, S., Driessen, A.J., Ehling-Schulz, M., Entian, K.D., Fischbach, M.A., Gerwick, L., Gerwick,

W.H., Gross, H., Gust, B., Hertweck, C., Hofte, M., Jensen, S.E., Ju, J., Katz, L., Kaysser, L., Klassen, J.L., Keller, N.P., Kormanec, J., Kuipers, O.P., Kuzuyama, T., Kyrpides, N.C., Kwon, H.J., Lautru, S., Lavigne, R., Lee, C.Y., Linquan, B., Liu, X., Liu, W., et al. 2015. Minimum Information about a Biosynthetic Gene cluster. *Nat Chem Biol*, **11**(9), 625-31.

Medema, M.H., Trefzer, A., Kovalchuk, A., van den Berg, M., Muller, U., Heijne, W., Wu, L., Alam, M.T., Ronning, C.M., Nierman, W.C., Bovenberg, R.A., Breitling, R., Takano, E. 2010. The sequence of a 1.8-mb bacterial linear plasmid reveals a rich evolutionary reservoir of secondary metabolic pathways. *Genome Biol Evol*, **2**, 212-24.

Meier-Kolthoff, J.P., Auch, A.F., Klenk, H.-P., Göker, M. 2013. Genome sequence-based species delimitation with confidence intervals and improved distance functions. *BMC Bioinformatics*, **14**(1), 60.

Meier-Kolthoff, J.P., Goker, M. 2019. TYGS is an automated high-throughput platform for state-of-the-art genome-based taxonomy. *Nat Commun*, **10**(1), 2182.

Meier-Kolthoff, J.P., Hahnke, R.L., Petersen, J., Scheuner, C., Michael, V., Fiebig, A., Rohde, C., Rohde, M., Fartmann, B., Goodwin, L.A., Chertkov, O., Reddy, T.B.K., Pati, A., Ivanova, N.N., Markowitz, V., Kyrpides, N.C., Woyke, T., Göker, M., Klenk, H.-P. 2014. Complete genome sequence of DSM 30083T, the type strain (U5/41T) of *Escherichia coli*, and a proposal for delineating subspecies in microbial taxonomy. *Stand in Genomic Sci*, **9**(1), 2.

Meier-Kolthoff, J.P., Klenk, H.P., Goker, M. 2014. Taxonomic use of DNA G+C content and DNA-DNA hybridization in the genomic age. *Int J Syst Evol Microbiol*, **64**(Pt 2), 352-356.

Meiswinkel, T.M., Gopinath, V., Lindner, S.N., Nampoothiri, K.M., Wendisch, V.F. 2013. Accelerated pentose utilization by *Corynebacterium glutamicum* for accelerated production of lysine, glutamate, ornithine and putrescine. *Microb Biotechnol*, **6**(2), 131-40.

Méndez, C., Brana, A.F., Manzanal, M.B., Hardisson, C. 1985. Role of substrate mycelium in colony development in *Streptomyces*. *Can J Microbiol*, **31**(5), 446-450.

Messner, K.R., Imlay, J.A. 2002. Mechanism of superoxide and hydrogen peroxide formation by fumarate reductase, succinate dehydrogenase, and aspartate oxidase. *J Biol Chem*, **277**(45), 42563-71.

Miao, V., Coëffet-LeGal, M.-F., Brian, P., Brost, R., Penn, J., Whiting, A., Martin, S., Ford, R., Parr, I., Bouchard, M., Silva, C.J., Wrigley, S.K., Baltz, R.H. 2005. Daptomycin biosynthesis in *Streptomyces roseosporus*: cloning and analysis of the gene cluster and revision of peptide stereochemistry. *Microbiol*, **151**(5), 1507-1523.

Miguélez, E.M., Hardisson, C., Manzanal, M.B. 1999. Hyphal Death during Colony

Development in *Streptomyces* antibioticus: Morphological Evidence for the Existence of a Process of Cell Deletion in a Multicellular Prokaryote. *J Cell Biol*, **145**, 515 - 525.

Milledge, J., Smith, B., Dyer, P., Harvey, P. 2014. Macroalgae-Derived Biofuel: A Review of Methods of Energy Extraction from Seaweed Biomass. *Energies*, **7**(11), 7194-7222.

Miller, J.R., Koren, S., Sutton, G. 2010. Assembly algorithms for next-generation sequencing data. *Genomics*, **95**(6), 315-27.

Mohy El-Din, S.M. 2018. Temporal variation in chemical composition of *Ulva lactuca* and *Corallina mediterranea*. *Int J Environ Sci Technol*, **16**(10), 5783-5796.

Moore, E.R., Mihaylova, S.A., Vandamme, P., Krichevsky, M.I., Dijkshoorn, L. 2010. Microbial systematics and taxonomy: relevance for a microbial commons. *Res Microbiol*, **161**(6), 430-8.

Moussa, M., Ebrahim, W., Bonus, M., Gohlke, H., Mándi, A., Kurtán, T., Hartmann, R., Kalscheuer, R., Lin, W., Liu, Z., Proksch, P. 2019. Co-culture of the fungus *Fusarium tricinctum* with *Streptomyces lividans* induces production of cryptic naphthoquinone dimers. *RSC Adv*, **9**(3), 1491-1500.

Murtey, M.D., Ramasamy, P. 2021. Life science sample preparations for scanning electron microscopy. *Acta Microscopica*, **30**(2), 80-91.

Myronovskyi, M., Luzhetskyy, A. 2019. Heterologous production of small molecules in the optimized *Streptomyces* hosts. *Nat Prod Rep*, **36**(9), 1281-1294.

Myronovskyi, M., Luzhetskyy, A. 2016. Native and engineered promoters in natural product discovery. *Nat Prod Rep*, **33**, 1006-1019.

Myronovskyi, M., Rosenkranzer, B., Nadmid, S., Pujic, P., Normand, P., Luzhetskyy, A. 2018. Generation of a cluster-free *Streptomyces albus* chassis strains for improved heterologous expression of secondary metabolite clusters. *Metab Eng*, **49**, 316-324.

Nadzan, A.M., Rinehart, K.L., Jr. 1976. Nybomycin. 8. Biosynthetic origin of the central ring carbons studied by 13C-labeled substrates. *J Am Chem Soc*, **98**(16), 5012-5014.

Naganawa, H., Wakashiro, T., Yagi, A., Kondo, S., Takita, T. 1970. Deoxynybomycin from a *Streptomyces*. *J Antibiot (Tokyo)*, **23**(7), 365-368.

Nagarajan, R., Boeck, L.D., Gorman, M., Hamill, R.L., Higgens, C.E., Hoehn, M.M., Stark, W.M., Whitney, J.G. 1971. beta.-Lactam antibiotics from *Streptomyces*. *J Am Chem Soc*, **93**(9), 2308-2310.

Nanopore, O. 2023. Guppy protocol.

Nauen, R., Smagghe, G. 2006. Mode of action of etoxazole. *Pest Manag Sci*, **62**(5), 379-382.

Nelson, M.L., Levy, S.B. 2011. 3.25 - Tetracyclines and Tetracycline Derivatives. in: *Comprehensive Biotechnology (Second Edition)*, (Ed.) M. Moo-Young, Academic Press. Burlington, pp. 269-283.

Offei, F., Mensah, M., Thygesen, A., Kemausuor, F. 2018. Seaweed Bioethanol Production: A

Process Selection Review on Hydrolysis and Fermentation. *Fermentation*, **4**(4), 99.

Ögmundarson, Ó., Sukumara, S., Laurent, A., Fantke, P. 2019. Environmental hotspots of lactic acid production systems. *GCB Bioenergy*, **12**(1), 19-38.

Ohnishi, Y., Ishikawa, J., Hara, H., Suzuki, H., Ikenoya, M., Ikeda, H., Yamashita, A., Hattori, M., Horinouchi, S. 2008. Genome sequence of the streptomycin-producing microorganism *Streptomyces griseus* IFO 13350. *J Bacteriol*, **190**(11), 4050-60.

Olano, C., Lombo, F., Mendez, C., Salas, J.A. 2008. Improving production of bioactive secondary metabolites in actinomycetes by metabolic engineering. *Metab Eng*, **10**(5), 281-92.

Ondov, B.D., Treangen, T.J., Melsted, P., Mallonee, A.B., Bergman, N.H., Koren, S., Phillippy, A.M. 2016. Mash: fast genome and metagenome distance estimation using MinHash. *Genome Biol*, **17**(1), 132.

Onishi, H.R., Pelak, B.A., Gerckens, L.S., Silver, L.L., Kahan, F.M., Chen, M.-H., Patchett, A.A., Galloway, S.M., Hyland, S.A., Anderson, M.S., Raetz, C.R.H. 1996. Antibacterial Agents That Inhibit Lipid A Biosynthesis. *Science*, **274**(5289), 980-982.

Pan, H.-Q., Cheng, J., Zhang, D.-F., Yu, S.-Y., Khieu, T.-N., Son, C.K., Jiang, Z., Hu, J.-C., Li, W.-J. 2015. *Streptomyces bohaiensis* sp. nov., a novel actinomycete isolated from *Scomberomorus niphonius* in the Bohai Sea. *J Antibiot (Tokyo)*, **68**(4), 246-252.

Park, J., Hong, S.-K., Chang, Y.K. 2015. Production of DagA and ethanol by sequential utilization of sugars in a mixed-sugar medium simulating microalgal hydrolysate. *Bioresour Technol*, **191**, 414-419.

Parkinson, E.I., Bair, J.S., Cismesia, M., Hergenrother, P.J. 2013. Efficient NQO1 Substrates are Potent and Selective Anticancer Agents. *ACS Chem Biol*, **8**(10), 2173-2183.

Parkinson, E.I., Bair, J.S., Nakamura, B.A., Lee, H.Y., Kuttab, H.I., Southgate, E.H., Lezmi, S., Lau, G.W., Hergenrother, P.J. 2015. Deoxynybomycins inhibit mutant DNA gyrase and rescue mice infected with fluoroquinolone-resistant bacteria. *Nat Commun*, **6**, 6947.

Parkinson, E.I., Hergenrother, P.J. 2015. Deoxynyboquinones as NQO1-Activated Cancer Therapeutics. *Acc Chem Res*, **48**(10), 2715-2723.

Parks, D.H., Imelfort, M., Skennerton, C.T., Hugenholtz, P., Tyson, G.W. 2015. CheckM: assessing the quality of microbial genomes recovered from isolates, single cells, and metagenomes. *Genome Res*, **25**(7), 1043-55.

Pauli, S., Kohlstedt, M., Lamber, J., Weiland, F., Becker, J., Wittmann, C. 2023. Systems metabolic engineering upgrades *Corynebacterium glutamicum* for selective high-level production of the chiral drug precursor and cell-protective extremolyte L-pipecolic acid. *Metab Eng*, **77**, 100-117.

Pei, X., Lei, Y., Zhang, H. 2024. Transcriptional regulators of secondary metabolite biosynthesis in *Streptomyces*. *World J Microbiol Biotechnol*, **40**(5), 156.

Penn, J., Li, X., Whiting, A., Latif, M., Gibson, T., Silva, C.J., Brian, P., Davies, J., Miao, V., Wrigley, S.K., Baltz, R.H. 2006. Heterologous production of daptomycin in *Streptomyces lividans*. *J Ind Microbiol Biotechnol*, **33**(2), 121-8.

Perez-Valero, A., Serna-Diestro, J., Villar, C.J., Lombo, F. 2024. Use of 3-Deoxy-D-arabino-heptulosonic acid 7-phosphate Synthase (DAHP Synthase) to Enhance the Heterologous Biosynthesis of Diosmetin and Chrysoeriol in an Engineered Strain of *Streptomyces albidoflavus*. *Int J Mol Sci*, **25**(5).

Poblete-Castro, I., Hoffmann, S.L., Becker, J., Wittmann, C. 2020. Cascaded valorization of seaweed using microbial cell factories. *Curr Opin Biotechnol*, **65**, 102-113.

Pommier, Y. 2013. Drugging Topoisomerases: Lessons and Challenges. *ACS Chem Biol*, **8**(1), 82-95.

Prakash, D., Nawani, N., Prakash, M., Bodas, M., Mandal, A., Khetmalas, M., Kapadnis, B. 2013. Actinomycetes: a repertory of green catalysts with a potential revenue resource. *Biomed Res Int*, **2013**, 264020.

Pullan, S.T., Chandra, G., Bibb, M.J., Merrick, M. 2011. Genome-wide analysis of the role of GlnR in *Streptomyces venezuelae* provides new insights into global nitrogen regulation in actinomycetes. *BMC Genomics*, **12**(1), 175.

RCoreTeam. 2020. R A language and environment for statistical computing, R Foundation for Statistical. in: *Computing*.

Reboleira, J., Silva, S., Chatzifragkou, A., Niranjan, K., Lemos, M.F.L. 2021. Seaweed fermentation within the fields of food and natural products. *Trends Food Sci Technol*, **116**, 1056-1073.

Redgrave, L.S., Sutton, S.B., Webber, M.A., Piddock, L.J. 2014. Fluoroquinolone resistance: mechanisms, impact on bacteria, and role in evolutionary success. *Trends Microbiol*, **22**(8), 438-45.

Reeves, A.R., Brikun, I.A., Cernota, W.H., Leach, B.I., Gonzalez, M.C., Weber, J.M. 2006. Effects of methylmalonyl-CoA mutase gene knockouts on erythromycin production in carbohydrate-based and oil-based fermentations of *Saccharopolyspora erythraea*. *J Ind Microbiol Biotechnol*, **33**(7), 600-9.

Risdian, C., Landwehr, W., Rohde, M., Schumann, P., Hahnke, R.L., Spröer, C., Bunk, B., Kämpfer, P., Schupp, P.J., Wink, J. 2021. *Streptomyces bathyalis* sp. nov., an actinobacterium isolated from the sponge in a deep sea. *Antonie Van Leeuwenhoek*, **114**(4), 425-435.

Rødde, R.S.H., Vårum, K.M., Larsen, B.A., Myklestad, S.M. 2004. Seasonal and geographical variation in the chemical composition of the red alga *Palmaria palmata* (L.) Kuntze. **47**(2), 125-133.

Rodriguez, E., Navone, L., Casati, P., Gramajo, H. 2012. Impact of malic enzymes on antibiotic

and triacylglycerol production in *Streptomyces coelicolor*. *Appl Environ Microbiol*, **78**(13), 4571-9.

Rodríguez Estévez, M., Myronovskyi, M., Gummerlich, N., Nadmid, S., Luzhetskyy, A. 2018. Heterologous Expression of the Nybomycin Gene Cluster from the Marine Strain *Streptomyces albus* subsp. *chlorinus* NRRL B-24108. *Mar Drugs*, **16**(11), 435.

Romero-Rodriguez, A., Rocha, D., Ruiz-Villafan, B., Guzman-Trampe, S., Maldonado-Carmona, N., Vazquez-Hernandez, M., Zelarayan, A., Rodriguez-Sanoja, R., Sanchez, S. 2017. Carbon catabolite regulation in *Streptomyces*: new insights and lessons learned. *World J Microbiol Biotechnol*, **33**(9), 162.

Rong, X., Guo, Y., Huang, Y. 2009. Proposal to reclassify the *Streptomyces albidoflavus* clade on the basis of multilocus sequence analysis and DNA-DNA hybridization, and taxonomic elucidation of *Streptomyces griseus* subsp. *solvifaciens*. *Syst Appl Microbiol*, **32**(5), 314-22.

Rong, X., Huang, Y. 2010. Taxonomic evaluation of the *Streptomyces griseus* clade using multilocus sequence analysis and DNA-DNA hybridization, with proposal to combine 29 species and three subspecies as 11 genomic species. *Int J Syst Evol Microbiol*, **60**(Pt 3), 696-703.

Rong, X., Huang, Y. 2012. Taxonomic evaluation of the *Streptomyces hygroscopicus* clade using multilocus sequence analysis and DNA-DNA hybridization, validating the MLSA scheme for systematics of the whole genus. *Syst Appl Microbiol*, **35**(1), 7-18.

Rossa, C.A., White, J., Kuiper, A., Postma, P.W., Bibb, M., Teixeira de Mattos, M.J. 2002. Carbon Flux Distribution in Antibiotic-Producing Chemostat Cultures of *Streptomyces lividans*. *Metab Eng*, **4**(2), 138-150.

Ruchala, J., Sibirny, A.A. 2021. Pentose metabolism and conversion to biofuels and high-value chemicals in yeasts. *FEMS Microbiol Rev*, **45**(4), fuaa069.

Ruiz, B., Chávez, A., Forero, A., García-Huante, Y., Romero, A., Sánchez, M., Rocha, D., Sánchez, B., Rodríguez-Sanoja, R., Sánchez, S., Langley, E. 2010. Production of microbial secondary metabolites: Regulation by the carbon source. *Crit Rev Microbio*, **36**(2), 146-167.

Ryu, Y.G., Butler, M.J., Chater, K.F., Lee, K.J. 2006. Engineering of primary carbohydrate metabolism for increased production of actinorhodin in *Streptomyces coelicolor*. *Appl Environ Microbiol*, **72**(11), 7132-7139.

Sánchez, S., Chávez, A., Forero, A., García-Huante, Y., Romero, A., Sánchez, M., Rocha, D., Sánchez, B., Ávalos, M., Guzmán-Trampe, S., Rodríguez-Sanoja, R., Langley, E., Ruiz, B. 2010. Carbon source regulation of antibiotic production. *J Antibiot (Tokyo)*, **63**(8), 442-459.

Santhanam, R., Rong, X., Huang, Y., Andrews, B.A., Asenjo, J.A., Goodfellow, M. 2013.

Streptomyces bullii sp. nov., isolated from a hyper-arid Atacama Desert soil. *Antonie Van Leeuwenhoek*, **103**(2), 367-73.

Sardari, S. 2017. Bioactive Compound Produced from *Actinomycetes* - *Streptomyces*. *Nov Approaches Drug Des Dev*, **1**(3).

Sasaki, M., Jojima, T., Kawaguchi, H., Inui, M., Yukawa, H. 2009. Engineering of pentose transport in *Corynebacterium glutamicum* to improve simultaneous utilization of mixed sugars. *Appl Microbiol Biotechnol*, **85**(1), 105-115.

Sauer, U., Eikmanns, B.J. 2005. The PEP-pyruvate-oxaloacetate node as the switch point for carbon flux distribution in bacteria. *FEMS Microbiol Rev*, **29**(4), 765-94.

Saurav, K., Kannabiran, K. 2010. Diversity and Optimization of process parameters for the growth of *Streptomyces* VITSVK9 spp. isolated from Bay of Bengal, India. *J Nat Environ Sci*, **1**(2), 56-65.

Schatz, A., Bugle, E., Waksman, S.A. 1944. Streptomycin, a substance exhibiting antibiotic activity against gram-positive and gram-negative bacteria. *Proc Soc Exp Biol Med*, **55**(1), 66-69.

Sekurova, O.N., Brautaset, T., Sletta, H., Borgos, S.E.F., Jakobsen, Ø.M., Ellingsen, T.E., Strøm, A.R., Valla, S., Zotchev, S.B. 2004. In Vivo Analysis of the Regulatory Genes in the Nystatin Biosynthetic Gene Cluster of *Streptomyces noursei* ATCC 11455 Reveals Their Differential Control Over Antibiotic Biosynthesis. *J Bacteriol*, **186**(5), 1345-1354.

Seo, K., Shu, W., Ruckert-Reed, C., Gerlinger, P., Erb, T.J., Kalinowski, J., Wittmann, C. 2023. From waste to health-supporting molecules: biosynthesis of natural products from lignin-, plastic- and seaweed-based monomers using metabolically engineered *Streptomyces lividans*. *Microb Cell Fact*, **22**(1), 262.

Seunghee, C., lt, sup, gt, Hee-Ju, N., Sisun, C., Eung-Soo, K. 2019. Heterologous Expression of Daptomycin Biosynthetic Gene Cluster Via *Streptomyces*; Artificial Chromosome Vector System. *J Microbiol Biotechnol*, **29**(12), 1931-1937.

Shirling, E.B., Gottlieb, D. 1966. Methods for characterization of *Streptomyces* species. *Int J Syst Evol Microbiol*, **16**, 313-340.

Sigle, S., Ladwig, N., Wohlleben, W., Muth, G. 2015. Synthesis of the spore envelope in the developmental life cycle of *Streptomyces coelicolor*. *Int J Med Microbiol*, **305**(2), 183-189.

Sissi, C., Cheng, B., Lombardo, V., Tse-Dinh, Y.C., Palumbo, M. 2013. Metal ion and inter-domain interactions as functional networks in *E. coli* topoisomerase I. *Gene*, **524**(2), 253-60.

Smith, E.M., Peterson, W.H., McCoy, E. 1954. Oligomycin, a new antiiungal antibiotic. *Antibiot Chemother (Northfield)*, **4**(9), 962-970.

Sprušanský, O., Řežuchová, B., Homerová, D., Kormanec, J. 2001. Expression of the gap

gene encoding glyceraldehyde-3-phosphate dehydrogenase of *Streptomyces aureofaciens* requires GapR, a member of the AraC/XylS family of transcriptional activators. *Microbiol*, **147**(5), 1291-1301.

Stackebrandt, E., Rainy, F.A., Ward-Rainey, N.L. 1997. Proposal for a New Hierarchic Classification System, Actinobacteria classis nov. *Int J Syst Evol Microbiol*, **47**(2), 479-491.

Stegmüller, J., Rodríguez Estévez, M., Shu, W., Gläser, L., Myronovskyi, M., Rückert-Reed, C., Kalinowski, J., Luzhetskyy, A., Wittmann, C. 2024. Systems metabolic engineering of the primary and secondary metabolism of *Streptomyces albidoflavus* enhances production of the reverse antibiotic nybomycin against multi-resistant *Staphylococcus aureus*. *Metab Eng*, **81**, 123-143.

Stiller, E.T., Vandeputte, J., Wachtel, J.L. 1955. Amphotericins A and B, antifungal antibiotics produced by a *Streptomycete*. II. The isolation and properties of the crystalline amphotericins. *Antibiot Annu*, **3**, 587-591.

Stratigopoulos, G., Bate, N., Cundliffe, E. 2004. Positive control of tylosin biosynthesis: pivotal role of TylR. *Mol Microbiol*, **54**(5), 1326-1334.

Strelitz, F., Flon, H., Asheshov, I.N. 1955. Nybomycin, a new antibiotic with antiphage and antibacterial properties. *Proc Natl Acad Sci USA*, **41**(9), 620-624.

Sun, L., Zeng, J., Cui, P., Wang, W., Yu, D., Zhan, J. 2018. Manipulation of two regulatory genes for efficient production of chromomycins in *Streptomyces reseiscleroticus*. *J Biol Eng*, **12**, 9.

Sur, S., Agrawal, D.K. 2016. Phosphatases and kinases regulating CDC25 activity in the cell cycle: clinical implications of CDC25 overexpression and potential treatment strategies. *Mol Cell Biochem*, **416**(1-2), 33-46.

Świątek, M.A., Gubbens, J., Bucca, G., Song, E., Yang, Y.-H., Laing, E., Kim, B.-G., Smith, C.P., Wezel, G.P.v. 2013. The ROK Family Regulator Rok7B7 Pleiotropically Affects Xylose Utilization, Carbon Catabolite Repression, and Antibiotic Production in *Streptomyces coelicolor*. *J Bacteriol*, **195**(6), 1236-1248.

Swiatek, M.A., Tenconi, E., Rigali, S., van Wezel, G.P. 2012. Functional analysis of the N-acetylglucosamine metabolic genes of *Streptomyces coelicolor* and role in control of development and antibiotic production. *J Bacteriol*, **194**(5), 1136-44.

Tajima, T., Tomita, K., Miyahara, H., Watanabe, K., Aki, T., Okamura, Y., Matsumura, Y., Nakashimada, Y., Kato, J. 2018. Efficient conversion of mannitol derived from brown seaweed to fructose for fermentation with a thraustochytrid. *J Biosci Bioeng*, **125**(2), 180-184.

Takahashi, Y., Nakashima, T. 2018. Actinomycetes, an Inexhaustible Source of Naturally Occurring Antibiotics. *Antibiotics (Basel)*, **7**(3), 74.

Takehana, Y., Umekita, M., Hatano, M., Kato, C., Sawa, R., Igarashi, M. 2017. Fradiamine A, a new siderophore from the deep-sea actinomycete *Streptomyces fradiae* MM456M-mF7. *J Antibiot (Tokyo)*, **70**(5), 611-615.

Tamura, K., Stecher, G., Kumar, S. 2021. MEGA11: Molecular Evolutionary Genetics Analysis Version 11. *Mol Biol Evol*, **38**(7), 3022-3027.

Tang, Z., Xiao, C., Zhuang, Y., Chu, J., Zhang, S., Herron, P.R., Hunter, I.S., Guo, M. 2011. Improved oxytetracycline production in *Streptomyces rimosus* M4018 by metabolic engineering of the G6PDH gene in the pentose phosphate pathway. *Enzyme Microb Technol*, **49**(1), 17-24.

Tatusova, T., DiCuccio, M., Badretdin, A., Chetvernin, V., Nawrocki, E.P., Zaslavsky, L., Lomsadze, A., Pruitt, K.D., Borodovsky, M., Ostell, J. 2016. NCBI prokaryotic genome annotation pipeline. *Nucleic Acids Res*, **44**(14), 6614-24.

Thykaer, J., Nielsen, J., Wohlleben, W., Weber, T., Gutknecht, M., Lantz, A.E., Stegmann, E. 2010. Increased glycopeptide production after overexpression of shikimate pathway genes being part of the balhimycin biosynthetic gene cluster. *Metab Eng*, **12**(5), 455-61.

Tian, X.P., Xu, Y., Zhang, J., Li, J., Chen, Z., Kim, C.J., Li, W.J., Zhang, C.S., Zhang, S. 2012. *Streptomyces oceani* sp. nov., a new obligate marine actinomycete isolated from a deep-sea sample of seep authigenic carbonate nodule in South China Sea. *Antonie Van Leeuwenhoek*, **102**(2), 335-343.

Tindall, B.J., Rossello-Mora, R., Busse, H.J., Ludwig, W., Kampfer, P. 2010. Notes on the characterization of prokaryote strains for taxonomic purposes. *Int J Syst Evol Microbiol*, **60**(Pt 1), 249-266.

Tong, Y., Charusanti, P., Zhang, L., Weber, T., Lee, S.Y. 2015. CRISPR-Cas9 Based Engineering of Actinomycetal Genomes. *ACS Synth Biol*, **4**(9), 1020-9.

Torres, M.D., Kraan, S., Domínguez, H. 2019. Seaweed biorefinery. *Rev in Environ Sci Biotechnol*, **18**(2), 335-388.

Toshiko, T., Jonathan, A., Polonia, H., María Elena, F. 2022. Multiplicity in the Genes of Carbon Metabolism in Antibiotic-Producing *Streptomycetes*. in: *Actinobacteria*, (Ed.) N.H. Wael, IntechOpen. Rijeka, pp. Ch. 5.

Turner, W., Greetham, D., Du, C. 2022. The characterisation of *Wickerhamomyces anomalus* M15, a highly tolerant yeast for bioethanol production using seaweed derived medium. *Front Bioeng Biotechnol*, **10**.

Umezawa, H., Hamada, M., Suhara, Y., Hashimoto, T., Ikekawa, T. 1965. Kasugamycin, a new antibiotic. *Antimicrob Agents Chemother*, **5**, 753-757.

Umezawa, H., Maeda, K., Takeuchi, T., Okami, Y. 1966. New antibiotics, bleomycin A & B. *J Antibiot (Tokyo)*, **19**(5), 200-209.

Umezawa, H., Ueda, M., Maeda, K., Yagishita, K., Kondō, S., Okami, Y., Utahara, R., Ōsato, Y., Nitta, K., Takeuchi, T. 1957. Production and Isolation of a New Antibiotic, Kanamycin. *J Antibiot, Series A*, **10**(5), 181-188.

van der Meij, A., Worsley, S.F., Hutchings, M.I., van Wezel, G.P. 2017. Chemical ecology of antibiotic production by actinomycetes. *FEMS Microbiol Rev*, **41**(3), 392-416.

van Wezel, G.P., McDowall, K.J. 2011. The regulation of the secondary metabolism of *Streptomyces*: new links and experimental advances. *Nat Prod Rep*, **28**(7), 1311-33.

Vandamme, P., Pot, B., Gillis, M., Vos, P.d., Kersters, K., Swings, J. 1996. Polyphasic taxonomy, a consensus approach to bacterial systematics. *Microbiol Rev*, **60**(2), 407-438.

Vézina, C., Kudelski, A., Sehgal, S.N. 1975. Rapamycin (AY-22, 989), a new antifungal antibiotic I. taxonomy of the producing *Streptomycete* and isolation of the active principle. *J Antibiot*, **28**(10), 721-726.

Vining, L.C., Stuttard, C. 1995. CHAPTER 18 - Chloramphenicol. in: *Genetics and Biochemistry of Antibiotic Production*, (Eds.) L.C. Vining, C. Stuttard, Butterworth-Heinemann. Boston, pp. 505-530.

Vitayakritsirikul, V., Jaemsaeng, R., Lohmaneeratana, K., Thanapipatsiri, A., Daduang, R., Chuawong, P., Thamchaipenet, A. 2015. Improvement of chloramphenicol production in *Streptomyces venezuelae* ATCC 10712 by overexpression of the *aroB* and *aroK* genes catalysing steps in the shikimate pathway. *Antonie Van Leeuwenhoek*, **109**(3), 379-388.

Waksman, S.A., Lechevalier, H.A. 1949. Neomycin, a New Antibiotic Active against Streptomycin-Resistant Bacteria, including Tuberculosis Organisms. *Science*, **109**(2830), 305-307.

Waksman, S.A., Lechevalier, H.A., Schaffner, C.P. 1965. Candicidin and other polyenic antifungal antibiotics: A review. *Bull World Health Organ*, **33**(2), 219.

Waksman, S.A., Woodruff, H.B. 1940. Bacteriostatic and bactericidal substances produced by a soil *Actinomyces*. *Proc Soc Exp Biol Med*, **45**(2), 609-614.

Wang, C., Wang, J., Yuan, J., Jiang, L., Jiang, X., Yang, B., Zhao, G., Liu, B., Huang, D. 2019. Generation of *Streptomyces hygroscopicus* cell factories with enhanced ascomycin production by combined elicitation and pathway-engineering strategies. *Biotechnol Bioeng*, **116**(12), 3382-3395.

Wang, X., Elshahawi, S.I., Ponomareva, L.V., Ye, Q., Liu, Y., Copley, G.C., Hower, J.C., Hatcher, B.E., Kharel, M.K., Van Lanen, S.G., She, Q.B., Voss, S.R., Thorson, J.S., Shaaban, K.A. 2019. Structure Determination, Functional Characterization, and Biosynthetic Implications of Nybomycin Metabolites from a Mining Reclamation Site-Associated *Streptomyces*. *J Nat Prod*, **82**(12), 3469-3476.

Wang, X.K., Jin, J.L. 2014. Crucial factor for increasing the conjugation frequency in

Streptomyces netropsis SD-07 and other strains. *FEMS Microbiol Lett*, **357**(1), 99-103.

Warnes, G.R., Bolker, B.M., Bonebakker, L., Gentleman, R., Huber, W., Liaw, A., Lumley, T., Maechler, M., Magnusson, A., Moeller, S., Schwartz, M., Venables, B.A.B. 2020. Various R Programming Tools for Plotting Data [R package gplots version 3.1.0].

Watabe, H. 1988. A new antibiotic SF2583A, 4-chloro-5-(3'-indolyl) oxazole, produced by *Streptomyces*. *Meiji Seika Kenkyu Nenpo*, **27**, 55-62.

Wayne, L.G., Brenner, D.J., Colwell, R.R., Grimont, P.A.D., Kandler, O., Krichevsky, M.I., Moore, L.H., Moore, W.E.C., Murray, R.G.E., Stackebrandt, E., Starr, M.P., Truper, H.G. 1987. Report of the Ad Hoc Committee on Reconciliation of Approaches to Bacterial Systematics. *Int J Syst Evol Microbiol*, **37**(4), 463-464.

Weisburg, W.G., Barns, S.M., Pelletier, D.A., Lane, D.J. 1991. 16S ribosomal DNA amplification for phylogenetic study. *J Bacteriol*, **173**(2), 697-703.

Wildermuth, H. 1970. Development and Organization of the Aerial Mycelium in *Streptomyces coelicolor*. *Microbiol*, **60**(1), 43-50.

Wildermuth, H., Hopwood, D.A. 1970. Septation During Sporulation in *Streptomyces coelicolor*. *Microbiol*, **60**(1), 51-59.

Winter, J.M., Moffitt, M.C., Zazopoulos, E., McAlpine, J.B., Dorrestein, P.C., Moore, B.S. 2007. Molecular basis for chloronium-mediated meroterpene cyclization: cloning, sequencing, and heterologous expression of the napyradiomycin biosynthetic gene cluster. *J Biol Chem*, **282**(22), 16362-8.

Wittmann, C., Hans, M., Heinzle, E. 2002. In vivo analysis of intracellular amino acid labelings by GC/MS. *Anal Biochem*, **307**(2), 379-382.

Wolfson, J.S., Hooper, D.C. 1989. Fluoroquinolone antimicrobial agents. *Clin Microbiol Rev* **2**(4), 378-424.

Wong, H., Ting, Y., Lin, H., Reichert, F., Myambo, K., Watt, K., Toy, P., Drummond, R. 1991. Genetic organization and regulation of the xylose degradation genes in *Streptomyces rubiginosus*. *J Bacteriol*, **173**(21), 6849-6858.

Wong, H.C., Ting, Y., Lin, H.C., Reichert, F., Myambo, K., Watt, K.W., Toy, P.L., Drummond, R.J. 1991. Genetic organization and regulation of the xylose degradation genes in *Streptomyces rubiginosus*. *J Bacteriol*, **173**(21), 6849-6858.

Worrall, J.A., Vijgenboom, E. 2010. Copper mining in *Streptomyces*: enzymes, natural products and development. *Nat Prod Rep*, **27**(5), 742-56.

Wu, H., Liu, W., Dong, D., Li, J., Zhang, D., Lu, C. 2014. *SlnM* gene overexpression with different promoters on natamycin production in *Streptomyces lydicus* A02. *J Ind Microbiol Biotechnol*, **41**(1), 163-172.

Wu, L., Ma, J. 2019. The Global Catalogue of Microorganisms (GCM) 10K type strain sequencing project: providing services to taxonomists for standard genome sequencing

and annotation. *Int J Syst Evol Microbiol*, **69**(4), 895-898.

Wu, S.J., Fotso, S., Li, F., Qin, S., Laatsch, H. 2007. Amorphane Sesquiterpenes from a Marine *Streptomyces* sp. *J Nat Prod*, **70**(2), 304-306.

Wu, Y., Shen, X., Yuan, Q., Yan, Y. 2016. Metabolic Engineering Strategies for Co-Utilization of Carbon Sources in Microbes. *Bioengineering (Basel)*, **3**(1), 10.

Xia, H., Li, X., Li, Z., Zhan, X., Mao, X., Li, Y. 2020. The Application of Regulatory Cascades in *Streptomyces*: Yield Enhancement and Metabolite Mining. *Front Microbiol*, **11**, 406.

Xu, D., Seghezzi, N., Esnault, C., Virolle, M.-J. 2010. Repression of Antibiotic Production and Sporulation in *Streptomyces coelicolor* by Overexpression of a TetR Family Transcriptional Regulator. *Appl Environ Microbiol*, **76**(23), 7741-7753.

Xu, R., Zhu, H., Zhang, H., Ju, J., Li, Q., Fu, S. 2023. Six Sets of Aromatic Polyketides Differing in Size and Shape Derive from a Single Biosynthetic Gene Cluster. *J Nat Prod*, **86**(6), 1512-1519.

Xu, Z., Ji, L., Tang, W., Guo, L., Gao, C., Chen, X., Liu, J., Hu, G., Liu, L. 2022. Metabolic engineering of *Streptomyces* to enhance the synthesis of valuable natural products. *Eng Microbiol*, **2**(2), 100022.

Xu, Z.F., Bo, S.T., Wang, M.J., Shi, J., Jiao, R.H., Sun, Y., Xu, Q., Tan, R.X., Ge, H.M. 2020. Discovery and biosynthesis of bosamycins from *Streptomyces* sp. 120454. *Chem Sci*, **11**(34), 9237-9245.

Yang, C., Qian, R., Xu, Y., Yi, J., Gu, Y., Liu, X., Yu, H., Jiao, B., Lu, X., Zhang, W. 2019. Marine Actinomycetes-derived Natural Products. *Curr Top Med Chem*, **19**(31), 2868-2918.

Yang, Q., Luan, M., Wang, M., Zhang, Y., Liu, G., Niu, G. 2024. Characterizing and Engineering Rhamnose-Inducible Regulatory Systems for Dynamic Control of Metabolic Pathways in *Streptomyces*. *ACS Synth Biol*, **13**(10), 3461-3470.

Yankovskaya, V., Horsefield, R., Törnroth, S., Luna-Chavez, C., Miyoshi, H., Léger, C., Byrne, B., Cecchini, G., Iwata, S. 2003. Architecture of Succinate Dehydrogenase and Reactive Oxygen Species Generation. *Science*, **299**(5607), 700-704.

Yao, R., Shimizu, K. 2013. Recent progress in metabolic engineering for the production of biofuels and biochemicals from renewable sources with particular emphasis on catabolite regulation and its modulation. *Process Biochem*, **48**(9), 1409-1417.

Yim, G., Wang, H.H., Davies, J. 2007. Antibiotics as signalling molecules. *Philos Trans R Soc Lond B Biol Sci*, **362**(1483), 1195-200.

Yim, S.S., Choi, J.W., Lee, S.H., Jeong, K.J. 2016. Modular Optimization of a Hemicellulose-Utilizing Pathway in *Corynebacterium glutamicum* for Consolidated Bioprocessing of Hemicellulosic Biomass. *ACS Synth Biol*, **5**(4), 334-43.

Yoon, S.H., Ha, S.M., Kwon, S., Lim, J., Kim, Y., Seo, H., Chun, J. 2017. Introducing EzBioCloud: a taxonomically united database of 16S rRNA gene sequences and whole-

genome assemblies. *Int J Syst Evol Microbiol*, **67**(5), 1613-1617.

Yoon, S.H., Ha, S.M., Lim, J., Kwon, S., Chun, J. 2017. A large-scale evaluation of algorithms to calculate average nucleotide identity. *Antonie Van Leeuwenhoek*, **110**(10), 1281-1286.

Yoshida, H., Bogaki, M., Nakamura, M., Nakamura, S. 1990. Quinolone resistance-determining region in the DNA gyrase *gyrA* gene of *Escherichia coli*. *Antimicrob Agents Chemother*, **34**(6), 1271-1272.

Zabala, D., Brana, A.F., Florez, A.B., Salas, J.A., Mendez, C. 2013. Engineering precursor metabolite pools for increasing production of antitumor mithramycins in *Streptomyces argillaceus*. *Metab Eng*, **20**, 187-97.

Zaburannyi, N., Rabyk, M., Ostash, B., Fedorenko, V., Luzhetskyy, A. 2014. Insights into naturally minimised *Streptomyces albus* J1074 genome. *BMC Genomics*, **15**(1), 97.

Zakalyukina, Y.V., Birykov, M.V., Lukianov, D.A., Shiriaev, D.I., Komarova, E.S., Skvortsov, D.A., Kostyukevich, Y., Tashlitsky, V.N., Polshakov, V.I., Nikolaev, E., Sergiev, P.V., Osterman, I.A. 2019. Nybomycin-producing *Streptomyces* isolated from carpenter ant *Camponotus vagus*. *Biochimie*, **160**, 93-99.

Zhang, H.Z., Zhao, Z.L., Zhou, C.H. 2018. Recent advance in oxazole-based medicinal chemistry. *Eur J Med Chem*, **144**, 444-492.

Zhang, L., Zhao, G., Ding, X. 2011. Tandem assembly of the epothilone biosynthetic gene cluster by in vitro site-specific recombination. *Sci Rep*, **1**(1), 141.

Zhang, S., Chen, T., Jia, J., Guo, L., Zhang, H., Li, C., Qiao, R. 2019. Establishment of a highly efficient conjugation protocol for *Streptomyces kanamyceticus* ATCC12853. *Microbiologyopen*, **8**(6), e00747.

Zhou, H., Wang, Y., Yu, Y., Bai, T., Chen, L., Liu, P., Guo, H., Zhu, C., Tao, M., Deng, Z. 2012. A non-restricting and non-methylating *Escherichia coli* strain for DNA cloning and high-throughput conjugation to *Streptomyces coelicolor*. *Curr Microbiol*, **64**(2), 185-90.

Zhou, T.C., Zhong, J.J. 2015. Production of validamycin A from hemicellulose hydrolysate by *Streptomyces hygroscopicus* 5008. *Bioresour Technol*, **175**, 160-166.

Zhu, H., Sandiford, S.K., van Wezel, G.P. 2014. Triggers and cues that activate antibiotic production by actinomycetes. *J Ind Microbiol Biotechnol*, **41**(2), 371-386.